

Large N Chern-Simons-matter fixed points with multiple flavors

Ofer Aharony, Ronny Frumkin, and Jonathan Mehl

Department of Particle Physics and Astrophysics, Weizmann Institute of Science, Rehovot 7610001, Israel

E-mail: ofer.aharony@weizmann.ac.il, ronny.frumkin@weizmann.ac.il,
jonathan.mehl@weizmann.ac.il

ABSTRACT: In this paper we analyze the 2+1d conformal fixed points arising from $SU(N_c)$ Chern-Simons-matter theories with multiple flavors $N_f > 1$ in the 't Hooft large N_c limit. The multi-flavor generalization of quasi-fermionic theories (fermions or critical scalars coupled to Chern-Simons gauge fields) is straightforward, but this is not true for quasi-bosonic theories (scalars or critical fermions coupled to Chern-Simons gauge fields). The latter theories have three flavor-singlet relevant operators and also three marginal operators, that become exactly marginal for infinite N_c , but have a non-zero beta function at order $1/N_c$. We compute the beta functions of these couplings in various weak coupling limits, and also discuss their general structure, generalizing previous computations for $N_f = 1$. We find that IR-stable fixed points of the marginal couplings exist for some values of N_f and of the 't Hooft coupling λ , but not for other values, and in one case we can explicitly follow how two pairs of fixed points merge and disappear as λ is increased. We also analyze the “Semi-Critical” conformal field theories that arise when fine-tuning two (rather than three) relevant operators, and compute the beta function for their (single) marginal coupling constant.

Contents

1	Introduction and summary of results	1
2	The theories studied in this paper	4
2.1	Fermion theories	5
2.2	Scalar theories	7
2.3	Summary and expected dualities	8
3	Review of the $N_f = 1$ results and formalism	10
3.1	General formalism	10
3.2	The beta function in the perturbative region	12
3.3	Discussion and hypothesis in the non-perturbative regime	15
4	Beta function structure for multiple flavors	15
4.1	Effective action for multiple flavors	16
4.2	Calculating the beta function	20
4.3	Analyzing the beta function structure	23
4.4	The large N_f limit	25
5	Regular boson theories with vanishing and small λ_B	27
5.1	Calculating the beta functions	27
5.2	The $N_f = 2$ case	31
5.3	The $N_f \geq 3$ case	34
5.4	The limit $N_f \rightarrow \infty$	37
5.5	General discussion – elimination, splitting, and merging of fixed points	44
6	The Critical Fermion theory with $\lambda_F = 0$	47
6.1	Computation of the β functions	47
6.2	Analysis of the flow	48
6.3	Solutions in the limit $N_f \rightarrow \infty$	50
7	Semi-Critical theories	51
7.1	Calculation of the beta functions	51
7.2	Semi-Critical Singlet theories	53
7.3	Semi-Critical Adjoint theories	55
8	Conclusions and future directions	56
A	Calculations for finite λ_B	59
A.1	The action and Feynman rules	59
A.2	The $\lambda = 0$ case	61
A.3	The $\lambda \ll 1$ case	65

B	Correlation functions for the critical boson theory at $\lambda = 0$	69
B.1	Effective action for σ	70
B.2	Amputated tree-level correlation functions for σ	72
B.3	Tree-level correlation functions	74
B.4	First $\ln(\Lambda)$ dependent sub-leading contribution to G_2	75
B.5	First sub-leading contribution to G_3	76
C	Correlation functions for the free fermion theories	77

1 Introduction and summary of results

2+1 dimensional conformal field theories arising by coupling matter to Chern-Simons gauge fields (“Chern-Simons-matter theories”) are interesting for many different reasons. Some of these theories are believed to arise in phase diagrams of condensed matter systems, as well as in 2 + 1 dimensional QCD (with or without bare Chern-Simons terms). The theories of fermions coupled to Chern-Simons (CS) gauge fields are believed to be dual to those of scalars coupled to Chern-Simons gauge fields [1–4], giving the simplest example of dualities between non-supersymmetric theories above 1 + 1 dimensions. In the large N_c limit of $SU(N_c)$ or $SO(N_c)$ theories (with fixed ’t Hooft coupling $\lambda \equiv \frac{N_c}{\kappa}$ where κ is the CS level), many things in these theories can be computed exactly, either by resumming the planar diagrams (whose difficulty is similar to vector models rather than to matrix models), or by using their approximate high-spin symmetry [5, 6]. The large N_c theories are also believed to be holographically dual to weakly coupled high-spin gravity theories on AdS_4 , giving a relatively simple example of non-supersymmetric holography [1, 7–11]¹.

The simplest Chern-Simons-matter theories (called “quasi-fermionic theories” [5, 6]) arise either by coupling a fermion in the fundamental representation of $SU(N_c)$ to $SU(N_c)$ CS gauge fields (“Regular Fermion (RF) theories”), or by coupling the critical $U(N_c)$ model to such gauge fields (“Critical Boson (CB) theories”)². The two descriptions are related by strong-weak-coupling duality, so that the full family of theories is given by either the fermionic or the bosonic theory with ’t Hooft coupling $-1 < \lambda \leq 1$ (we will denote the ’t Hooft coupling in the scalar description by λ_B , and the one in the fermionic description by λ_F). These theories have a single relevant operator whose coefficient (the mass term in the fermionic theory) must be fine-tuned to flow to a fixed point (recall that Chern-Simons couplings are quantized and do not run under the renormalization group). In the large N_c limit the single-trace spectrum of these theories consists of a scalar operator of dimension $\Delta = 2 + \mathcal{O}\left(\frac{1}{N_c}\right)$, and of currents of every integer spin s , whose anomalous dimensions (for $s > 2$) go as $\frac{1}{N_c}$.

¹In this paper we will discuss theories that have either only fermions or only scalars coupled to Chern-Simons gauge fields; the features and dualities mentioned above can also be generalized to theories with both scalars and fermions, some of which are supersymmetric [12–24].

²All the theories discussed in this paper also have $SO(N_c)$ versions, which for large N_c are very similar to the $SU(N_c)$ theories in terms of our discussion here, so we will not discuss them separately.

There is also a family of “quasi-bosonic theories” that requires additional fine-tunings. These theories arise either by coupling a scalar in the fundamental representation of $SU(N_c)$ to $SU(N_c)$ CS gauge fields (“Regular Boson (RB) theories”), or by coupling the $U(N_c)$ Gross-Neveu model to such gauge fields (“Critical Fermion (CF) theories”). These theories have two relevant operators, which in the scalar language are the ϕ^2 and $(\phi^2)^2$ operators, and both need to be fine-tuned to flow to a fixed point. The main difference in the spectrum of these theories compared to the quasi-fermionic ones is that the single-trace scalar operator has dimension $\Delta = 1 + \mathcal{O}\left(\frac{1}{N_c}\right)$.

The “quasi-bosonic theories” have a $(\phi^2)^3$ “triple-trace” operator that is exactly marginal in the large N_c limit, but has a finite beta function for finite N_c (going as $\frac{1}{N_c}$ at large N_c). Thus, to analyze if these fixed points exist for finite large N_c and how much fine-tuning is required to flow to them, one has to carefully analyze this beta function, and this was done in [25]. It was shown there that at weak coupling, either from the bosonic side ($\lambda_B \rightarrow 0$, equivalent to $|\lambda_F| \rightarrow 1$) or from the fermionic side of the duality ($\lambda_F \rightarrow 0$, equivalent to $|\lambda_B| \rightarrow 1$), the theory has one IR-stable and two UV-stable fixed points for the extra coupling, and it was conjectured that this remains true for all values of the ’t Hooft coupling λ . With this assumption, flowing to the IR-stable fixed point requires two fine-tunings of the two relevant operators.

The discussion above, and most of the analysis of these theories in the literature, was for the case of a single flavor of matter fields in the fundamental representation of $SU(N_c)$, $N_f = 1$. It is straightforward to generalize these theories to $N_f > 1$ flavors of fermion or scalar fields, with couplings that preserve an $SU(N_f)$ global symmetry (in addition to the $U(1)$ global symmetry of the $N_f = 1$ theory).

For the “quasi-fermionic theories” this does not change much. These have scalar operators of dimension $\Delta \simeq 2$ in both the singlet and adjoint representations of the $SU(N_f)$ global symmetry, but they still require (for all λ) only a single fine-tuning in order to flow to the fixed point (from an $SU(N_f)$ -symmetric starting point).

For the “quasi-bosonic theories” that will be our focus in this paper, the situation is very different. These theories have scalar operators in the singlet+adjoint representations of $SU(N_f)$ with dimensions $\Delta = 1 + \mathcal{O}\left(\frac{1}{N_c}\right)$, which we can denote by \mathcal{O}_S and \mathcal{O}_A , respectively, and this has two dramatic consequences:

- These theories now have three relevant operators, schematically given by flavor-singlets coming from \mathcal{O}_S , \mathcal{O}_S^2 and \mathcal{O}_A^2 . This means that we need to perform at least three fine-tunings in order to flow to these theories and not just two.
- These theories have (for $N_f \geq 3$) three flavor-singlet marginal operators that are all exactly marginal in the large N_c limit, schematically of the form \mathcal{O}_S^3 , $\mathcal{O}_S\mathcal{O}_A^2$ and \mathcal{O}_A^3 . For finite large N_c , all of their couplings acquire beta functions, which must be computed in order to see if they have IR-stable fixed points (beyond the three relevant operators mentioned above).

Our main goal in this paper is to analyze the beta functions of the marginal couplings in these theories, generalizing the computations of [25], and to see for which values of λ and

N_f they have IR-stable fixed points. In addition to analyzing fixed values of N_f as N_c becomes large, it is also interesting to analyze the case of $1 \ll N_f \ll N_c$ (including the limit of large N_c with fixed small N_f/N_c), and we will see that some computations become more tractable in this case.

As we mentioned, in order to flow to the “quasi-bosonic theories” for $N_f > 1$ we need to tune three relevant operators, which can be thought of as a mass term and two independent four-fermi/four-scalar couplings. We can also choose to fine-tune just one of the four-fermi/four-scalar couplings and not both of them. This leads to “Semi-Critical theories”, in which either the dimension of the singlet scalar is $\Delta = 1 + \mathcal{O}\left(\frac{1}{N_c}\right)$ and that of the adjoint scalar is $\Delta = 2 + \mathcal{O}\left(\frac{1}{N_c}\right)$, or vice versa. These theories are in many ways in-between the “quasi-fermionic” and the “quasi-bosonic” theories. In particular, each class of theories has just one marginal coupling (that becomes exactly marginal for infinite N_c), whose beta function needs to be computed to look for IR-stable fixed points (beyond the two relevant operators of each of these theories).

We begin in section 2 by defining precisely all the theories discussed above, and describing their relevant and marginal couplings, and the expected dualities and flows between them.

In section 3 we review the results of [25] on the $N_f = 1$ theory and its fixed points.

In section 4 we analyze the general form of the beta functions in the “quasi-bosonic theories” for all values of λ . We show that, as for $N_f = 1$, the beta functions for all three marginal operators begin at order $\frac{1}{N_c}$, and at this order they are polynomials of degree three. We also analyze the large N_f limit (with $N_f \ll N_c$), and show that in some scaling of the couplings (corresponding to a planar limit for $SU(N_f)$), the beta functions simplify in this limit.

In section 5 we compute explicitly the beta functions in the theories with scalars when they are weakly coupled ($\lambda_B \rightarrow 0$). We show that, as for $N_f = 1$, for $\lambda_B = 0$ the free theory (with vanishing marginal deformations) is a degenerate fixed point, which splits for small finite λ_B . We find that for $N_f = 2$ and for $N_f \geq 5$ there is an IR-stable fixed point for the marginal couplings at small λ_B , but that no such fixed point exists for $N_f = 3, 4$. At large N_f we find that the IR-stable fixed point merges with another fixed point and disappears at $|\lambda_B| = 24\pi/N_f$, such that for $24\pi/N_f < |\lambda_B| \ll 1$ there is no IR-stable fixed point. We classify also all the other fixed points, and discuss how they can change as we change λ . The small λ_B analysis is relevant also for weakly coupled fixed points at finite (not necessarily large) N_c , and in appendix A.3.1 we analyze precisely for which values of N_c and N_f weakly coupled IR-stable fixed points exist.

In section 6 we do the same in the limit where the fermionic description is weakly coupled. In this limit we find that for all $N_f > 1$ there is no IR-stable fixed point. The simplest conjecture would be that for $N_f \geq 5$ such a fixed point exists for small enough λ_B , but disappears as $|\lambda_B|$ is increased.

In section 7 we compute the beta functions for the two “Semi-Critical theories”. These beta functions (for the single marginal coupling that exists in each of these theories) are again third order polynomials at order $\frac{1}{N_c}$. In both of these theories the $\lambda_B \rightarrow 0$ limit is

not a free theory (it includes a non-trivial fixed point), so our computations in this limit depend on some unknown coefficients. In the “Semi-Critical singlet” theories (where the dimension of the scalar flavor-singlet $\simeq 1$ while that of the scalar flavor-adjoint $\simeq 2$) we find that for $\lambda_B \rightarrow 0$ an IR-stable fixed point (for the marginal coupling) exists at large enough N_f (we cannot tell how large it needs to be), while for $\lambda_F \rightarrow 0$ there is an IR-stable fixed point for all N_f . The “Semi-Critical adjoint” theory for $N_f = 2$ has no marginal coupling so there is a fixed point where we need to fine-tune just the two relevant deformations. For $N_f = 3$ we find that as $\lambda_B \rightarrow 0$ the theory has one IR-stable fixed point, while for $\lambda_F \rightarrow 0$ it has two IR-stable fixed points, so presumably one of these fixed points merges with another fixed point as we increase $|\lambda_F|$. For $N_f \geq 4$ there is always an IR-stable fixed point for small $|\lambda_F|$, while for small $|\lambda_B|$ we cannot determine the existence of an IR-stable fixed point for any value of N_f .

We end in section 8 with a summary of our results and some future directions. Several appendices contain technical results needed for computations in the main text.

2 The theories studied in this paper

In this paper we study Chern-Simons-matter theories with N_f massless complex scalars or Dirac fermions in the fundamental representation of an $SU(N_c)$ gauge group in $d = 3$ dimensions.

We denote the scalar fields as $\phi^{c,i}$ (or $\psi^{c,i}$ for fermions), where $c = 1, \dots, N_c$ is the color index, and $i = 1, \dots, N_f$ is the flavor index. Here, and in the rest of this paper, we use a, b, c, \dots to denote color indices and i, j, k, \dots to denote flavor indices.

We assume that the gauge field is described by a level κ Chern-Simons (CS) action, given in Euclidean space by

$$S_{CS}(A) = \frac{\kappa}{4\pi} \int d^3x \left(-\frac{i}{2} \epsilon^{\mu\nu\rho} A_{\mu}^{\bar{a}} \partial_{\nu} A_{\rho}^{\bar{a}} - \frac{i}{6} \epsilon^{\mu\nu\rho} f^{\bar{a}\bar{b}\bar{c}} A_{\mu}^{\bar{a}} A_{\nu}^{\bar{b}} A_{\rho}^{\bar{c}} \right) \quad (2.1)$$

where $\bar{a}, \bar{b}, \bar{c}, \dots$ are adjoint color indices. Conventions for generators of the color group are given in Appendix A. We will study these theories mainly in the ’t Hooft limit where $N_c, |\kappa| \rightarrow \infty$ with fixed N_f , while the ’t Hooft coupling $\lambda \equiv \frac{N_c}{\kappa}$ ³ is finite and takes values⁴ between $0 \leq |\lambda| \leq 1$. When considering the possible dualities between fermion and scalar (boson) theories, we will add the super/subscript F, B to indicate the level, coupling and N_c of the fermion and scalar theories, respectively⁵. In this paper we consider only $SU(N_c)$ gauge theories, but in the ’t Hooft limit that we consider they are the same as $U(N_c)$ gauge theories; dualities sometimes exchange $SU(N)$ and $U(N)$ theories [3, 26] but the distinction will not be important in this work.

³Because λ is the ratio of two integers it has no continuous renormalization group flow.

⁴We follow the conventions of [25], where the CS coupling is written in the dimensional reduction scheme, in which it obeys $|\kappa| \geq N_c$; it is related to the level k coming from a high-energy Yang-Mills-Chern-Simons theory by $\kappa = k + N_c \text{sign}(k)$.

⁵The number of flavors N_f will always be assumed to be the same in both theories.

The actions of the fermionic and scalar theories include kinetic terms

$$\begin{aligned} S_F(A, \psi) &= \int d^3x \bar{\psi}_{i,b} \not{D}_{ba} \psi^{i,a}, \\ S_B(A, \phi) &= \int d^3x \left(D_\mu^{ba} \phi_{i,a} \right)^\dagger (D_{bc}^\mu \phi^{i,c}). \end{aligned} \quad (2.2)$$

Both theories have a $U(N_f)$ flavor symmetry, and we will assume that any additional interactions also preserve this symmetry.

In order to avoid cumbersome notation, we'll usually drop either the color or flavor index whenever the context is clear. In the following subsections we'll review the allowed interactions, and versions of these theories that include additional auxiliary fields.

2.1 Fermion theories

2.1.1 Regular and Critical Fermions

The theory that includes only the fermion and the CS term is called the Regular Fermion (RF) theory

$$S_{RF}(A, \psi) = S_{CS}(A) + S_F(A, \psi). \quad (2.3)$$

In the 't Hooft large N_c limit, the anomalous dimensions of ψ and of its composites are $O(\frac{1}{N_c})$. Thus, in the large N_c limit this theory has a single relevant operator – the fermion mass term $\bar{\psi}\psi$, which we will fine-tune to zero – and no marginal interactions. Upon fine-tuning the mass to zero the action (2.3) describes a conformal theory. At least at weak coupling, one place where this theory arises is in the IR limit of the QCD-Chern-Simons theory where we add also a Yang-Mills term to (2.3).

To define the critical fermion theories, we introduce a new auxiliary field ζ_j^i , and couple it to the fermion bilinears $M_i^j \equiv \frac{4\pi}{\kappa_F} \bar{\psi}_{c,i} \psi^{c,j}$. Note that in this normalization, at leading order in the 't Hooft large N_c limit, n -point functions of M scale as N_c^{1-n} . At leading order in large N_c , ζ has conformal dimension $\Delta = 1$, so after adding this auxiliary field the large N_c theory has three (for $N_f > 1$) new relevant interactions, ζ_i^i , $(\zeta_i^i)^2$ and $\zeta_i^j \zeta_j^i$, which need to be fine-tuned to get a conformal field theory. On the other hand, the mass term mentioned above is no longer an independent deformation since it is determined by the equation of motion of ζ . In addition, in the large N_c limit there are three different types of marginal ζ^3 deformations, corresponding to different ways of contracting the flavor indices:

$$\mathcal{L}_{int}^F = -\zeta_j^i M_i^j + \frac{\bar{g}_1^F}{3!} (\zeta_i^i)^3 + \frac{\bar{g}_2^F}{2} \zeta_i^i \zeta_j^k \zeta_k^j + \frac{\bar{g}_3^F}{3} \zeta_i^j \zeta_j^k \zeta_k^i. \quad (2.4)$$

The resulting theory (with the three relevant operators appropriately fine-tuned) is called the Critical Fermion (CF) theory

$$S_{CF}(A, \phi, \zeta) = S_{CS}(A) + S_F(A, \psi) + \int d^3x \mathcal{L}_{int}^F. \quad (2.5)$$

In the 't Hooft limit, we need to scale $\bar{g}_n^F \equiv \frac{\bar{\lambda}_n^F \cdot (\lambda_F)^3}{(N_c^F)^2}$, with $\bar{\lambda}_n^F$ finite⁶. In the extreme large N_c limit all three marginal deformations are exactly marginal, but for large finite N_c they

⁶The factor of $(\lambda_F)^3$ in this equation is for later convenience.

acquire beta functions, and our goal in this paper will be to analyze the fixed points and the flow of these beta functions (generalizing the analysis of [25] for $N_f = 1$).

In some cases it's more convenient to write the interaction term in **the representation basis**, such that the $SU(N_f)$ flavor transformations are manifest. We define

$$M_S \equiv M_i^i, \quad (M_A)_i^j \equiv M_i^j - \frac{\delta_i^j}{N_f} M_S, \quad (2.6)$$

and similarly for ζ . We call M_S the singlet structure and M_A the adjoint structure. To distinguish from the representation basis, we call the form (2.4) **the index basis**. The interaction term written in the representation basis is

$$\mathcal{L}_{int}^F = -\frac{1}{N_f} M_S \zeta_S - \text{tr}(M_A \zeta_A) + \frac{g_{SSS}^F}{3!} \zeta_S^3 + \frac{g_{SAA}^F}{2!} \zeta_S \text{tr}(\zeta_A \zeta_A) + \frac{g_{AAA}^F}{3} \text{tr}(\zeta_A \zeta_A \zeta_A), \quad (2.7)$$

where the traces are over the flavor indices, and the relation between the couplings in the index (\bar{g}_n) and in the representation (g_n) basis is given by

$$\begin{aligned} g_{SSS} &= \bar{g}_1 + \frac{3}{N_f} \bar{g}_2 + \frac{2}{N_f^2} \bar{g}_3 & \bar{g}_1 &= g_{SSS} - \frac{3}{N_f} g_{SAA} + \frac{4}{N_f^2} g_{AAA} \\ g_{SAA} &= \bar{g}_2 + \frac{2}{N_f} \bar{g}_3 & \bar{g}_2 &= g_{SAA} - \frac{2}{N_f} g_{AAA} \\ g_{AAA} &= \bar{g}_3 & \bar{g}_3 &= g_{AAA}. \end{aligned} \quad (2.8)$$

Note that for the special case of $N_f = 2$, the trace of three identical adjoints vanishes, so there is no g_{AAA} coupling in this case.

In what follows we'll use both the representation and the index basis. From now on, unless the context demands it, we'll omit the $\text{tr}()$ for brevity, such that any multiplication of the adjoints is assumed to be traced over.

2.1.2 Semi-Critical fermions

The form of (2.7) gives rise to a natural generalization: instead of adding auxiliary fields coupling to both M_A and M_S , we can add a field coupling only to one of them. We call the resulting theories Semi-Critical theories (because only the singlet/adjoint degrees of freedom become critical).

The actions for these theories are given by

$$S_{CF_S}(A, \phi, \zeta_S) = S_{CS}(A) + S_F(A, \psi) + \int d^3x \left(-\frac{1}{N_f} M_S \zeta_S + \frac{g_{SSS}^F}{3!} \zeta_S^3 \right), \quad (2.9a)$$

$$S_{CF_A}(A, \phi, \zeta_A) = S_{CS}(A) + S_F(A, \psi) + \int d^3x \left(-M_A \zeta_A + \frac{g_{AAA}^F}{3!} \zeta_A^3 \right), \quad (2.9b)$$

where we now have just a single interaction term that is marginal at large N_c . In the CF_S theory, the singlet degree of freedom is critical and the adjoint is regular, and vice versa for CF_A . The CF_S theory has (at large N_c) two relevant operators that need to be fine-tuned, ζ_S and ζ_S^2 . The CF_A theory also has (at large N_c) two such operators, which are ζ_A^2 and

M_S . The existence of these fixed points at finite N_c depends on having fixed points for the ζ^3 couplings, and we will analyze this question below in section 7⁷. If we ignore the marginal operators, then we can flow from the CF theory to the CF_S theory by turning on the ζ_A^2 deformation, or to the CF_A theory by turning on the ζ_S^2 deformation, while generic relevant deformations (still fine-tuning the fermion mass to zero) lead to the RF theory. Similarly, we can flow from the CF_A and CF_S theories to the RF theory.

2.2 Scalar theories

2.2.1 The Regular Boson theory

Naively, as in the fermionic case, one would like to define a Regular Boson theory by $S_B + S_{CS}$. This theory would have (in the large N_c limit) three relevant ϕ^2 and ϕ^4 operators that need to be fine-tuned to reach a fixed point. But it also has three marginal deformations (at large N_c), which must be added to the action since for finite N_c they would flow (even if we start without such interactions but only with CS interactions). As in the fermionic case, there are three different ways of contracting the ϕ field indices [27]

$$\mathcal{L}_{int}^B = \frac{\bar{g}_1^B}{3!} (\bar{\phi}_{c,i} \phi^{c,i})^3 + \frac{\bar{g}_2^B}{2} \bar{\phi}_{a,i} \phi^{a,i} \bar{\phi}_{b,j} \phi^{b,k} \bar{\phi}_{c,k} \phi^{c,j} + \frac{\bar{g}_3^B}{3} \bar{\phi}_{a,i} \phi^{a,j} \bar{\phi}_{b,j} \phi^{b,k} \bar{\phi}_{c,k} \phi^{c,i}. \quad (2.10)$$

The simplest bosonic theory that we can write, called the Regular Boson (RB) theory, is thus

$$S_{RB}(A, \phi) = S_{CS}(A) + S_B(A, \phi) + \int d^3x \mathcal{L}_{int}^B. \quad (2.11)$$

As for the CF theories, in some cases it's more convenient to write the interaction terms in the representation basis (see section 2.1.1). We define $\tilde{M}_j^i \equiv \bar{\phi}_{c,j} \phi^{c,i}$, and using the notation of (2.6), we can rewrite the interaction terms in (2.10) as

$$\mathcal{L}_{int}^B = \frac{g_{SSS}^B}{3!} \tilde{M}_S^3 + \frac{g_{SAA}^B}{2!} \tilde{M}_S \text{tr}(\tilde{M}_A \tilde{M}_A) + \frac{g_{AAA}^B}{3} \text{tr}(\tilde{M}_A \tilde{M}_A \tilde{M}_A). \quad (2.12)$$

The relation between the couplings in the index basis $(\bar{g}_1^B, \bar{g}_2^B, \bar{g}_3^B)$ and in the representation basis $(g_{SSS}^B, g_{SAA}^B, g_{AAA}^B)$ is given by (2.8). In the 't Hooft limit, we need to scale $\bar{g}_n^B \equiv \frac{\bar{\lambda}_n^B}{(N_c^B)^2}$, with $\bar{\lambda}_n^B$ finite⁸.

In order to relate this theory to the formalism used for critical theories (as in section 2.1.2), we can rewrite the RB theory in a different way. We introduce two new auxiliary fields: σ , that will act as a Lagrange multiplier, and ζ . We now write

$$\mathcal{L}_{int}^B = \sigma_i^j \tilde{M}_j^i - \sigma_i^j \zeta_j^i + \frac{\bar{g}_1^B}{3!} (\zeta_i^i)^3 + \frac{\bar{g}_2^B}{2} \zeta_i^i \zeta_j^k \zeta_k^j + \frac{\bar{g}_3^B}{3} \zeta_i^j \zeta_j^k \zeta_k^i, \quad (2.13)$$

or equivalently in the representation basis

$$\mathcal{L}_{int}^B = \frac{1}{N_f} \sigma_S \tilde{M}_S + \sigma_A \tilde{M}_A - \frac{1}{N_f} \sigma_S \zeta_S - \sigma_A \zeta_A + \frac{g_{SSS}^B}{3!} \zeta_S^3 + \frac{g_{SAA}^B}{2!} \zeta_S (\zeta_A \zeta_A) + \frac{g_{AAA}^B}{3} (\zeta_A \zeta_A \zeta_A), \quad (2.14)$$

⁷For the special case of $N_f = 2$ there is no g_{AAA} coupling, so the CF_A theory has no marginal operators at large N_c and describes a conformal theory.

⁸Note the difference between the definition of $\bar{\lambda}_n^B$ and the definition of $\bar{\lambda}_n^F$ below (2.5).

where $\zeta_{A/S}$, $\sigma_{A/S}$ and $\tilde{M}_{A/S}$ were defined similarly to $M_{A/S}$ in (2.6). In this way, the theory with the interaction term includes 4 fields $S_{RB}(A, \phi, \sigma, \zeta)$, but it is obviously equivalent to (2.11) after integrating out σ and ζ .

2.2.2 Critical and Semi-Critical Boson theories

Again, the form (2.14) gives rise to a natural generalization. Instead of adding both fields ζ_A and ζ_S to the Lagrangian, we can add either or none of them. The resulting theories are the Semi-Critical or Critical Boson (CB) theories, respectively,

$$S_{CB}(A, \phi, \sigma) = S_{CS}(A) + S_B(A, \phi) + \int d^3x \left(\frac{1}{N_f} \sigma_S \tilde{M}_S + \sigma_A \tilde{M}_A \right), \quad (2.15a)$$

$$S_{CB_A}(A, \phi, \sigma, \zeta_S) = S_{CS}(A) + S_B(A, \phi) + \int d^3x \left(\frac{1}{N_f} \sigma_S \tilde{M}_S + \sigma_A \tilde{M}_A - \frac{1}{N_f} \sigma_S \zeta_S + \frac{g_{SSS}^B}{3!} \zeta_S^3 \right), \quad (2.15b)$$

$$S_{CB_S}(A, \phi, \sigma, \zeta_A) = S_{CS}(A) + S_B(A, \phi) + \int d^3x \left(\frac{1}{N_f} \sigma_S \tilde{M}_S + \sigma_A \tilde{M}_A - \sigma_A \zeta_A + \frac{g_{AAA}^B}{3} \zeta_A^3 \right). \quad (2.15c)$$

Note that in the CB_S theory the singlet degree of freedom is critical, and therefore the marginal interactions involve only the adjoint degrees of freedom⁹ (and vice versa for CB_A). The CB theory has one relevant operator σ_S (of dimension $\Delta = 2$ in the large N_c limit) and no marginal operators. The CB_S theory has two relevant operators, σ_S and ζ_A^2 , and one marginal operator in the large N_c limit. Similarly, the CB_A theory has two relevant operators, ζ_S and ζ_S^2 , and one marginal operator in the large N_c limit.

One can flow from the RB theory to the CB_S , CB_A or CB theories, by turning on ϕ^4 couplings (or ζ^2 couplings in the description (2.13)). We can also formally write the RB (and also $CB_{A/S}$) theory as a Legendre transform of the CB theory, as

$$S_{RB}(A, \phi, \sigma, \zeta) = S_{CB}(A, \phi, \sigma) + \int d^3x \left(-\sigma_i^j \zeta_j^i + \frac{\bar{g}_1^B}{3!} (\zeta_i^i)^3 + \frac{\bar{g}_2^B}{2} \zeta_i^i \zeta_j^k \zeta_k^j + \frac{\bar{g}_3^B}{3} \zeta_i^j \zeta_j^k \zeta_k^i \right). \quad (2.16)$$

2.3 Summary and expected dualities

To summarize, we have presented eight theories: four scalar and four fermionic. The properties of these theories, including their interaction terms, are summarized in table 1. All of the scalar theories and all of the fermionic theories are related, as described above, by renormalization group (RG) flows (or alternatively by Legendre transforms), which are summarized in figure 1¹⁰.

⁹Because $\sigma_{S/A}$ acts as a Lagrange multiplier which sets the composite operators $\tilde{M}_{S/A}$ to zero, we cannot add interactions involving these operators to the Lagrangian.

¹⁰Since the flows involve multi-trace operators made from the scalar operators, the 3-point correlation functions of higher-spin operators will be the same in all of these theories at leading order in $1/N_c$; however, higher-point correlation functions, and higher-order corrections in $1/N_c$, will be different. This is similar to the relation between the RF/CB and CF/RB theories for $N_f = 1$.

Scalars		Fermions		Running Marginal Couplings
RB	(2.14) (see also (2.11))	CF	(2.7)	$g_{SSS}, g_{SAA}, g_{AAA}$
CB_A	$\frac{1}{N_f}\sigma_S\tilde{M}_S + \sigma_A\tilde{M}_A - \frac{1}{N_f}\sigma_S\zeta_S + \frac{g_{SSS}^B}{3!}\zeta_S^3$	CF_S	$-\frac{1}{N_f}M_S\zeta_S + \frac{g_{SSS}^F}{3!}\zeta_S^3$	g_{SSS}
CB_S	$\frac{1}{N_f}\sigma_S\tilde{M}_S + \sigma_A\tilde{M}_A - \sigma_A\zeta_A + \frac{g_{AAA}^B}{3}\zeta_A^3$	CF_A	$-M_A\zeta_A + \frac{g_{AAA}^F}{3}\zeta_A^3$	g_{AAA}
CB	$\frac{1}{N_f}\sigma_S\tilde{M}_S + \sigma_A\tilde{M}_A$	RF	<i>none</i>	<i>none</i>

Table 1. The different theories considered in this paper and their interaction terms. The two theories on each row are conjectured to be dual, as explained in the text.

There is strong evidence that there is a duality in the 't Hooft limit between the $CB \leftrightarrow RF$ theories [2–4, 28–39], with σ_i^j dual to M_i^j . While this has mostly been studied for $N_f = 1$, the same evidence holds also for larger finite values of N_f in the 't Hooft limit. It has been conjectured [3, 4] that this duality is true even at finite N_c , although this is not as well established. Given that the different theories are related (at least at large N_c) by Legendre transforms, a duality between the $CB \leftrightarrow RF$ theories (the last row in table 1) implies dualities between the $RB \leftrightarrow CF$ theories and between the $CB_{A/S} \leftrightarrow CF_{S/A}$ theories (the other rows of the table, note the exchange of subscript A and S). Of course, the existence of the fixed points on the first three lines depends on having fixed points for their marginal couplings, which we will investigate in detail below; we conjecture that any fixed point for the scalar theories is dual to a corresponding fixed point for the fermionic theories.

The relation between the Chern-Simons couplings and level between the dual theories is¹¹:

$$\lambda_F = \begin{cases} \lambda_B - 1 & \lambda_B > 0 \\ 1 + \lambda_B & \lambda_B < 0 \end{cases}, \quad \kappa_F = -\kappa_B. \quad (2.17)$$

This is a strong-weak duality with respect to the gauge interaction, which can help us understand the behavior of the theories at regimes where perturbation theory is no longer valid. Naively we would expect the couplings g_n^F to map to g_n^B under the duality, but this is subtle because the dual RF and CB theories have different contact terms, and for $N_f = 1$ it was found [25] that this leads to a relative shift by a constant between g_{SSS}^F and g_{SSS}^B (the only coupling that exists in that case). Similar shifts for one or more of the g_n presumably are present also for $N_f > 1$. Since shifting the coefficient by a constant does not change the structure of the β function, which is our main topic in this paper, this will not affect our discussion below. In any case, we will not use the duality in most of our analysis, except when trying to interpolate the behavior of the fixed points between weak and strong coupling (in either set of variables). The theories discussed above are also conjectured to be dual to high-spin gravity theories (that are generalizations of Vasiliev's

¹¹This implies that N_c must also change under this duality, and in the theories above there is N_c^B for scalars and N_c^F for fermions.

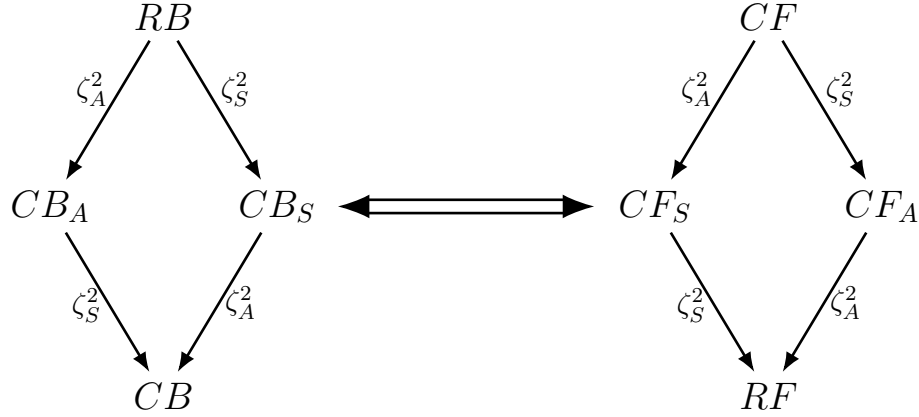


Figure 1. The RG flows between the theories discussed in this section are depicted, with arrows labeled by the relevant operators that are turned on to generate them. The lowest relevant operator, ζ_S , is fine-tuned to the fixed point throughout these flows; turning it on leads to a flow to a pure CS theory.

high-spin gravity, in which all the bulk fields are adjoints of $U(N_f)$, but we will not use this here.

3 Review of the $N_f = 1$ results and formalism

The case of $N_f = 1$ was extensively studied in [25], where a formalism was developed for computing the beta function for the marginal coupling, that will also be useful for the current computations.

In this section we'll briefly review the formalism and the results for the $N_f = 1$ case, and in the following sections we'll present the generalization to arbitrary N_f . For the $N_f = 1$ case the theories presented in section 2 are significantly simplified: there is no adjoint structure (see, e.g., (2.6)), and therefore there is only one running coupling g_{SSS} . Moreover, the Semi-Critical theories do not exist, so we can consider only the RB and CF theories.

3.1 General formalism

The main idea of the formalism presented in [25] is to compute an effective action for the field ζ , which can be expressed for the CF theory in terms of expectation values of M 's in the RF theory, and for the RB theory in terms of expectation values of σ 's in the CB theory. Then, we can use this effective action to compute the order $\frac{1}{N_c}$ correction to the 2 and 3-point correlation functions for ζ , from which we derive the beta function. The effective action for ζ takes the form

$$S^{eff}(\zeta) = \frac{g_{SSS}}{3!} \int \zeta^3 d^3x - \sum_{n=2}^{\infty} \frac{1}{n!} \int d\Pi_n \left\langle \tilde{J}(-p_1) \cdots \tilde{J}(-p_n) \right\rangle_{\text{connected}} \zeta(p_1) \cdots \zeta(p_n) \quad (3.1)$$

with

$$d\Pi_n \equiv (2\pi)^3 \delta \left(\sum_{i=1}^n p_i \right) \prod_{i=1}^n \frac{d^3 p_i}{(2\pi)^3}, \quad (3.2)$$

and \tilde{J} representing σ (in the CB theories) or M (in the RF theories).

In the CF case one can compute the expectation values for $M = \frac{4\pi}{\kappa_F} \bar{\psi} \psi$ using the Feynman rules that are derived from the RF theory (2.3). In the RB case the situation is more delicate, as the expectation values should be evaluated in the CB theory (2.15a). σ is then also a field, so one needs first to compute the effective action for σ and then, using this new action, to compute the effective action for ζ .

It can be shown that in the 't Hooft limit the leading contribution (of order $\frac{1}{N_c}$) to the beta function come from 1-loop diagrams in ζ , contributing to its 3-point function, and therefore one needs to compute the sum in (3.1) only up to $n = 5$. The result is

$$\begin{aligned} S^{eff}(\zeta) = & \frac{G_2}{2} \int \frac{d^3 q}{(2\pi)^3} |q| \left| \frac{q}{\Lambda} \right|^{2\gamma} \zeta(q) \zeta(-q) \\ & + \frac{G_3}{3!} \int \frac{d^3 q_1}{(2\pi)^3} \frac{d^3 q_2}{(2\pi)^3} \frac{d^3 q_3}{(2\pi)^3} (2\pi)^3 \delta(q_1 + q_2 + q_3) \zeta(q_1) \zeta(q_2) \zeta(q_3) \\ & + \frac{\delta G_3}{3!} \int \frac{d^3 q_1}{(2\pi)^3} \frac{d^3 q_2}{(2\pi)^3} \frac{d^3 q_3}{(2\pi)^3} (2\pi)^3 \delta(q_1 + q_2 + q_3) \log \left(\frac{\Lambda}{|q_1| + |q_2| + |q_3|} \right) \zeta(q_1) \zeta(q_2) \zeta(q_3) \\ & - \frac{1}{4!} \int d\Pi_4 G_4(q_1, q_2, q_3, q_4) \zeta(q_1) \zeta(q_2) \zeta(q_3) \zeta(q_4) \\ & - \frac{1}{5!} \int d\Pi_5 G_5(q_1, q_2, q_3, q_4, q_5) \zeta(q_1) \zeta(q_2) \zeta(q_3) \zeta(q_4) \zeta(q_5), \end{aligned} \quad (3.3)$$

where Λ is the UV cut-off used in the regularization, γ is the anomalous dimension of \tilde{J} , and it was useful to write explicitly the momentum dependence of the 2 and 3 point functions. The momentum dependence of the 5 and 4-point functions is important only in a special kinematic limit, for which it is given by¹²

$$G_4(p, -p, k, -k) = \tilde{G}_4 \left[-\frac{2}{|p|} + \frac{|k|}{|p|^2} + \frac{(p \cdot k)^2}{|p|^4 |k|} + \mathcal{O}\left(\frac{k^2}{p^3}\right) \right] \quad \text{for } p \gg k, \quad (3.4a)$$

$$G_5(p, -p, 0, 0, 0) = \frac{\tilde{G}_5}{p^2}. \quad (3.4b)$$

The leading large N_c scaling of the various coefficients is given by

$$G_2 = \mathcal{O}\left(\frac{1}{N_c}\right), \quad \gamma = \mathcal{O}\left(\frac{1}{N_c}\right), \quad G_3 = \mathcal{O}\left(\frac{1}{N_c^2}\right), \quad \delta G_3 = \mathcal{O}\left(\frac{1}{N_c^3}\right), \quad \tilde{G}_4 = \mathcal{O}\left(\frac{1}{N_c^3}\right), \quad \tilde{G}_5 = \mathcal{O}\left(\frac{1}{N_c^4}\right). \quad (3.5)$$

Using this action one can first compute the anomalous dimension of ζ by computing the 1-loop corrections to the 2-point correlation function, as shown in figure 2, and find that it is given by

$$\gamma' = \gamma + \frac{\tilde{G}_4}{6\pi^2 G_2^2}. \quad (3.6)$$

¹²More precisely we take $G_5(p, -p - p_1 - p_2 - p_3, p_1, p_2, p_3)$ with $|p| \gg |p_1|, |p_2|, |p_3|$.

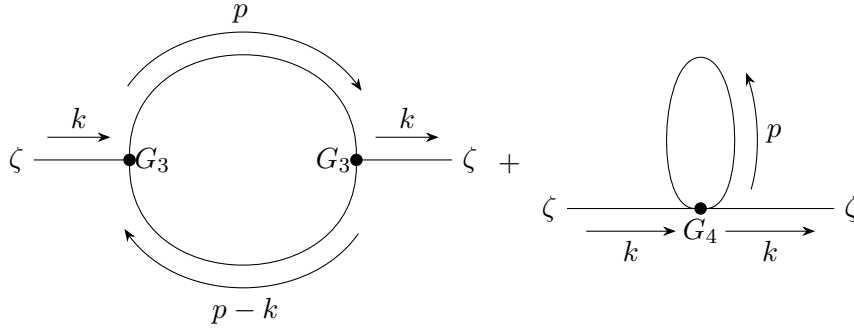


Figure 2. Feynman diagrams that contribute to the 2-point function of ζ . The left diagram doesn't have a logarithmic divergence in the cutoff Λ and therefore does not contribute to the anomalous dimension γ' . In order to extract the logarithmic divergence of the right diagram, only the kinematical region of (3.4) is needed.

Computing the amputated 3-point correlation function, as shown in figure 3, and using the Callan-Symanzik equation we can then find the beta function for G_3 in terms of G_n and γ as

$$\beta(g_{SSS}) = \left(\frac{\tilde{G}_5}{4\pi^2 G_2} - \delta G_3 \right) - G_3 \left(-\frac{3\tilde{G}_4}{2\pi^2 G_2^2} + 3\gamma' \right) - \frac{G_3^3}{2\pi^2 G_2^3}. \quad (3.7)$$

Note that in the large N_c limit G_3 is of order $\frac{1}{N_c^2}$, while each term on the right-hand side (using (3.5)) is $O\left(\frac{1}{N_c^3}\right)$, such that the beta function is suppressed by $\frac{1}{N_c}$. Equation (3.7) contains this leading contribution in $\frac{1}{N_c}$, exactly as a function of the 't Hooft couplings λ_{SSS} and λ . G_3 is equal to g_{SSS} up to a constant (that differs for fermions and bosons), this means that the beta function for g_{SSS} will be a cubic polynomial, with a negative coefficient for the third power (since G_2 is always positive from unitarity).

Illustrations of the possible beta functions (3.7) are given in figure 4. Generically, there are either one or no stable points in the IR, and either one or two fixed points in the UV.

3.2 The beta function in the perturbative region

Some of the values of the correlation functions G_n are known in the literature to all orders in the coupling λ , while others are known either only to leading order or in a specific kinematic limit (see [25] for a full summary of the known results). The values at $\lambda_{B/F} = 0$ ¹³ are shown in Table 2¹⁴. We can now substitute these values in (3.7) to find the CF and RB beta functions in these limits.

¹³For fermions we take the limit $\lambda_F \rightarrow 0$, using λ_{SSS}^F as defined in section 2.1.1.

¹⁴The relation between the notation used here and in [25] can be read off by comparing the action (3.3) with (3.17) there. Care must be taken in relating the signs of different factors between the fermionic and bosonic theories, e.g. in the notation of [25] $\gamma'_B = \frac{\delta'_B}{\kappa_B}$ but $\gamma'_F = -\frac{\delta'_F}{\kappa_F}$, which can be checked by requiring the duality (2.17) to hold.

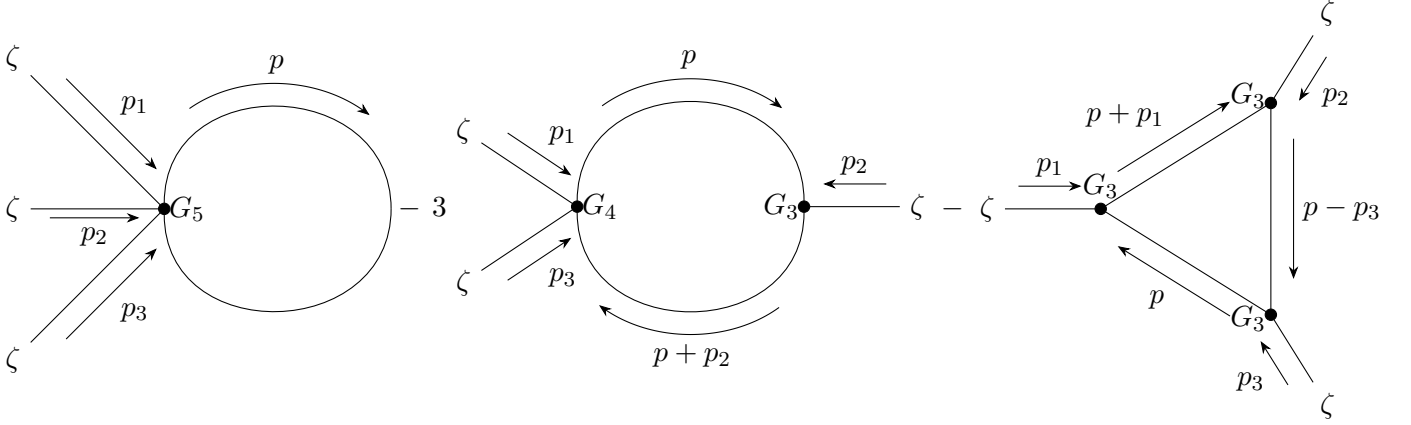


Figure 3. Feynman diagrams that contribute to the amputated 3-point function of ζ . Together with the tree level diagram for δG_3 and the anomalous dimension, they contribute to the beta function (3.7). It can be seen that for beta function computations, only the kinematic region in (3.4) contributes.

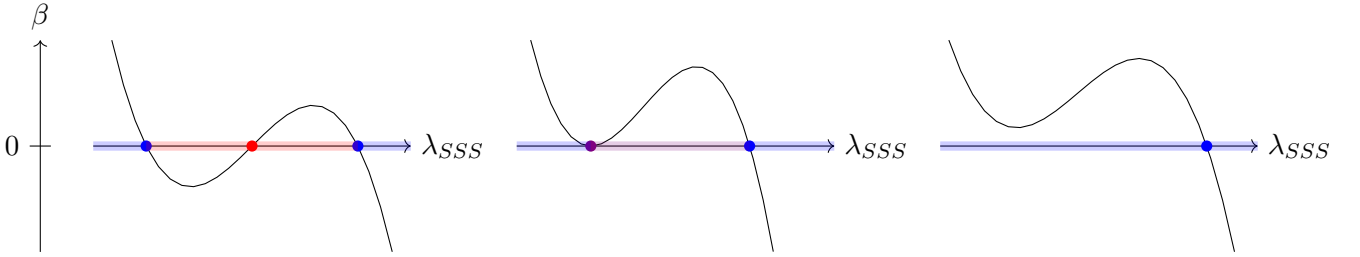


Figure 4. Illustrations of the three possibilities for the beta function in (3.7). UV fixed points are denoted in blue, and IR fixed points in red. Points denoted by blue on the horizontal axis flow to (plus or minus) infinite coupling in the IR, while points denoted by red flow to the IR fixed point. The middle case corresponds to a non generic case, which under small perturbations will result in either the left or right cases. The purple point is a stable fixed point in the IR from one direction, and points denoted by purple on the horizontal axis flow in the IR to this point.

The beta function for the CF theory with $\lambda_F = 0$ is

$$\beta(\lambda_{SSS}^F) = \frac{1}{\pi^2 N_c^F} \left[32\lambda_{SSS}^F - (\lambda_{SSS}^F)^3 \frac{1}{16\pi^6} \right]. \quad (3.8)$$

This beta function has three roots and corresponds to the case on the left in figure 4. The IR fixed point $\lambda_{SSS}^F = 0$ has a finite domain of attraction $\lambda_{SSS}^F \in (-16\sqrt{2}\pi^3, 16\sqrt{2}\pi^3)$, and so turning on a finite small λ_F will not alter the number or type of fixed points.

The situation for the bosons is somewhat more complicated. The values of \tilde{G}_5 and

Coupling	Bosons	Fermions
G_2	$\frac{8}{\lambda_B \kappa_B}$	$2\pi^2 \frac{\lambda_F}{\kappa_F}$
G_3	$g_{SSS}^B - \frac{128}{(N_c^B)^2}$	g_{SSS}^F
δG_3	see (3.9)	0
\tilde{G}_4	$\frac{2^{11}}{\lambda_B^3 \kappa_B^3}$	$\frac{\lambda_F}{2\kappa_F^3} (4\pi)^4$
\tilde{G}_5	see (3.9)	0
γ	$-\frac{16}{3\pi^2 \lambda_B \kappa_B}$	0
γ'	0	$\frac{16}{3\pi^2 \lambda_F \kappa_F}$

Table 2. The known values of G_n , γ and γ' in the limits $\lambda_{B/F} \rightarrow 0$ [2, 25, 40–45]. For the fermions with $\lambda_F = 0$, \tilde{G}_3 and \tilde{G}_5 vanish due to parity. The vanishing of γ' for bosons and γ for fermions in the appropriate limits can be understood because the RB and RF theories are free as $\lambda_{B/F} \rightarrow 0$.

δG_3 are unknown in that case¹⁵. However, they are related in the limit $\lambda_B = 0$ by¹⁶

$$\frac{\tilde{G}_5}{4\pi^2 G_2} - \delta G_3 \stackrel{\lambda_B=0}{=} \frac{4096}{N_B^3 \pi^2}. \quad (3.9)$$

In this formalism, this is due to the fact that both \tilde{G}_5 and δG_3 get contributions from the same set of diagrams (see Appendix B in [25]). Plugging this into (3.7) and expressing the result in term of λ_{SSS}^B (as defined in section 2.2.1) we find¹⁷

$$\beta(\lambda_{SSS}^B) = \frac{3}{8\pi^2 N_c^B} (\lambda_{SSS}^B)^2 \left[1 - \frac{\lambda_{SSS}^B}{384} \right]. \quad (3.10)$$

This beta function has a double root at $\lambda_{SSS}^B = 0$, which corresponds to the middle case in figure 4 (the other root is at $\lambda_{SSS}^B = 384$ and is UV stable). A small perturbation making λ_B finite can therefore either create an IR-stable point, or remove this fixed point completely.

In order to understand which of these options is realized, one must consider finite λ_B . This was done for finite N_c directly in the RB formalism (2.11) in the region $\lambda_B^2 \sim \lambda_{SSS}^B \ll 1$ [48–50]¹⁸. The beta function for small λ_{SSS}^B was found to be

$$\beta(\lambda_{SSS}^B) = \frac{1}{N_c^B \pi^2} \left[\frac{3}{2} \left(\frac{\lambda_B}{4\pi} \right)^4 - \frac{5}{2} \lambda_{SSS}^B \left(\frac{\lambda_B}{4\pi} \right)^2 + \frac{3}{8} (\lambda_{SSS}^B)^2 \right]. \quad (3.11)$$

¹⁵It was conjectured that once \tilde{G}_5 is computed for $\lambda_B = 0$ it will be possible to interpolate it to arbitrary values of λ [46].

¹⁶The easiest way to see this is to note that due to the fact that the $N_f = 1$ version of (2.11) is free when $\lambda_B = 0$ and $g_{SSS}^B = 0$, the beta function should also vanish at this point, and this completely determines the constant part of (3.7). Thus, even though \tilde{G}_5 is unknown, it will not play a role in this case.

¹⁷This result can also be obtained directly from (2.11) in the usual way [47].

¹⁸This was first done in [48]. Later, [49] presented a simplified version for $SO(N_c)$, which were expanded for other gauge groups (including $U(N_c)$) in [50] (note a small typo in the prefactor of λ^4 in equation (9) of [49], which is fixed in equation (3.1) in [50] for the $SO(N_c)$ case. The $SU(N_c)$ case is given, to leading order in N_c , by a factor of two compared to equation (3.1) in [50]. The prefactor in (3.2) in [50] for $U(N_c)$ is a mistake, as evident by explicitly summing all the diagram. See Appendix B in [50]). In terms of their notation $\frac{\lambda_B}{4\pi} = \lambda$, $\lambda_{SSS}^B = \lambda_6$, and we only take leading order in $\frac{1}{N_c}$. As mentioned above, in the 't Hooft limit the beta function is the same for $SU(N_c)$ and $U(N_c)$ gauge groups, up to a factor of 2.

The $\lambda_{SSS}^B = 0$ fixed point is thus split to $\lambda_{SSS}^B = \frac{2}{3} \left(\frac{\lambda_B}{4\pi} \right)^2$ and $\lambda_{SSS}^B = 6 \left(\frac{\lambda_B}{4\pi} \right)^2$, with the second one an IR-stable fixed point.

3.3 Discussion and hypothesis in the non-perturbative regime

Using the RB-CF duality mentioned in section 2.3 we can view these beta functions as the limits of the beta function of the same theory as $\lambda \rightarrow 0, 1$. Both beta functions have 2 UV stable fixed points and one IR-stable fixed point. This, together with other considerations, led the authors of [25] to conjecture that there is an IR-stable fixed point for **any** intermediate value of λ .

We can also see from the beta functions that the size of the region which flows to the IR-stable point stays finite even as $\lambda_B \rightarrow 0$, and therefore landing on this point does not require substantial fine tuning (in figure 4 this corresponds to a finite length of the purple region). This region is always compact, bounded between the two UV stable points.

In the following we'll find that some of the features mentioned above carry over also to the $N_f > 1$ cases. In particular, we'll find degenerate roots of the beta functions in the RB theories as $\lambda_B \rightarrow 0$, so we'll need to generalize the small λ_B computation there, while the critical (and Semi-Critical) theories do not have such a degeneracy. In contrast, the behavior of the IR-stable fixed points and the region that flows to them will be very different for $N_f > 1$.

4 Beta function structure for multiple flavors

Chern-Simons-matter theories with multiple flavors have several marginal interactions (see (2.4) and (2.10)), which leads to intricate beta functions. In this section, we analyze (to leading order in $\frac{1}{N_c}$) the generic structure of the beta functions of the marginal couplings for the CF (2.5) and RB (2.11) theories.

The crucial observation is that to leading order in $\frac{1}{N_c}$, *the diagrams which contribute to the beta functions in the $N_f > 1$ case are the same as in the $N_f = 1$ case*, the only difference is that the interaction vertices acquire additional flavor index structure¹⁹. We can thus use similar tools to those presented in section 3, focusing on the effective action of the ζ_j^i fields.

The section is organized as follow: In section 4.1 we present the effective action of the ζ_j^i , and parameterize its coefficients. In section 4.2 we present the calculation of the anomalous dimensions and of the beta functions. In section 4.3 we analyze the structure of the beta functions, and general features which can be extracted from their form. Finally, in section 4.4, we discuss the limit of a large number of flavors $N_f \rightarrow \infty$ (but still with $N_f \ll N_c$).

¹⁹The momentum dependence of the diagrams, as well as the order of $\frac{1}{N_c}$ at which each diagram contributes, stays the same.

4.1 Effective action for multiple flavors

4.1.1 General structure

Our first step, in both the CF and RB theories, is to write the path integral in terms of the ζ_j^i fields only, integrating out all other fields. Generalizing the $N_f = 1$ case above, the effective action of ζ_j^i takes the form

$$S^{eff}(\zeta_j^i) = \int d^3x \left[\frac{\bar{g}_1}{3!} (\zeta_i^i)^3 + \frac{\bar{g}_2}{2} \zeta_i^i \zeta_j^k \zeta_k^j + \frac{\bar{g}_3}{3} \zeta_i^j \zeta_j^k \zeta_k^i \right] - \sum_{n=2}^{\infty} \frac{1}{n!} \int d\Pi_n \left\langle \tilde{J}_{i_1}^{j_1}(-p_1) \cdots \tilde{J}_{i_n}^{j_n}(-p_n) \right\rangle_{\text{connected}} \zeta_{j_1}^{i_1}(p_1) \cdots \zeta_{j_n}^{i_n}(p_n), \quad (4.1)$$

where \tilde{J}_i^j represents σ_i^j (in the scalar case) or M_i^j (in the fermionic case).

In the 't Hooft limit, the leading contribution to the beta functions of the marginal couplings is of order $\frac{1}{N_c}$. As in the $N_f = 1$ case, we then need to expand the sum in (4.1) only up to $n = 5$, so that it can be rewritten as

$$S^{eff}(\zeta) = \frac{1}{2} \int \frac{d^3q}{(2\pi)^3} |q| \left((G_2)_{i_1, i_2}^{j_1, j_2} + (\delta G_2)_{i_1, i_2}^{j_1, j_2} \log\left(\frac{q}{\Lambda}\right) \right) \zeta_{j_1}^{i_1}(q) \zeta_{j_2}^{i_2}(-q) + \frac{1}{3!} \int d\Pi_3 (G_3)_{i_1, i_2, i_3}^{j_1, j_2, j_3}(p_1, p_2, p_3) \zeta_{j_1}^{i_1}(p_1) \zeta_{j_2}^{i_2}(p_2) \zeta_{j_3}^{i_3}(p_3) + \frac{1}{3!} \int d\Pi_3 (\delta G_3)_{i_1, i_2, i_3}^{j_1, j_2, j_3}(p_1, p_2, p_3) \log\left(\frac{\Lambda}{|p_1| + |p_2| + |p_3|}\right) \zeta_{j_1}^{i_1}(p_1) \zeta_{j_2}^{i_2}(p_2) \zeta_{j_3}^{i_3}(p_3) - \frac{1}{4!} \int d\Pi_4 (G_4)_{i_1, i_2, i_3, i_4}^{j_1, j_2, j_3, j_4}(p_i) \zeta_{j_1}^{i_1}(p_1) \zeta_{j_2}^{i_2}(p_2) \zeta_{j_3}^{i_3}(p_3) \zeta_{j_4}^{i_4}(p_4) - \frac{1}{5!} \int d\Pi_5 (G_5)_{i_1, i_2, i_3, i_4, i_5}^{j_1, j_2, j_3, j_4, j_5}(p_i) \zeta_{j_1}^{i_1}(p_1) \zeta_{j_2}^{i_2}(p_2) \zeta_{j_3}^{i_3}(p_3) \zeta_{j_4}^{i_4}(p_4) \zeta_{j_5}^{i_5}(p_5), \quad (4.2)$$

where the \bar{g}_n couplings in (4.1) are inserted into $(G_3)_{i_1, i_2, i_3}^{j_1, j_2, j_3}$ in the second line of (4.2). This is the generalization of (3.3)²⁰.

The coefficients $(G_n)_{i_1, \dots, i_n}^{j_1, \dots, j_n}(p_1, \dots, p_n)$ in (4.2) can be greatly simplified in our limits, since for each coefficient we consider only its leading order in $\frac{1}{N_c}$. In the following discussion, we concentrate on their parametrization in the CF theory, with the conclusions being the same for the RB theory.

4.1.2 Parameterizing G_2 and δG_2

The two-point function of two mesons in the CF theory is given by a sum of diagrams with two distinct ‘topologies’, shown in figure 5. In one type of diagrams (on the left-hand side), the fermion line which starts with flavor index j_1 (j_2), connects to the flavor index i_2 (i_1); this results in a contribution to the two-point function with the flavor structure $\delta_{i_2}^{j_1} \delta_{i_1}^{j_2}$. Note that the only fermion interactions in the RF theory are with gluons, and those preserve the flavor index, and so it is valid to assign a flavor to a fermion line. Diagrams

²⁰The anomalous dimension γ in (3.3) is expressed here as $\delta G_2 = 2G_2\gamma$ for $N_f = 1$.

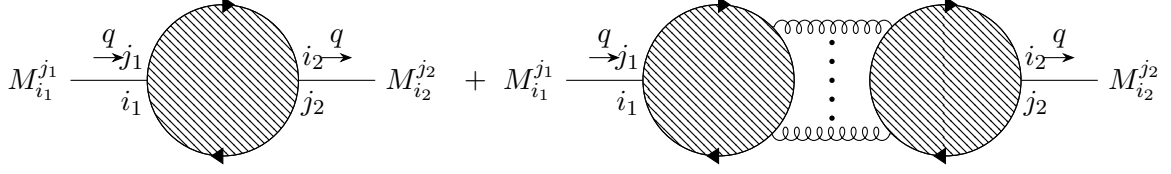


Figure 5. Two ‘topologies’ contributing to the 2-point function (4.3). The shaded area includes possible gluon lines and interactions (the diagram on the right is schematic and actually there can be many different types of gluon structures). The diagrams on the right start at one higher order in $\frac{1}{N_c}$ in the ’t Hooft large N_c limit.

like this start at order $\frac{1}{N_c}$, when the gluon diagram filling the disk in figure 5 is planar and there are no extra fermion loops [51]. For the second type of diagrams (on the right-hand side in the figure), the fermion line connects each meson to itself, resulting in the structure $\delta_{i_1}^{j_1} \delta_{i_2}^{j_2}$. These diagrams start with “annulus diagrams” of order $\frac{1}{N_c^2}$.

Since we are interested only in the leading order result of $\frac{1}{N_c}$, we can take the structure of the two-point function to be of the form²¹

$$(G_2)_{i_1, i_2}^{j_1, j_2} = G_2 \delta_{i_2}^{j_1} \delta_{i_1}^{j_2}, \quad (4.3)$$

where by dimensional analysis, G_2 is constant²².

However, we are interested also in δG_2 , which is suppressed compared to G_2 by an extra factor of $\frac{1}{N_c}$. Thus, both types of diagrams can contribute to δG_2 , and we parameterize it by

$$(\delta G_2)_{i_1, i_2}^{j_1, j_2} = 2G_2 \gamma_A \delta_{i_1}^{j_2} \delta_{i_2}^{j_1} + 2\frac{G_2}{N_f} (\gamma_S - \gamma_A) \delta_{i_1}^{j_1} \delta_{i_2}^{j_2}, \quad (4.4)$$

where we explain the subscripts in $\gamma_{A/S}$ below. Once again, $\gamma_{A/S}$ are constants and do not depend on the momentum, by dimensional analysis.

The general classification by ‘topologies’ for the diagrams can be extended to $n > 2$. More concretely, for any n , the leading contribution at large N_c comes only from diagrams where all the fermion lines exiting the mesons are connected (in some cyclic order) along a single fermion loop, as in figure 6. A diagram in which there are several connected pieces gives a subleading contribution, with each added ‘connected’ piece reducing the contribution of this diagram by a factor of $\frac{1}{N_c}$.

Before continuing to $n > 2$, we have two comments. First, since (4.3) is diagonal at leading order in $\frac{1}{N_c}$, it is easy to find the propagator of the ζ fields to leading order in $\frac{1}{N_c}$,

$$(G_2^{-1})_{j_1, j_2}^{i_1, i_2}(q) \equiv \left\langle \zeta_{j_1}^{i_1}(q) \zeta_{j_2}^{i_2}(-q) \right\rangle = \frac{1}{|q| G_2} \delta_{j_2}^{i_1} \delta_{j_1}^{i_2}. \quad (4.5)$$

We will use (4.5) in evaluating the Feynman diagrams below.

²¹Note that here, and in the following, we leave the dependence on $\lambda_{F/B}$ implicit in the parametrization.

²²Note that G_2 is actually known for any value of $\lambda_{B/F}$. This follows from the fact that only the planar diagrams (left diagram in figure 5) contribute to G_2 in leading order, and this diagram is the same as for the single flavor case, which is known in the literature [2, 25].

Second, the theory preserves the $SU(N_f)$ flavor symmetry, and quantities multiplying $\zeta_{j_1}^{i_1}$ can be written in terms of the representation basis. For two ζ fields

$$\left(a\delta_{i_1}^{j_2}\delta_{i_2}^{j_1} + b\delta_{i_1}^{j_1}\delta_{i_2}^{j_2}\right)\zeta_{j_1}^{i_1}\zeta_{j_2}^{i_2} = a(\zeta_A)_j^i(\zeta_A)_i^j + \left(\frac{a}{N_f} + b\right)\zeta_S\zeta_S, \quad (4.6)$$

and so using the parametrization in (4.3) and (4.4), the first line of the effective action (4.2) can be written as

$$\left((G_2)_{i_1,i_2}^{j_1,j_2} + (\delta G_2)_{i_1,i_2}^{j_1,j_2} \log\left(\frac{q}{\Lambda}\right)\right)\zeta_{j_1}^{i_1}\zeta_{j_2}^{i_2} = G_2\left(\frac{q}{\Lambda}\right)^{2\gamma_A}(\zeta_A)_j^i(\zeta_A)_i^j + \frac{G_2}{N_f}\left(\frac{q}{\Lambda}\right)^{2\gamma_S}\zeta_S\zeta_S. \quad (4.7)$$

We see that γ_A and γ_S can be identified with the ‘classical’ anomalous dimension of the ζ_A and ζ_S fields (classical in the sense that ζ loops have not been taken into account).

4.1.3 Parameterizing G_3 and δG_3

For $n = 3$, we have three different possible structures of flavor indices. The general G_3 can therefore be written as

$$(G_3)_{i_1,i_2,i_3}^{j_1,j_2,j_3} = \left[\begin{array}{c} \bar{G}_{3,1}\left(\delta_{i_1}^{j_1}\delta_{i_2}^{j_2}\delta_{i_3}^{j_3}\right) + \\ \bar{G}_{3,2}\left(\delta_{i_1}^{j_1}\delta_{i_2}^{j_3}\delta_{i_3}^{j_2} + \delta_{i_2}^{j_2}\delta_{i_1}^{j_3}\delta_{i_3}^{j_1} + \delta_{i_3}^{j_3}\delta_{i_1}^{j_2}\delta_{i_2}^{j_1}\right) + \\ \bar{G}_{3,3}\left(\delta_{i_1}^{j_2}\delta_{i_2}^{j_3}\delta_{i_3}^{j_1} + \delta_{i_1}^{j_3}\delta_{i_2}^{j_1}\delta_{i_3}^{j_2}\right) \end{array} \right]. \quad (4.8)$$

Following the previous discussion, the leading order large N_c contributions from the correlation functions of mesons appear only in $\bar{G}_{3,3}$. We thus find

$$\bar{G}_{3,1} = \bar{g}_1, \quad \bar{G}_{3,2} = \bar{g}_2, \quad \bar{G}_{3,3} = \bar{g}_3 - \left\langle \tilde{J}_1^2(-p_1)\tilde{J}_2^3(-p_2)\tilde{J}_3^1(-p_3) \right\rangle_{\text{leading}}. \quad (4.9)$$

For δG_3 , we are interested in coefficients with a factor of $\frac{1}{N_c}$ compared to G_3 , and so we can write

$$(\delta G_3)_{i_1,i_2,i_3}^{j_1,j_2,j_3} = \delta\bar{G}_{3,2}\left(\delta_{i_1}^{j_1}\delta_{i_2}^{j_3}\delta_{i_3}^{j_2} + \delta_{i_2}^{j_2}\delta_{i_1}^{j_3}\delta_{i_3}^{j_1} + \delta_{i_3}^{j_3}\delta_{i_1}^{j_2}\delta_{i_2}^{j_1}\right) + \delta\bar{G}_{3,3}\left(\delta_{i_1}^{j_2}\delta_{i_2}^{j_3}\delta_{i_3}^{j_1} + \delta_{i_1}^{j_3}\delta_{i_2}^{j_1}\delta_{i_3}^{j_2}\right), \quad (4.10)$$

where we implicitly used $\delta\bar{G}_{3,1} = 0$ since its calculation contains three disconnected pieces, so it not at the order in $\frac{1}{N_c}$ that we are interested in.

The parametrization adopted in (4.9) and (4.10) is natural within the index basis, which is more convenient for explicit calculations. However, for the purposes of presentation and gaining conceptual insight, it is more advantageous to write the beta functions in the representation basis, with the transformation given in (2.8). To facilitate the understanding of the results, in the following we use $G_{SSS}, G_{SAA}, G_{AAA}$ instead of $\bar{G}_{3,1}, \bar{G}_{3,2}, \bar{G}_{3,3}$ and $\delta G_{SSS}, \delta G_{SAA}, \delta G_{AAA}$ instead of $\delta\bar{G}_{3,1}, \delta\bar{G}_{3,2}, \delta\bar{G}_{3,3}$.

4.1.4 Parameterizing G_4 and G_5

For $n = 4$ we need only the leading order results, which means only diagrams with one ‘connected’ piece, and only in a specific momentum limit (we want $(G_4)_{i_1,i_2,i_3,i_4}^{j_1,j_2,j_3,j_4}(p, -p, k, -k)$

in the limit $|p| \gg |k|$). By dimensional analysis, at the leading and first subleading orders in $\frac{1}{|p|}$, there can be only three momentum terms which contribute: $\frac{1}{|p|}$, $\frac{|k|}{|p|^2}$, $\frac{(p \cdot k)^2}{|p|^4 |k|}$, as in (3.4)²³. However, here there is a slight complication: once we fix the momenta of the different operators, different flavor structures correspond to different diagrams. This is evident in the examples in figure 6. The diagram on the left is proportional to $\delta_{i_2}^{j_1} \delta_{i_3}^{j_2} \delta_{i_4}^{j_3} \delta_{i_1}^{j_4}$, and the diagram on the right to $\delta_{i_3}^{j_1} \delta_{i_2}^{j_2} \delta_{i_4}^{j_3} \delta_{i_1}^{j_4}$. Each structure will have a different momentum dependence, and so we assign different coefficients to them. There is a symmetry of taking $p \rightarrow -p$ and $k \rightarrow -k$, and so in total there are only 2 options – either p is ‘near’ $-p$ (left diagram) or p is ‘far’ from $-p$ (right diagram). We conclude that the general structure of G_4 is²⁴

$$(G_4)_{i_1, i_2, i_3, i_4}^{j_1, j_2, j_3, j_4}(p, -p, k, -k) = \frac{1}{|p|} \left(\frac{|k|}{|p|} \left(G_{4,1,N} \left(\delta_{i_2}^{j_1} \delta_{i_3}^{j_2} \delta_{i_4}^{j_3} \delta_{i_1}^{j_4} + \delta_{i_2}^{j_1} \delta_{i_4}^{j_2} \delta_{i_3}^{j_3} \delta_{i_1}^{j_4} + \delta_{i_1}^{j_2} \delta_{i_3}^{j_1} \delta_{i_4}^{j_3} \delta_{i_2}^{j_4} + \delta_{i_1}^{j_2} \delta_{i_4}^{j_1} \delta_{i_3}^{j_3} \delta_{i_2}^{j_4} \right) + G_{4,1,F} \left(\delta_{i_3}^{j_1} \delta_{i_2}^{j_2} \delta_{i_4}^{j_3} \delta_{i_1}^{j_4} + \delta_{i_4}^{j_1} \delta_{i_2}^{j_2} \delta_{i_3}^{j_3} \delta_{i_1}^{j_4} \right) \right) + \frac{(p \cdot k)^2}{|p|^3 |k|} \left(G_{4,2,N} \left(\delta_{i_2}^{j_1} \delta_{i_3}^{j_2} \delta_{i_4}^{j_3} \delta_{i_1}^{j_4} + \delta_{i_2}^{j_1} \delta_{i_4}^{j_2} \delta_{i_3}^{j_3} \delta_{i_1}^{j_4} + \delta_{i_1}^{j_2} \delta_{i_3}^{j_1} \delta_{i_4}^{j_3} \delta_{i_2}^{j_4} + \delta_{i_1}^{j_2} \delta_{i_4}^{j_1} \delta_{i_3}^{j_3} \delta_{i_2}^{j_4} \right) + G_{4,2,F} \left(\delta_{i_3}^{j_1} \delta_{i_2}^{j_2} \delta_{i_4}^{j_3} \delta_{i_1}^{j_4} + \delta_{i_4}^{j_1} \delta_{i_2}^{j_2} \delta_{i_3}^{j_3} \delta_{i_1}^{j_4} \right) \right) + \frac{(p \cdot k)^2}{|p|^3 |k|} \left(G_{4,3,N} \left(\delta_{i_2}^{j_1} \delta_{i_3}^{j_2} \delta_{i_4}^{j_3} \delta_{i_1}^{j_4} + \delta_{i_2}^{j_1} \delta_{i_4}^{j_2} \delta_{i_3}^{j_3} \delta_{i_1}^{j_4} + \delta_{i_1}^{j_2} \delta_{i_3}^{j_1} \delta_{i_4}^{j_3} \delta_{i_2}^{j_4} + \delta_{i_1}^{j_2} \delta_{i_4}^{j_1} \delta_{i_3}^{j_3} \delta_{i_2}^{j_4} \right) + G_{4,3,F} \left(\delta_{i_3}^{j_1} \delta_{i_2}^{j_2} \delta_{i_4}^{j_3} \delta_{i_1}^{j_4} + \delta_{i_4}^{j_1} \delta_{i_2}^{j_2} \delta_{i_3}^{j_3} \delta_{i_1}^{j_4} \right) \right) \right), \quad (4.11)$$

where the subscript N stands for ‘Near’ and F for ‘Far’²⁵.

The $n = 5$ case is similar to the $n = 4$ case. We need only the leading order in $\frac{1}{N_c}$, and only for $(G_5)_{i_1, i_2, i_3, i_4, i_5}^{j_1, j_2, j_3, j_4, j_5}(p, -p, 0, 0, 0)$ (namely, the other momenta are small compared to p). As in the $n = 4$ case, there are two structures, where the p meson is ‘near’ or ‘far’ from the $-p$ meson. The only momentum contribution which we care about has the form $\frac{1}{|p|^2}$, and so we can write²⁶

$$(G_5)_{i_1, i_2, i_3, i_4, i_5}^{j_1, j_2, j_3, j_4, j_5}(p, -p, 0, 0, 0) = \frac{1}{|p|^2} \left(\begin{array}{l} G_{5,N} \left(\delta_{i_2}^{j_1} \delta_{i_3}^{j_2} \delta_{i_4}^{j_3} \delta_{i_5}^{j_4} \delta_{i_1}^{j_5} + (3, 4, 5) + (1 \leftrightarrow 2) \right) + \\ G_{5,F} \left(\delta_{i_3}^{j_1} \delta_{i_2}^{j_2} \delta_{i_4}^{j_3} \delta_{i_5}^{j_4} \delta_{i_1}^{j_5} + (3, 4, 5) + (1 \leftrightarrow 2) \right) \end{array} \right), \quad (4.12)$$

²³There can be in general also contributions of the type $\frac{k \cdot p}{|p|^3}$ or $\frac{k \cdot p}{|p|^2 |k|}$, however, they will cancel when integrating over p .

²⁴Note that in the calculation below, when we use the 4-point function we integrate over all values of p , and odd functions of p in G_4 will not contribute to the beta function. Thus, we do not use $(G_4)_{i_1, i_2, i_3, i_4}^{j_1, j_2, j_3, j_4}(p, -p, k, -k)$ per se, but the symmetrized combination

$$\frac{1}{2} \left[(G_4)_{i_1, i_2, i_3, i_4}^{j_1, j_2, j_3, j_4}(-p, p, k, -k) + (G_4)_{i_1, i_2, i_3, i_4}^{j_1, j_2, j_3, j_4}(p, -p, k, -k) \right].$$

This, instead of $(G_4)_{i_1, i_2, i_3, i_4}^{j_1, j_2, j_3, j_4}(p, -p, k, -k)$ alone, is what the parametrization in (4.11) stands for. Indeed, we calculate in Appendix B the symmetrized quantity for the CB theory with $\lambda_B = 0$, and show that this quantity is well defined and free from IR divergences, rather than the non-symmetrized G_4 .

²⁵For the $N_f = 1$ case the 4-point function is known exactly for any value of λ [42, 52], and this fixes some specific combinations of the $N_f > 1$ coefficients as described in (4.23) below. It is possible that using the same techniques one can compute each of these terms separately, for $G_{4,1,N/F}$ this was done in [42].

²⁶Note that as described in footnote 24 for G_4 , we use only the symmetrized version of G_5 .

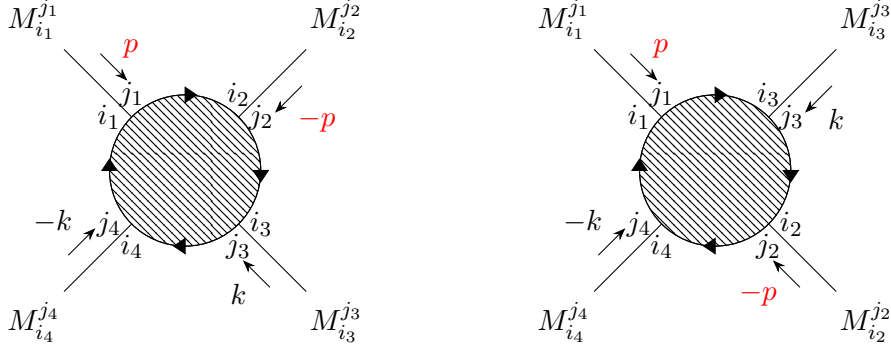


Figure 6. Two momentum structures that contribute to the 4-point function in the kinematic limit discussed in the text. Either the two external lines of momentum $\pm p$ are near each other in the cyclic order (left), or they are separated by another external line (right).

where all the non-written permutations are given by permutations of the indices $\{3, 4, 5\}$ and exchanging $1 \leftrightarrow 2$. All in all, we have 24 terms, corresponding to the number of permutations of the 5 mesons up to cyclic permutations.

4.2 Calculating the beta function

The calculation of the beta function proceeds in a similar fashion to the calculation reviewed in section 3; one has to compute the diagrams in figures 2 and 3, adding the appropriate flavor structures.

For the 2-point function, as in the $N_f = 1$ case, the logarithmic UV divergence comes only from the right diagram of figure 2

$$\begin{aligned}
 (\delta\Gamma_2)^{j_1, j_2}_{i_1, i_2}(q) &= -\frac{1}{2} \int \frac{d^3 p}{(2\pi)^3} (G_2^{-1})^{i_3, i_4}_{j_3, j_4}(p) (G_4)^{j_3, j_4, j_1, j_2}_{i_3, i_4, i_1, i_2}(p, -p, q, -q) \\
 &= \left(\frac{N_f (3G_{4,2,N} + G_{4,3,N})}{3\pi^2 G_2} \delta_{i_2}^{j_1} \delta_{i_1}^{j_2} + \frac{3G_{4,2,F} + G_{4,3,F}}{6\pi^2 G_2} \delta_{i_1}^{j_1} \delta_{i_2}^{j_2} \right) |q| \log\left(\frac{q}{\Lambda}\right), \quad (4.13)
 \end{aligned}$$

where we used $\int \frac{d^3 p}{(2\pi)^3} \frac{|q|}{|p|^3} = \frac{|q|}{2\pi^2} \log(\Lambda)$ and $\int \frac{d^3 p}{(2\pi)^3} \frac{(p \cdot q)^2}{|p|^5 |q|} = \frac{|q|}{6\pi^2} \log(\Lambda)$.

For the 3-point function, we need to take into account all the diagrams in figure 3. The computation is more lengthy but straightforward and we find (the dots are to abbreviate the full structures presented in (4.8))

$$(\delta\Gamma_3)^{j_1, j_2, j_3}_{i_1, i_2, i_3} = \left[\delta\bar{\Gamma}_{3,1} \left(\delta_{i_1}^{j_1} \delta_{i_2}^{j_2} \delta_{i_3}^{j_3} \right) + \delta\bar{\Gamma}_{3,2} \left(\delta_{i_1}^{j_1} \delta_{i_2}^{j_3} \delta_{i_3}^{j_2} + \dots \right) + \delta\bar{\Gamma}_{3,3} \left(\delta_{i_1}^{j_2} \delta_{i_2}^{j_3} \delta_{i_3}^{j_1} + \dots \right) \right] \log(\Lambda), \quad (4.14)$$

where

$$\begin{aligned}
 \delta\bar{\Gamma}_{3,1} &= \left(\frac{3\bar{G}_{3,2} G_{4,1,F}}{2\pi^2 G_2^2} + \frac{\bar{G}_{3,1}^3 N_f^3 + \bar{G}_{3,2}^3 (N_f^2 + 14) + 9\bar{G}_{3,1}^2 \bar{G}_{3,2} N_f^2}{2\pi^2 G_2^3} \right. \\
 &\quad \left. + \frac{24\bar{G}_{3,1} \bar{G}_{3,2}^2 N_f + 6\bar{G}_{3,3} (\bar{G}_{3,2}^2 N_f + \bar{G}_{3,1}^2 N_f + 4\bar{G}_{3,1} \bar{G}_{3,2}) + 6\bar{G}_{3,3}^2 \bar{G}_{3,2}}{2\pi^2 G_2^3} \right) \log(\Lambda), \quad (4.15)
 \end{aligned}$$

$$\delta\bar{\Gamma}_{3,2} = \left(-\frac{G_{5,F}}{\pi^2 G_2^2} + \frac{2\bar{G}_{3,3}(G_{4,1,F} + G_{4,1,N}) + \bar{G}_{3,1}(G_{4,1,F} + 2G_{4,1,N}) + 2\bar{G}_{3,2}N_f G_{4,1,N}}{2\pi^2 G_2^2} \right. \\ \left. + \frac{2\bar{G}_{3,3}^2(\bar{G}_{3,2}N_f + 2\bar{G}_{3,1}) + 2\bar{G}_{3,2}\bar{G}_{3,3}(2\bar{G}_{3,1}N_f + 7\bar{G}_{3,2}) + \bar{G}_{3,2}^2N_f(\bar{G}_{3,1}N_f + 4\bar{G}_{3,2}) + 2\bar{G}_{3,3}^3}{2\pi^2 G_2^3} \right) \log(\Lambda), \quad (4.16)$$

and

$$\delta\bar{\Gamma}_{3,3} = \left(-\frac{3N_f G_{5,N}}{2\pi^2 G_2^2} + \frac{\bar{G}_{3,3}(\bar{G}_{3,3}^2 N_f + 3\bar{G}_{3,2}^2 N_f + 12\bar{G}_{3,2}\bar{G}_{3,3})}{2\pi^2 G_2^3} \right. \\ \left. + \frac{3(\bar{G}_{3,2}(G_{4,1,F} + 2G_{4,1,N}) + \bar{G}_{3,3}N_f G_{4,1,N})}{2\pi^2 G_2^2} \right) \log(\Lambda). \quad (4.17)$$

We can now use the above results to write the regulated 1-loop correction to the inverse of the ζ_i^j propagator and to the amputated 3-point function:

$$(\Gamma_2)_{i_1, i_2}^{j_1, j_2}(q) \equiv |q|(G_2)_{i_1, i_2}^{j_1, j_2} + |q|(\delta G_2)_{i_1, i_2}^{j_1, j_2} \log\left(\frac{q}{\Lambda}\right) + (\delta\Gamma_2)_{i_1, i_2}^{j_1, j_2}(q), \quad (4.18)$$

$$\left\langle \zeta_{j_1}^{i_1}(q_1) \zeta_{j_2}^{i_2}(q_2) \zeta_{j_3}^{i_3}(q_3) \right\rangle_{\text{amputated}} = (G_3)_{i_1, i_2, i_3}^{j_1, j_2, j_3} + (\delta G_3)_{i_1, i_2, i_3}^{j_1, j_2, j_3} \log(\Lambda) + (\delta\Gamma_3)_{i_1, i_2, i_3}^{j_1, j_2, j_3}, \quad (4.19)$$

where we emphasize that $\delta\Gamma_2$ and $\delta\Gamma_3$ have a factor of $\log(\Lambda)$ inside them.

To proceed with the beta functions calculation, one has to renormalize the ζ fields. To preserve the $SU(N_f)$ flavor symmetry of the theory, the renormalization of all the fields in the adjoint ζ_A structure must be the same, and thus there are two renormalization conditions – one for ζ_S and one for all the fields in ζ_A .

Thus, we need to project the equations above into the representation basis. For the two-point function this is done using (4.6), so together with (4.3), (4.4) and (4.13), we get that

$$(\Gamma_2)_{i_1, i_2}^{j_1, j_2}(q) \zeta_{j_1}^{i_1}(q) \zeta_{j_2}^{i_2}(-q) = G_2 \left(\frac{q}{\Lambda}\right)^{2\gamma'_A} |q| (\zeta_A)_j^i(q) (\zeta_A)_i^j(-q) + \frac{G_2}{N_f} |q| \left(\frac{q}{\Lambda}\right)^{2\gamma'_S} \zeta_S(q) \zeta_S(-q) \quad (4.20)$$

with the one loop corrected anomalous dimensions

$$\gamma'_A = \gamma_A + \frac{N_f(3G_{4,2,N} + G_{4,3,N})}{6\pi^2 G_2^2}, \quad \gamma'_S = \gamma_S + \frac{N_f(3G_{4,2,F} + G_{4,3,F} + 6G_{4,2,N} + 2G_{4,3,N})}{12\pi^2 G_2^2}. \quad (4.21)$$

Proceeding in the same manner as in section 3 and [25], and using (2.8) to relate the 3-point structures in the index basis to the representation basis, we find that the beta functions of the G_{SSS} , G_{SAA} , G_{AAA} couplings are

$$\begin{aligned}
\beta_{G_{SSS}} &= \frac{1}{\pi^2 G_2} \frac{3(G_{5,F} + G_{5,N})}{N_f} - \delta G_{SSS} - G_{SSS} \left(3\gamma'_S + \frac{3(G_{4,1,F} + 2G_{4,1,N})}{2\pi^2 G_2^2 N_f} \right) \\
&\quad - G_{SAA} \left(\frac{3(N_f^2 - 1)(G_{4,1,F} + 2G_{4,1,N})}{2\pi^2 G_2^2 N_f^2} \right) - \frac{1}{2\pi^2 G_2^3} (N_f^3 G_{SSS}^3 + (N_f^2 - 1) G_{SAA}^3), \\
\beta_{G_{SAA}} &= \frac{1}{\pi^2 G_2} (G_{5,F} + 3G_{5,N}) - \delta G_{SAA} - G_{SSS} \left(\frac{G_{4,1,F} + 2G_{4,1,N}}{2\pi^2 G_2^2} \right) \\
&\quad - G_{SAA} \left(\gamma'_S + 2\gamma'_A + \frac{3G_{4,1,F} + 2(N_f^2 + 3)G_{4,1,N}}{2\pi^2 G_2^2 N_f} \right) \\
&\quad - G_{AAA} \left(\frac{(N_f^2 - 4)(G_{4,1,F} + 2G_{4,1,N})}{\pi^2 G_2^2 N_f^2} \right) \\
&\quad - \frac{1}{2\pi^2 G_2^3} \left(N_f^2 G_{SSS} G_{SAA}^2 + N_f G_{SAA}^3 + 2 \frac{(N_f^2 - 4)}{N_f} G_{SAA} G_{AAA}^2 \right), \\
\beta_{G_{AAA}} &= \frac{3}{2\pi^2 G_2} N_f G_{5,N} - \delta G_{AAA} - G_{SAA} \left(\frac{3(G_{4,1,F} + 2G_{4,1,N})}{2\pi^2 G_2^2} \right) \\
&\quad - G_{AAA} \left(3\gamma'_A + \frac{3(N_f^2 - 4)G_{4,1,N} - 6G_{4,1,F}}{2\pi^2 G_2^2 N_f} \right) \\
&\quad - \frac{1}{2\pi^2 G_2^3} \left(3N_f G_{SAA}^2 G_{AAA} + \frac{(N_f^2 - 12)}{N_f} G_{AAA}^3 \right).
\end{aligned} \tag{4.22}$$

Those serve as the analog of (3.7) in the single flavor case.

As a check, we note that this computation reproduces the single flavor result presented in section 3. For $N_f = 1$, there is only the SSS structure, and indeed $\beta_{G_{SSS}}$ depends on G_{SSS} only. Comparing the parametrization of \tilde{G}_4 and \tilde{G}_5 (3.4) in the single flavor case and the parametrization of (4.11) and (4.12) we find

$$\begin{aligned}
&\tilde{G}_5 = 12G_{5,N} + 12G_{5,F}, \\
&\text{for } N_f = 1 : \quad \begin{aligned} -2\tilde{G}_4 &= 4G_{4,1,N} + 2G_{4,1,F}, \\ \tilde{G}_4 &= 4G_{4,2,N} + 2G_{4,2,F}, \\ \tilde{G}_4 &= 4G_{4,3,N} + 2G_{4,3,F}. \end{aligned}
\end{aligned} \tag{4.23}$$

Substituting (4.23) into equations (4.21) and (4.22) reproduces the $N_f = 1$ results in (3.6) and (3.7).

We can find the beta functions (4.22) exactly (at leading order in $\frac{1}{N_c}$) for the RB theory with $\lambda_B = 0$ and the CF theory with $\lambda_F = 0$. The correlation functions in those cases are calculated analytically in Appendices B and C. The results are summarized in table 3. We study those cases in detail in sections 5 and 6.

Element	coupling	Bosons	Fermions
G_2		$\frac{8}{\lambda_B \kappa_B}$	$2\pi^2 \frac{\lambda_F}{\kappa_F}$
G_3	G_{SSS}	$g_1^B - \frac{128}{N_f^2 (N_c^B)^2}$	g_1^F
	G_{SAA}	$g_2^B - \frac{128}{N_f (N_c^B)^2}$	g_2^F
	G_{AAA}	$g_3^B - \frac{64}{(N_c^B)^2}$	g_3^F
δG_3	δG_{SSS}	$\frac{4096(3s_{5,F} + 3s_{5,N} - 1)}{(N_c^B)^3 N_f \pi^2}$	0
	δG_{SAA}	$\frac{2048(2s_{5,F} + 6s_{5,N} - 1)}{(N_c^B)^3 \pi^2}$	0
	δG_{AAA}	$\frac{512N_f(12s_{5,N} - 1)}{(N_c^B)^3 \pi^2}$	0
G_4	$G_{4,1,N}$	$-\frac{1}{8} \frac{8^4}{\lambda_B^3 \kappa_B^3}$	$-\frac{1}{8} (4\pi)^4 \frac{\lambda_F}{\kappa_F^3}$
	$G_{4,2,N}$	0	0
	$G_{4,3,N}$	$\frac{1}{8} \frac{8^4}{\lambda_B^3 \kappa_B^3}$	$\frac{1}{8} (4\pi)^4 \frac{\lambda_F}{\kappa_F^3}$
	$G_{4,1,F}$	$-\frac{1}{4} \frac{8^4}{\lambda_B^3 \kappa_B^3}$	$-\frac{1}{4} (4\pi)^4 \frac{\lambda_F}{\kappa_F^3}$
	$G_{4,2,F}$	$\frac{1}{4} \frac{8^4}{\lambda_B^3 \kappa_B^3}$	$\frac{1}{4} (4\pi)^4 \frac{\lambda_F}{\kappa_F^3}$
	$G_{4,3,F}$	0	0
G_5	$G_{5,N/F}$	$\frac{8^5}{(N_c^B)^4} s_{5,N/F}$	0
γ_S		$-\frac{1}{N_c^B} \frac{16N_f}{3\pi^2}$	0
γ'_S		0	$\frac{1}{N_c^F} \frac{16N_f}{3\pi^2}$
γ_A		$-\frac{1}{N_c^B} \frac{4N_f}{3\pi^2}$	0
γ'_A		0	$\frac{1}{N_c^F} \frac{4N_f}{3\pi^2}$

Table 3. Summary of the results of Appendices B (bosons) and C (fermions). These are the coefficients that appear in (4.22) when $\lambda_{B/F} \rightarrow 0$ and they are used to derive (6.2), and as an alternative method to derive (5.2). (2.8) is used to transform from the index basis in the text to the representation basis in this table. $s_{5,N/F}$ are defined in (B.11) (see also (B.15)) and their values are unknown.

4.3 Analyzing the beta function structure

In the following sections 5 and 6 we compute the beta functions in two specific limits. Here, we wish to emphasize several general aspects of the beta functions presented in (4.22):

1. We are interested in the beta functions in terms of the finite 't Hooft couplings $\lambda_{SSS}, \lambda_{SAA}, \lambda_{AAA}$ (see section 2.3). The connection between them and $G_{SSS}, G_{SAA}, G_{AAA}$ is given by shifting by some constants (provided in the index basis in (4.9)) and rescaling. Substituting the explicit dependence on N_c , one gets that the beta functions for the finite 't Hooft couplings scale as $\sim \frac{1}{N_c}$. Furthermore, as emphasized in the paragraph below equation (3.7), at leading order in $\frac{1}{N_c}$, the beta functions found are *exact* to all orders in $\lambda_{SSS}, \lambda_{SAA}, \lambda_{AAA}$ [25].
2. The beta functions for $\lambda_{SSS}, \lambda_{SAA}, \lambda_{AAA}$ are 3 polynomials of degree 3. To find the fixed points of this system, we set all the beta functions to zero. Such a system of

real equations can have in general between 1 and 27 real solutions (see section 5.5.1 for more details), and so these are the minimal and maximal possible numbers of fixed points in the system (at large N_c).

3. Note that the beta functions in (4.22) have a special form: no G_{AAA} dependence in $\beta_{G_{SSS}}$ and no G_{SSS} dependence in $\beta_{G_{AAA}}$.
4. One way to find the fixed points is to relate them to a single complicated equation in one variable. The property mentioned in the previous item implies that one can solve third-order equations for G_{SSS} and for G_{AAA} in terms of G_{SAA} . One can then substitute each of the 9 possible options into $\beta_{G_{SAA}}$, and get an equation just for G_{SAA} .
5. The cubic terms in each of the beta functions (the last term in each equation) are the same for all our theories, up to an overall factor of G_2^3 . These terms are not affected by shifting the λ_n by constants, and G_2 is always positive by unitarity. Thus, the analysis of the flow for very large values of $\lambda_{SSS}, \lambda_{SAA}, \lambda_{AAA}$ (when the cubic part dominates the beta function) will be the same in all our theories and for any values of λ_F or λ_B . We will analyze this flow in sections 5.2.2 and 5.3.2.
6. We mentioned above the simplification of the beta functions for $N_f = 1$, where only the G_{SSS} coupling exists, and G_{SAA} does not appear in its beta function because of factors of $(N_f^2 - 1)$. There is a similar simplification for $N_f = 2$, where the structure associated with G_{AAA} does not exist, and indeed it does not appear in the other two beta functions; in $\beta_{G_{SAA}}$ this is because its coefficients are proportional to $(N_f^2 - 4)$.
7. The general structure of the beta functions is similar to the $N_f = 1$ case in (3.7), with constant terms, linear terms, and cubic terms, but no quadratic term, because they arise from the same diagrams just with different flavor indices. The δG_3 terms, as well as the G_5 Feynman diagram (the left diagram in figure 3), lead to the constant parts. The renormalization of the two-point functions (manifested by the anomalous dimensions) and the $G_4 - G_3$ Feynman diagram (the middle diagram in figure 3) lead to the linear parts, and the G_3^3 Feynman diagram (the right diagram in figure 3) corresponds to the cubic part. It is easy to see from the diagrams why the specific linear and cubic terms that we have in (4.22) arise, see for instance figure 7. The λ_n couplings are shifted from G_n by constants, so their beta functions will contain some quadratic terms, but otherwise they will have the same properties.
8. For each $N_f \geq 3$, there are 10 parameters that determine the beta functions and thus the fixed points and the flows between them²⁷: the 3 constant terms in each beta function and the 7 prefactors of the linear terms.

²⁷The prefactors of the cubic terms are equal in all of the beta functions, and so it can be set to 1 by rescaling.

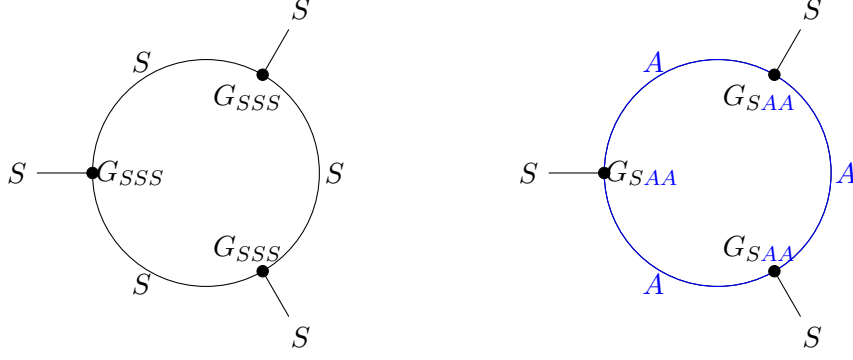


Figure 7. The structures contributing to the cubic terms in $\beta_{G_{SSS}}$: either all the interactions are SSS vertices and the internal lines are ζ_S , or they are all SAA vertices and the internal lines are ζ_A .

4.4 The large N_f limit

In our analysis, we consider the limit $N_c \rightarrow \infty$, retaining only the leading non-trivial terms of order $\frac{1}{N_c}$ in the beta functions. While the previous analysis was conducted for a fixed number of flavors N_f , we now extend it to the large N_f limit, assuming $N_f \ll N_c$.

In the $N_f \rightarrow \infty$ limit we have (on top of the N_c -scalings discussed above)

$$\begin{aligned} \gamma'_A, \gamma'_S, \delta G_{AAA} &\sim N_f, \\ \delta G_{SAA} &\sim 1, \\ \delta G_{SSS} &\sim \frac{1}{N_f}, \end{aligned} \tag{4.24}$$

with the rest of the parameters having no scaling under N_f . (See table 3 for examples of these parameter scalings in free theories.)

It is interesting to ask what are the possible N_f scalings of the fixed points associated with (4.22), in the limit $N_f \rightarrow \infty$ and for constant λ . In other words, denoting the couplings as

$$G_{SSS} = \frac{Y_{SSS}}{N_f^a} + \mathcal{O}\left(\frac{1}{N_f^{a+\epsilon}}\right), \quad G_{SAA} = \frac{Y_{SAA}}{N_f^b} + \mathcal{O}\left(\frac{1}{N_f^{b+\epsilon}}\right), \quad G_{AAA} = \frac{Y_{AAA}}{N_f^c} + \mathcal{O}\left(\frac{1}{N_f^{c+\epsilon}}\right), \tag{4.25}$$

what are the possible values of (a, b, c) with $\epsilon > 0$.

Plugging (4.25) into (4.22) and using the scalings (4.24), we can write the beta functions as sums of terms with different powers of N_f that depend on a , b and c . Generically (i.e, if no special relation between the different components of (4.22) holds) we expect to get a root of the beta functions (i.e, a fixed point) only when at least two terms in the sum that contribute to the leading N_f power²⁸ are the same. We find that this condition holds only for

$$(a, b, c) : \quad \left(\frac{2}{3}, \frac{1}{3}, 0\right), (1, 1, 0), (2, 1, 0), \tag{4.26}$$

²⁸Which terms are leading and which are subleading, as well as what is the leading power, depends on a , b and c .

and any other leading scaling is forbidden.

In sections 5.4 and 6.3, we will see explicit examples of solutions of the types $(\frac{2}{3}, \frac{1}{3}, 0)$ and $(2, 1, 0)$ ²⁹. The $(2, 1, 0)$ solution is particularly interesting, as we discuss in the following.

4.4.1 The (2,1,0) scaling

Since our gauge-invariant operators are $N_f \times N_f$ matrices, this scaling is the natural one associated with the standard large N_f limit of matrix models, with single- $SU(N_f)$ -trace terms dominating, and other terms suppressed by powers of N_f . The large N_f limit is most natural to write in the index basis, in which it is natural to scale

$$\bar{g}_1 = \frac{\bar{Y}_1}{N_f^2}, \quad \bar{g}_2 = \frac{\bar{Y}_2}{N_f}, \quad \bar{g}_3 = \bar{Y}_3, \quad (4.27)$$

with the \bar{Y}_i 's fixed in the large N_f limit. Using the relation (2.8) between the index and representation basis, this is equivalent to taking

$$G_{SSS} = \frac{Y_{SSS}}{N_f^2}, \quad G_{SAA} = \frac{Y_{SAA}}{N_f}, \quad G_{AAA} = Y_{AAA}, \quad (4.28)$$

which is seen to correspond to the third solution in (4.26). In this limit the beta functions simplify, and we find as expected from general large- N_f arguments that the flow of the single-trace coupling (which is the dominant contribution to Y_{AAA}) decouples from the flow of the other couplings, and the flow of the double-trace (the dominant contribution to Y_{SAA}) decouples from the triple-trace.

One can show that this is the case explicitly in the parametrization chosen using (4.24). The resulting beta functions, at leading order in $1/N_f$, are

$$\begin{aligned} \frac{\beta_{Y_{SSS}}}{N_f} &= \left(\frac{3(G_{5,F} + G_{5,N})}{\pi^2 G_2} - N_f \delta G_{SSS} \right) - Y_{SSS} \left(3 \frac{\gamma'_S}{N_f} \right) \\ &\quad - Y_{SAA} \left(\frac{3(G_{4,1,F} + 2G_{4,1,N})}{2\pi^2 G_2^2} \right) - \frac{1}{2\pi^2 G_2^3} Y_{SAA}^3 + \mathcal{O}\left(\frac{1}{N_f}\right), \\ \frac{\beta_{Y_{SAA}}}{N_f} &= \left(\frac{G_{5,F} + 3G_{5,N}}{\pi^2 G_2} - \delta G_{SAA} \right) - Y_{SAA} \left(\frac{\gamma'_S}{N_f} + 2 \frac{\gamma'_A}{N_f} + \frac{G_{4,1,N}}{\pi^2 G_2^2} \right) \\ &\quad - Y_{AAA} \left(\frac{G_{4,1,F} + 2G_{4,1,N}}{\pi^2 G_2^2} \right) - \frac{1}{2\pi^2 G_2^3} 2Y_{SAA} Y_{AAA}^2 + \mathcal{O}\left(\frac{1}{N_f}\right), \\ \frac{\beta_{Y_{AAA}}}{N_f} &= \left(\frac{3G_{5,N}}{2\pi^2 G_2} - \frac{\delta G_{AAA}}{N_f} \right) - Y_{AAA} \left(3 \frac{\gamma'_A}{N_f} + \frac{3G_{4,1,N}}{2\pi^2 G_2^2} \right) - \frac{1}{2\pi^2 G_2^3} Y_{AAA}^3 + \mathcal{O}\left(\frac{1}{N_f}\right). \end{aligned} \quad (4.29)$$

Note that all the terms on the right-hand side are $O(1)$ in the large N_f limit. Upon rewriting (4.29) in terms of the finite 't Hooft couplings $y_n = N_c^2 Y_n$, the beta functions for

²⁹The type $(1, 1, 0)$ requires $\gamma'_S < 0$, which does not happen for the values of $\lambda_{B/F}$ considered in this paper.

y_n become proportional to $\frac{N_f}{N_c} \ll 1$. We see that indeed, the flow of Y_{AAA} does not depend on the other couplings, and the flow of Y_{SAA} does not depend on Y_{SSS} .

In searching for fixed points, it is possible in this limit to solve the equations iteratively: we first solve $\beta_{Y_{AAA}} = 0$, which is a cubic polynomial in Y_{AAA} , that generically has 1 or 3 zeros. Next, we can substitute this solution to $\beta_{Y_{SAA}} = 0$ to get Y_{SAA} , and repeat the process to find Y_{SSS} . Since $\beta_{Y_{SAA}}$ and $\beta_{Y_{SSS}}$ are linear in Y_{SAA} and Y_{SSS} respectively, we find that there are always between 1 and 3 solutions with the scaling (4.28).

The argument above holds unless the linear terms in the leading order equation (4.29) happen to vanish. If for one of the solutions of Y_{AAA} , the prefactor of Y_{SAA} in its beta function vanishes, which happens when

$$\left(\frac{3G_{5,N}}{2\pi^2 G_2} - \frac{\delta G_{AAA}}{N_f} \right)^2 = -\pi^2 G_2^3 \left(2\frac{\gamma'_A}{N_f} + \frac{G_{4,1,N}}{\pi^2 G_2^2} + \frac{\gamma'_S}{N_f} \right) \left(2\frac{\gamma'_A}{N_f} + \frac{G_{4,1,N}}{\pi^2 G_2^2} - \frac{1}{2} \frac{\gamma'_S}{N_f} \right)^2, \quad (4.30)$$

or the prefactor of Y_{SSS} in its beta function vanishes, which happens when $\gamma'_S = 0$, then it is not enough to look at the leading order terms (4.29) to find all possible solutions with the leading scaling of (4.28). We will see examples of these degeneracies in sections 5.4 and 6.3. However, for generic values of the 't Hooft coupling λ we do not expect such degeneracies to hold.

5 Regular boson theories with vanishing and small λ_B

In this section, we analyze in detail the number of fixed points and the flows coming from the beta functions of the marginal couplings $\lambda_{SSS}^B, \lambda_{SAA}^B, \lambda_{AAA}^B$, in the weakly coupled limit of the RB theories defined in section 2.2.1. We will ignore the subscript and superscript B , as we concentrate only on scalar theories in this section.

We first calculate the exact beta functions at leading order in $\frac{1}{N_c}$ for the ‘gluon free’ theory with $\lambda = 0$. As for the single flavor case (see (3.10) and figure 4), the free point $\lambda_{SSS} = \lambda_{SAA} = \lambda_{AAA} = 0$ is a degenerate fixed point in this case. To observe its splitting to several fixed points at finite λ , we calculate the beta function for $\lambda \ll 1$ ³⁰ in the vicinity of this point, and show that an IR-stable fixed point emerges.

The structure of this section is as follow: in section 5.1 we compute the beta function in two regimes of interest, when $\lambda = 0$ and when $\lambda^2 \sim \lambda_n \ll 1$. We then analyze the fixed points structure and the flows for $N_f = 2$ and for $N_f \geq 3$, in sections 5.2 and 5.3, respectively. In section 5.4, we comment on the solutions for fixed points at large values of N_f . We conclude in section 5.5 with a general discussion of the possible behavior of the fixed points as we change λ .

5.1 Calculating the beta functions

In this section we outline the calculations of the beta functions for the $\lambda = 0$ case and for the perturbative $\lambda \ll 1$ case. The full details of the calculations, including conventions for the Lie algebra generators, renormalization conditions, and the contribution of each Feynman diagram, are presented in Appendix A.

³⁰A subtlety in this definition arises for large N_f , which we discuss in section 5.1.2.

5.1.1 The $\lambda = 0$ case

The RB theory (2.11) with $\lambda = 0$ has the simple Lagrangian

$$\mathcal{L} = \partial_\mu \bar{\phi}_{i,a} \partial_\mu \phi^{i,a} + \frac{\bar{g}_1^B}{3!} (\bar{\phi}_{c,i} \phi^{c,i})^3 + \frac{\bar{g}_2^B}{2} \bar{\phi}_{a,i} \phi^{a,i} \bar{\phi}_{b,j} \phi^{b,k} \bar{\phi}_{c,k} \phi^{c,j} + \frac{\bar{g}_3^B}{3} \bar{\phi}_{a,i} \phi^{a,j} \bar{\phi}_{b,j} \phi^{b,k} \bar{\phi}_{c,k} \phi^{c,i}, \quad (5.1)$$

which contains only six-scalar vertices. In the 't Hooft limit we are working in, there are only two diagrams which contribute to the 6-point correlation function, corresponding to two and three interaction vertices. The diagrams are presented in figure 8. We leave the proof that in this formalism, those are the only two diagrams that contribute in the leading 't Hooft limit, to Appendix A.2.

Evaluating the diagrams, the beta functions are found to be³¹

$$\begin{aligned} 2^{10} \pi^2 N_c \beta_{SSS} &= 2^6 \left(6N_f \lambda_{SSS}^2 + 6 \frac{(N_f^2 - 1)}{N_f} \lambda_{SAA}^2 \right) - (N_f^3 \lambda_{SSS}^3 + (N_f^2 - 1) \lambda_{SAA}^3), \\ 2^{10} \pi^2 N_c \beta_{SAA} &= 2^6 \left(4N_f \lambda_{SSS} \lambda_{SAA} + 8 \lambda_{SAA}^2 + 4 \frac{(N_f^2 - 4)}{N_f} \lambda_{SAA} \lambda_{AAA} + 4 \frac{(N_f^2 - 4)}{N_f^2} \lambda_{AAA}^2 \right) \\ &\quad - \left(N_f^2 \lambda_{SSS} \lambda_{SAA}^2 + N_f \lambda_{SAA}^3 + 2 \frac{(N_f^2 - 4)}{N_f} \lambda_{SAA} \lambda_{AAA}^2 \right), \\ 2^{10} \pi^2 N_c \beta_{AAA} &= 2^6 \left(3N_f \lambda_{SAA}^2 + \frac{3(N_f^2 - 12)}{N_f} \lambda_{AAA}^2 + 12 \lambda_{SAA} \lambda_{AAA} \right) \\ &\quad - \left(3N_f \lambda_{SAA}^2 \lambda_{AAA} + \frac{(N_f^2 - 12)}{N_f} \lambda_{AAA}^3 \right). \end{aligned} \quad (5.2)$$

It is also possible to evaluate the beta function in this case directly using the formalism presented in section 4. In Appendix B we calculate the correlation functions for RB theories with $\lambda = 0$. Substituting the results summarized in table 3 in (4.22) reproduces (5.2).

The beta functions (5.2) are a simple special case of the general possible form of the beta functions for RB theories, which is presented in (4.22). The reduction to the $N_f = 1$ and $N_f = 2$ cases is straightforward by ignoring β_{SAA} and/or β_{AAA} (as manifested by the $N_f^2 - 1$ and $N_f^2 - 4$ factors, see item 6 in section 4.3). Also, one can explicitly check that redefining the couplings by $\lambda_{SSS} \rightarrow \lambda_{SSS} + \frac{128}{N_f^2}$, $\lambda_{SAA} \rightarrow \lambda_{SAA} + \frac{128}{N_f}$, $\lambda_{AAA} \rightarrow \lambda_{AAA} + 64$ removes the quadratic terms in all of the equations and brings them to the form of section 4³².

³¹The result for the $SO(N_c)$ case, which includes an additional factor of two compared to (5.2), was also computed in [27], though with a different normalization of the couplings.

³²Note that without the general formalism presented in section 4, this property is rather surprising, since unlike the one coupling case in which it is always possible to redefine the variable in a cubic polynomial to remove the quadratic part, this is not true for a generic system of three cubic polynomials with three variables.

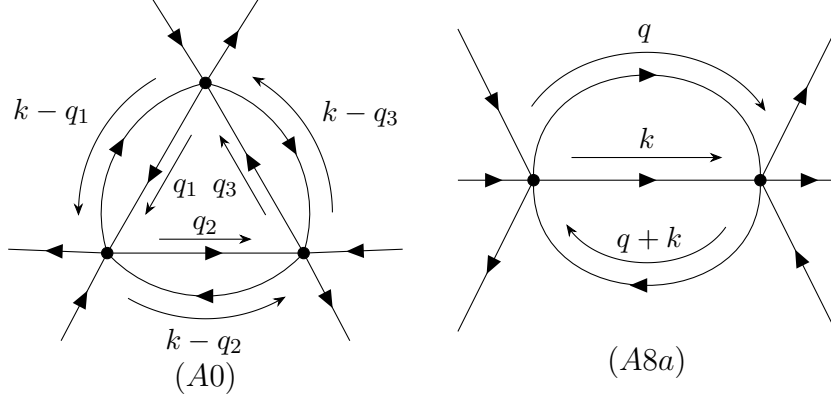


Figure 8. The only two diagrams contributing to the beta function of RB theories when $\lambda = 0$, at leading order in the 't Hooft $\frac{1}{N_c}$ expansion, when the external legs have zero momentum.

In sections 5.2 and 5.3 we present a full analysis of the fixed point structure and the flow which results from the beta functions (5.2). Note that in the $\lambda = 0$ theory the beta functions do not contain any constants or linear terms. An immediate consequence of this is that there is a degenerate fixed point at $(\lambda_{SSS}, \lambda_{SAA}, \lambda_{AAA}) = (0, 0, 0)$, which is simply the free massless scalar theory, and that will either split or vanish when turning on a finite λ (the three dimensional analog of figure 4). To determine what happens to this point, we'll turn on a small but finite λ , and use perturbation theory to compute the beta functions near this free point $\lambda_n = 0$.

5.1.2 Finite $\lambda \ll 1$ in the vicinity of the free theory

In order to calculate the beta functions at finite $\lambda \ll 1$ near $\lambda_n = 0$, one has to take into account the full action of the RB theory (2.11).

This calculation, for a Lagrangian involving both relevant terms and fermions (see equation 23 in [48]), was first performed in [48] (see equation 34), for a $SU(N_c)$ gauge group with finite N_c and one flavor. It involved a very large number of Feynman diagrams. In [49]³³ (and later in [50, 53]), the authors showed that in the region $\lambda_n \sim \lambda^2 \ll 1$, there are 11³⁴ diagrams that contribute to the 6-point vertex (figure 9), and 4 that contribute to the propagator (figure 10). Adding flavors does not alter the number of diagrams, but only adds flavor indices to each scalar line.

The full calculation of the 2-loop beta function is presented in Appendix A.3, with the result in the representation basis³⁵

³³The calculation in [49] was done for the $SO(N_c)$ gauge group with $N_f = 1$.

³⁴In [49], there are 8 diagrams contributing to the 6-point vertex for real scalars. For complex scalars, the orientation of the scalar lines splits diagrams A1 and A8.

³⁵Note that the quadratic term in (5.3) is the same as in (5.2) since in both, the only diagram that contributes to the quadratic term in the 't Hooft limit is A8a.

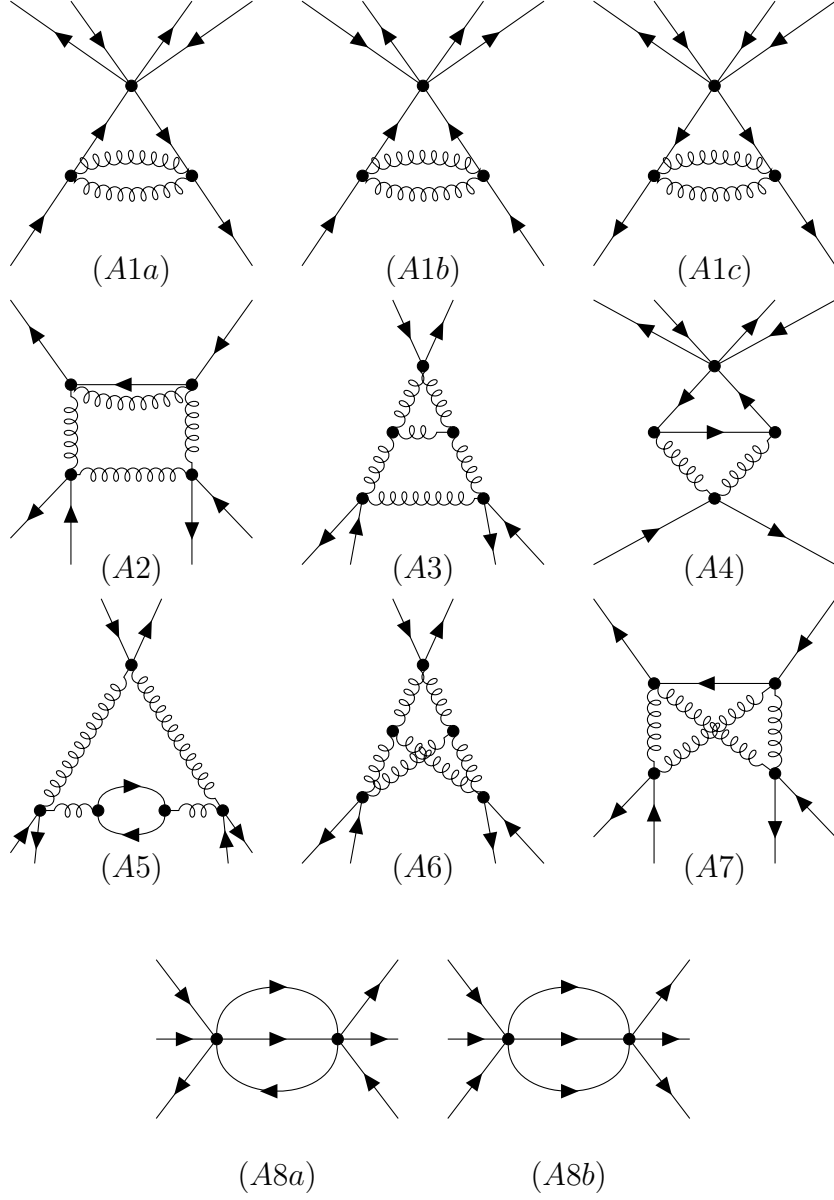


Figure 9. Diagrams that contribute to the 2-loop correction to the 6-point vertex. Each external line carries a color and a flavor index.

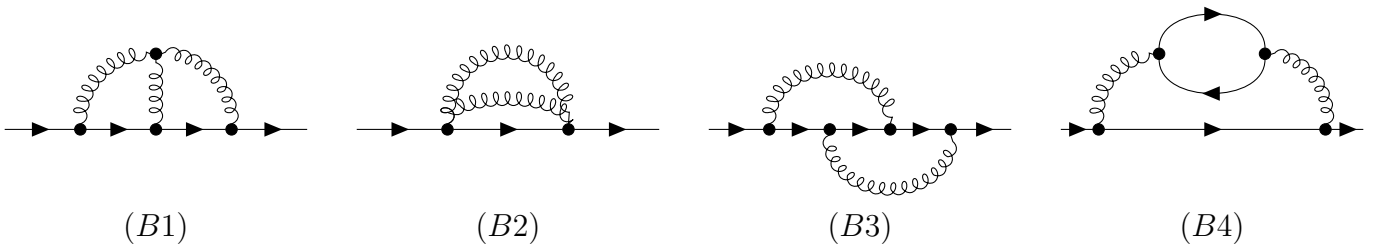


Figure 10. Diagrams that contribute to the 2-loop correction to the scalar propagator.

$$\begin{aligned}
16\pi^2 N_c \beta_{SSS} &= \left(\frac{\lambda}{4\pi}\right)^4 \frac{24}{N_f} - \left(\frac{\lambda}{4\pi}\right)^2 \frac{8 \left(\lambda_{SSS} N_f (2N_f^2 + 3) + 3\lambda_{SAA} (N_f^2 - 1) \right)}{N_f^2} \\
&\quad + 6\lambda_{SSS}^2 N_f + \frac{6\lambda_{SAA}^2 (N_f^2 - 1)}{N_f}, \\
16\pi^2 N_c \beta_{SAA} &= 12 \left(\frac{\lambda}{4\pi}\right)^4 - \left(\frac{\lambda}{4\pi}\right)^2 \frac{4 \left(N_f (2\lambda_{SSS} N_f + 3\lambda_{SAA} (N_f^2 + 2)) + 4\lambda_{AAA} (N_f^2 - 4) \right)}{N_f^2} \\
&\quad + \frac{4 \left(\lambda_{SAA} N_f^2 (\lambda_{SSS} N_f + 2\lambda_{SAA}) + \lambda_{SAA} \lambda_{AAA} (N_f^2 - 4) N_f + \lambda_{AAA}^2 (N_f^2 - 4) \right)}{N_f^2}, \\
16\pi^2 N_c \beta_{AAA} &= 3N_f \left(\frac{\lambda}{4\pi}\right)^4 + \left(\frac{\lambda}{4\pi}\right)^2 \left(-10\lambda_{AAA} N_f + \frac{48\lambda_{AAA}}{N_f} - 24\lambda_{SAA} \right) \\
&\quad + 3 \left(\lambda_{SAA}^2 N_f + \frac{\lambda_{AAA}^2 (N_f^2 - 12)}{N_f} + 4\lambda_{AAA} \lambda_{SAA} \right).
\end{aligned} \tag{5.3}$$

As a consistency check, we see that for $N_f = 1$, β_{SSS} reduces to (3.11), and there is a $N_f^2 - 4$ factor in front of λ_{AAA} in β_{SAA} (so that for $N_f = 2$, β_{AAA} decouples from β_{SSS} and β_{SAA}).

As in the $N_f = 1$ case, we analyze the splitting of the degenerate free fixed point at $\lambda = 0$ using (5.3). The resulting fixed points are located at couplings of order λ^2 , i.e. $\lambda_{SSS}, \lambda_{SAA}, \lambda_{AAA} \sim \lambda^2 \ll 1$. This hierarchy will justify the use of perturbation theory to the order considered in the derivation of (5.3), if all next order terms will be smaller. In (5.2) the cubic terms come with factors proportional to powers of N_f (up to N_f^3), therefore this perturbative approach is fully justified only for $\lambda \ll \frac{1}{N_f}$. For finite N_f this subtlety is of little importance, and in section 5.4.3 we'll discuss this regime in the case of large N_f .

We note that the computations presented in Appendix A.3 were carried out without invoking any specific assumptions regarding N_c or N_f . The 't Hooft limit was imposed only in the final step. This allows for the perturbative analysis to be extended to finite values of N_c as well. In Appendix A.3.1, we investigate whether an infrared (IR)-stable fixed point persists for finite values of N_c .

5.2 The $N_f = 2$ case

We can now analyze the fixed point structure and the flow of the beta functions in (5.2) and (5.3). We start with the $N_f = 2$ case, in which we have only β_{SSS} and β_{SAA} .

5.2.1 Analysis for $\lambda = 0$

For $\lambda = 0$, we find from (5.2) that there are 4 fixed points

$$(\lambda_{SSS}, \lambda_{SAA}) : (0, 0), (\sim 80, \sim 199), (96, 0), (96, 192). \tag{5.4}$$

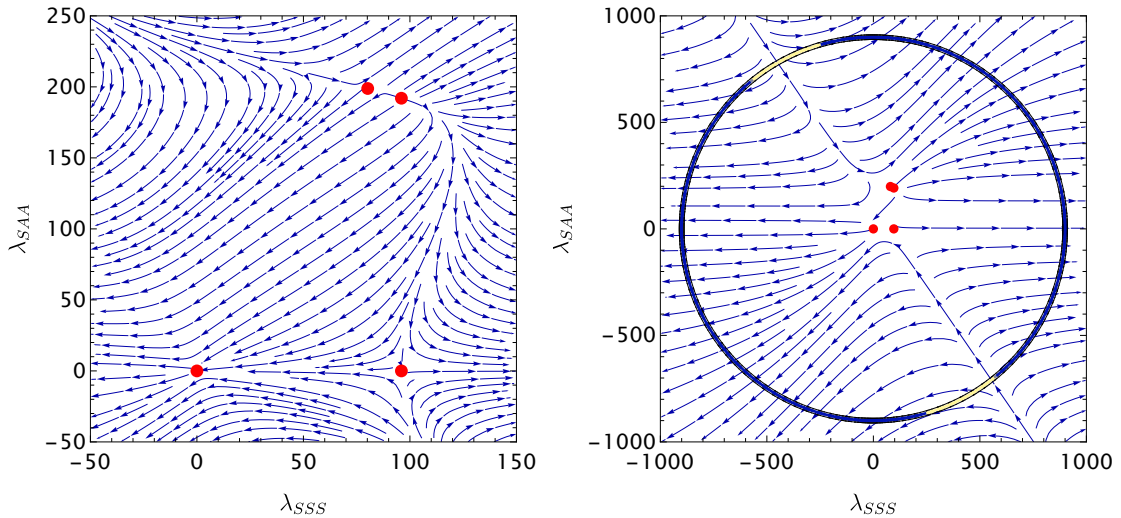


Figure 11. The flow to the IR of (minus) (5.2) for $N_f = 2$ and $\lambda = 0$. The fixed points (5.4) are shown in red. **Left:** The flow near the fixed points. **Right:** The flows “at infinity”, the color of the circle encodes whether the flow goes outward (blue), or inward (yellow). Note that the angular size of the outward and inward regions stays finite as $\lambda_n \rightarrow \infty$.

Diagonalization of the derivative matrix of the beta function at these points $\partial_i \beta_j$ shows that (see section 5.5.2 for more details)

- The free point $(0, 0)$ has two zero eigenvalues and is thus degenerate.
- The $(\sim 80, \sim 199)$ and $(96, 0)$ points have both positive and negative eigenvalues, which means that they are mixed points and not UV nor IR-stable.
- The $(96, 192)$ point has only positive eigenvalues, so it is UV-stable [27].

The RG flow of the couplings is shown in the streamplot in the left panel of figure 11, which shows the behaviors of the fixed points mentioned above (note that arrows represent flows to the IR).

5.2.2 Analysis of large λ_n

An interesting aspect of the RG flow is its behavior for large values of λ_n . In this region, we consider only the cubic terms in (5.2), and, as we discuss in section 4 (see item 5 in section 4.3), this behavior is universal for any value of λ .

We compute the direction of the flow (inward or outward) predicted from the cubic terms in the right panel of figure 11, where we plot a circle centered at the origin with large radius, on top of a stream plot like that in the left panel.

For finite λ , angles for which the flow points inward can either land at an IR-stable point, or turn around and flow to infinity. Angles for which the flow points outward will only flow to infinity. This simple test restricts the possible domains of attraction of a possible IR fixed point.

	γ	$\text{ind}_p = (-1)^\gamma$	Num. of points	$\sum \text{ind}_p$
IR fixed points	0	+1	1	1
Mixed fixed points	1	-1	4	-4
UV fixed points	2	+1	2	2
Total			7	-1

Table 4. Summary of the $N_f = 2$ fixed points with $\lambda \ll 1$. We denote by γ the number of relevant directions at each point. The importance of ind_p is discussed in section 5.5.2.

5.2.3 Analysis for $\lambda \ll 1$

We can now use the perturbative results obtained in (5.3) to see what happens to the degenerate free fixed point when turning on a finite λ . Solving the equations, we find four fixed points at

$$\begin{aligned}
(\lambda_{SSS}, \lambda_{SAA}) : & \left(\frac{1}{6} \left(\frac{\lambda}{4\pi} \right)^2, \frac{1}{3} \left(\frac{\lambda}{4\pi} \right)^2 \right), \left(\frac{3}{2} \left(\frac{\lambda}{4\pi} \right)^2, 3 \left(\frac{\lambda}{4\pi} \right)^2 \right), \\
& \left(\frac{1}{42} (131 - 2\sqrt{22}) \left(\frac{\lambda}{4\pi} \right)^2, \frac{1}{7} (5 - 2\sqrt{22}) \left(\frac{\lambda}{4\pi} \right)^2 \right), \\
& \left(\frac{1}{42} (2\sqrt{22} + 131) \left(\frac{\lambda}{4\pi} \right)^2, \frac{1}{7} (2\sqrt{22} + 5) \left(\frac{\lambda}{4\pi} \right)^2 \right).
\end{aligned} \tag{5.5}$$

The first point $\left(\frac{1}{6} \left(\frac{\lambda}{4\pi} \right)^2, \frac{1}{3} \left(\frac{\lambda}{4\pi} \right)^2 \right)$ is UV-stable, the last point is IR-stable, and the middle two points are mixed. We summarize the number of fixed points of any type for $\lambda \ll 1$ in table 4.

The stream plot zoomed on the points in (5.5) is given in the left panel of figure 12. As can be seen from the figure, couplings inside the ‘polygon’ created by the perturbative fixed points flow to the IR fixed point. This shows that the area in the coupling space which flows to the IR-stable point is bounded from below by $\sim \lambda^4$.

To find the global structure of the flows to the IR fixed point, we solved equations (5.2) and (5.3) together, by adding the linear and constant terms in (5.3) to (5.2). Since $\lambda \ll 1$, this has a minor effect on the flow far from $\lambda_n = 0$, but it splits the degenerate fixed point into the four points in (5.5).

In the right panel of figure 12 we show the basin of attraction to the IR fixed point for $\lambda = 0.2$. We see from this figure that there is deformation of the UV-stable fixed point at (96, 192) which flows to the IR fixed point, and passes near the mixed fixed point (96, 0). We also see that unlike the single flavor case in section 3, here the domain of attraction is non-compact, namely there is a flow to the IR-stable fixed point from infinity. We have checked numerically that the size of the basin of attraction of the IR-stable point decreases continuously to 0 as λ decreases. This stands in contrast to the single flavor case, in which the IR-stable fixed point’s basin of attraction stays finite even as $\lambda \rightarrow 0$, and is compact.

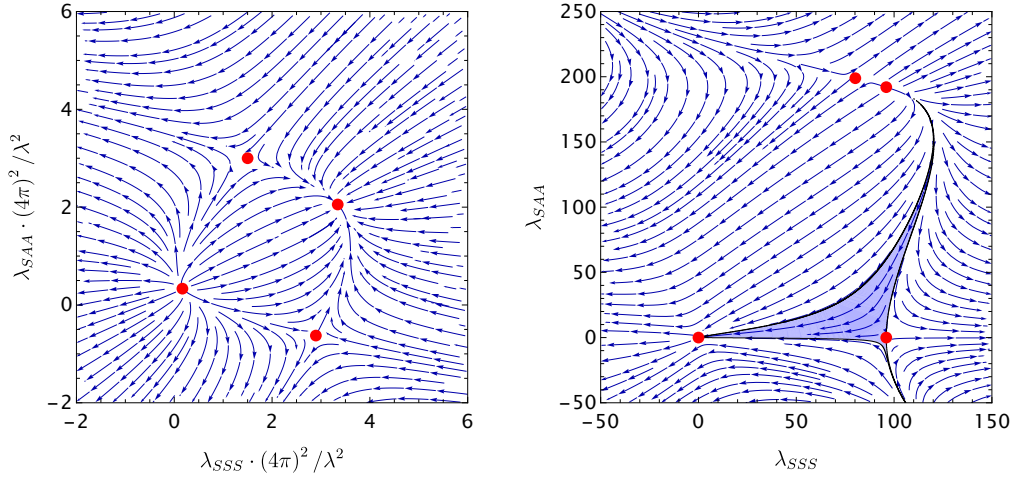


Figure 12. **Left:** Stream plot of flow to the IR of (minus) (5.3) for $N_f = 2$ and $\lambda = 0.2$. The fixed points (5.5) are shown in red. **Right:** The basin of attraction of the IR fixed point, overlaid on the beta function flows shown in figure 11.

5.3 The $N_f \geq 3$ case

In this section we analyze the fixed points structure and the flows for the $N_f \geq 3$ case. Unlike $N_f = 2$, now the flow is three dimensional.

5.3.1 Analysis for $\lambda = 0$

The number of fixed points predicted by the beta functions (5.2) depends on the number of flavors N_f , and can be found directly by solving the equations for each N_f . We summarize the number of fixed points, and the number of relevant directions of each such fixed point (obtained by diagonalizing the derivative matrix of the beta function $\partial_i \beta_j$ at each point, and counting the number of negative eigenvalues), in table 5.

Out of all the fixed points, there are three fixed points with simple expressions [27]

$$(\lambda_{SSS}, \lambda_{SAA}, \lambda_{AAA}) : (0, 0, 0), \left(\frac{384}{N_f^2}, 0, 0 \right), \left(\frac{384}{N_f^2}, \frac{384}{N_f}, 192 \right). \quad (5.6)$$

The additional 4 fixed points that exist for $N_f \geq 10$ converge to the point $(0, 0, 192)$ as we take $N_f \rightarrow \infty$. We elaborate on this limit in section 5.4.

Unlike the cases $N_f = 1, 2$, for $N_f \geq 3$ there are two fixed points in which the derivative matrix of the beta function $\partial_i \beta_j$ is a degenerate matrix. For the point $(0, 0, 0)$ we have $\partial_i \beta_j = 0$, and so it is degenerate in all of the directions. For the point $\left(\frac{384}{N_f^2}, 0, 0 \right)$ there is one zero, one positive, and one negative eigenvalue. The point $\left(\frac{384}{N_f^2}, \frac{384}{N_f}, 192 \right)$ is a mixed fixed point.

N_f	$\gamma = 0$ IR-stable	$\gamma = 1$	$\gamma = 2$	$\gamma = 3$ UV stable	Degenerate points	Total num. of fixed points	$\sum \text{ind}_p$
3	0	1	4	0	2	7	3
4-9	0	0	2	1	2	5	1
10\leq	0	0	3	2	2	7	1

Table 5. Summary of the $N_f > 2$ fixed points with $\lambda = 0$. We denote by γ the number of relevant directions at each point. In our case, the degenerate points do not contribute to the sum in the last column, whose importance is explained in section 5.5.2. The fact that this sum differs between $N_f = 3$ and $N_f > 3$ is also discussed in section 5.5.2.

5.3.2 Analysis of large λ_n

One can perform a similar analysis to the one done in section 5.2.2 and analyze the RG flow for large couplings, considering only the (universal) cubic terms. Since the RG flow in this case is three dimensional, the origin is circled by a sphere S^2 instead of S^1 as in the $N_f = 2$ case.

We parametrize the different couplings on the sphere as

$$\lambda_{AAA} = R \cos(\theta), \lambda_{SAA} = R \sin(\theta) \sin(\phi), \lambda_{SSS} = R \sin(\theta) \cos(\phi), \quad (5.7)$$

with $R \rightarrow \infty$. The direction of the flow, as a function of $\theta \in [0, \pi]$ and $\phi \in [0, 2\pi]$, for different values of N_f , is shown in figure 13. We see that there is a qualitative difference between the behavior for $N_f = 3$ and for $N_f > 3$ (which are all similar to each other), which is that for $\theta \sim 0, \pi$ the flow for $N_f = 3$ is inward, unlike the $N_f > 3$ case. This stems from the factor of $(N_f^2 - 12)$ in front of λ_{AAA}^3 in β_{AAA} in (5.2), which flips sign between $N_f = 3$ and $N_f = 4$.

5.3.3 Analysis for $\lambda \ll 1$

We now turn to study what happens to the degenerate *free* fixed point when we turn on a small coupling λ .

Solving the beta functions (5.3) for various values of N_f , we find that the free point splits into 6 points (with the exception of $N_f = 4$), where there is always a UV-stable fixed point, and for $N_f \geq 5$ there is also an IR-stable fixed point. Two of the points have simple solutions (the second point is for any $N_f \geq 4$):

$$(\lambda_{SSS}, \lambda_{SAA}, \lambda_{AAA}) : \left(\frac{6}{N_f^2} \left(\frac{\lambda}{4\pi} \right)^2, \frac{6}{N_f} \left(\frac{\lambda}{4\pi} \right)^2, 3 \left(\frac{\lambda}{4\pi} \right)^2 \right), \quad (5.8)$$

$$\left(\frac{2}{3N_f^2} \left(\frac{\lambda}{4\pi} \right)^2, \frac{2}{3N_f} \left(\frac{\lambda}{4\pi} \right)^2, \frac{1}{3} \left(\frac{\lambda}{4\pi} \right)^2 \right),$$

where the first point in (5.8) is mixed, while the second point is UV-stable. We summarize the number of fixed points and their types in table 6. As apparent from (5.2), the coupling values scale as λ^2 .

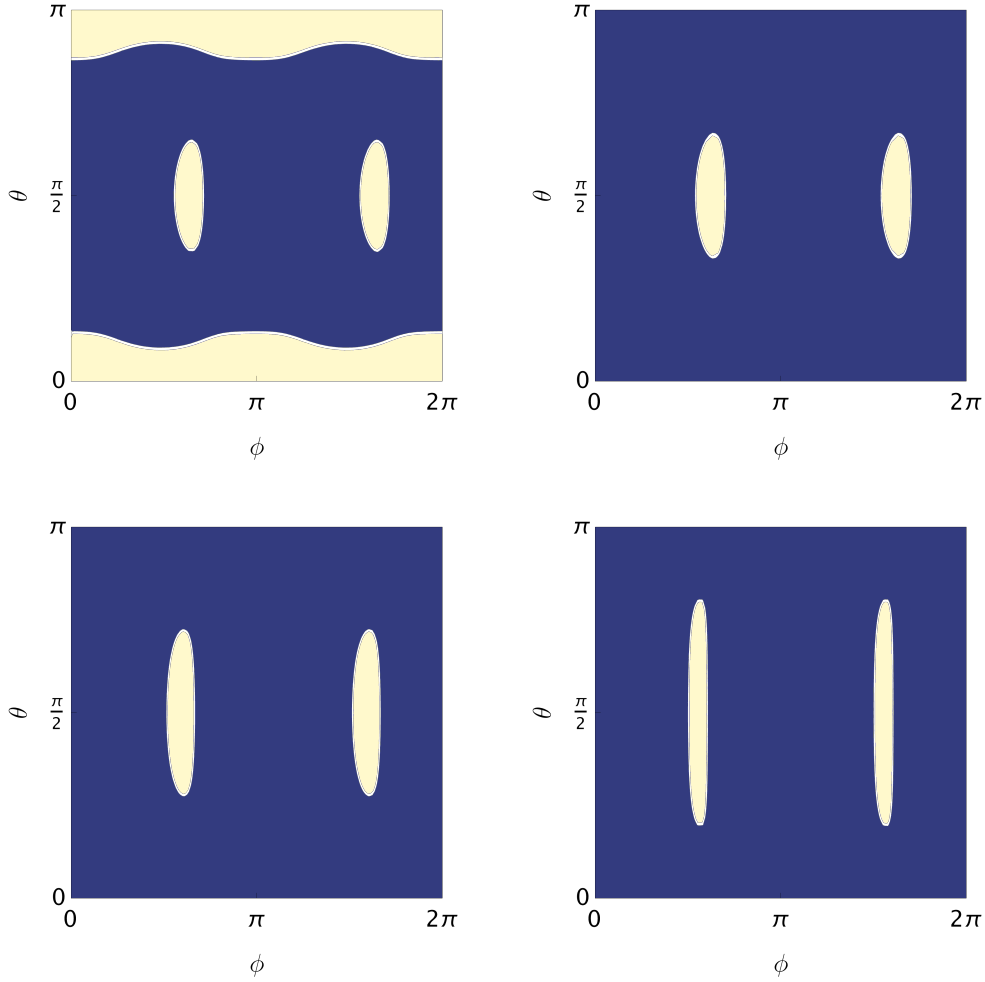


Figure 13. Direction of the flow to the IR of (minus) the cubic term in (5.2) for $N_f = 3$ (**upper left**), for $N_f = 4$ (**upper right**), for $N_f = 10$ (**bottom left**), and for $N_f = 50$ (**bottom right**). **Blue**- The direction is outward (to infinity), **Yellow**- The direction is inward.

For $N_f \geq 5$, We find that the 3D polygon generated by the points is in the basin of attraction of the IR-stable fixed point, so the area of the basin of attraction grows at least as λ^6 . Furthermore, we also find that there is a direction from infinity that flows to the IR-stable fixed point. Like in the $N_f = 2$ case, it seems that the area of the basin of attraction goes to zero smoothly as $\lambda \rightarrow 0$.

The methods presented above are insufficient to determine what happens to the degenerate fixed point $\left(\frac{384}{N_f^2}, 0, 0\right)$, which may be eliminated by the small- λ corrections or split into several non-degenerate fixed points. The beta functions (5.3) were calculated in perturbation theory around the free fixed point, and not around a point for which one of the couplings (λ_{SSS}) is finite. However, since already for $\lambda = 0$ this fixed point had an IR-unstable direction, it is clear that it cannot lead to an IR-stable fixed point at small

N_f	$\gamma = 0$ IR-stable	$\gamma = 1$	$\gamma = 2$	$\gamma = 3$ UV stable	Total num. of fixed Points
3	0	2	3	1	6
4	0	1	2	1	4
5 \leq	1	2	2	1	6

Table 6. Summary of $N_f > 2$ and $\lambda \ll 1$ fixed points near $(0, 0, 0)$. We denote by γ the number relevant directions at each point. Note that there are no longer any degenerate fixed points in that area. Also note that the sum $\sum \text{ind}_p$ for these points is 0 for any N_f , this is because all these points came from a splitting of a degenerate fixed point, as explained in section 5.5.2.

λ . In section 5.4.3, we show that in the large N_f limit in which the CS coupling scales as $\lambda \sim \frac{1}{N_f}$, this point can be treated perturbatively, and that it splits for small λ .

5.4 The limit $N_f \rightarrow \infty$

In this section we focus on the limit $N_f \rightarrow \infty$. We start by taking the limit $N_f \rightarrow \infty$ of the beta functions (5.2) and (5.3), and show that the derivation of (5.3) is inconsistent with this limit. Then, we take a double scaling limit, in which we can use the calculation above, and we show that the IR-stable fixed point merges with another fixed point and disappears as λ is increased. Finally, we look concretely at the $(2, 1, 0)$ scaling.

All the solutions found in this section are presented to leading relevant order in $\frac{1}{N_f}$, we drop the $\mathcal{O}(N_f^{-\alpha})$ notation for convenience whenever explicit solutions are discussed.

5.4.1 The $\lambda = 0$ case

It is interesting to check how the fixed point solutions found above behave in the large $N_f \rightarrow \infty$. A naive approach would be to scale the parameters according to the scalings of (4.26), and solve at leading order in the large N_f expansion (e.g. substituting into (4.29) the values in table 3).

However, this does not give us all the possible solutions with that leading order scaling of N_f . The reason is that the leading order of the N_f expansion might vanish, or give us degenerate answers (see section 5.4.4 for a concrete example of degeneracy that forces us to use the next orders). Thus, we need to use the subleading orders of $\frac{1}{N_f}$ to determine the couplings, and those depend on the subleading scalings of the running couplings λ_n .

Therefore, in order to apply perturbation theory correctly, one has to write the couplings as a series

$$\begin{aligned}
\lambda_{SSS} &= \frac{1}{N_f^a} \left(y_{SSS} + \frac{z_{SSS}}{N_f} + \frac{w_{SSS}}{N_f^2} + \frac{x_{SSS}}{N_f^3} \dots \right), \\
\lambda_{SAA} &= \frac{1}{N_f^b} \left(y_{SAA} + \frac{z_{SAA}}{N_f} + \frac{w_{SAA}}{N_f^2} + \frac{x_{SAA}}{N_f^3} \dots \right), \\
\lambda_{AAA} &= \frac{1}{N_f^c} \left(y_{AAA} + \frac{z_{AAA}}{N_f} + \frac{w_{AAA}}{N_f^2} + \frac{x_{AAA}}{N_f^3} \dots \right),
\end{aligned} \tag{5.9}$$

with a , b , c as in (4.26), and to solve the vanishing of the beta functions (5.2) order by order in $\frac{1}{N_f}$ for $y_n, z_n, w_n, x_n, \dots$ ³⁶. Doing so, we find that at leading order in $\frac{1}{N_f}$, the three analytic solutions presented in (5.6), two additional UV-stable fixed points

$$(\lambda_{SSS}, \lambda_{SAA}, \lambda_{AAA}) : \left(\frac{384\sqrt{2}}{N_f^2}, \frac{384}{N_f} - \frac{768(-1+\sqrt{2})}{N_f^3}, 192 + \frac{3072(-1+\sqrt{2})}{N_f^4} \right), \quad (5.10)$$

$$\left(\frac{-384\sqrt{2}}{N_f^2}, \frac{384}{N_f} + \frac{768(1+\sqrt{2})}{N_f^3}, 192 - \frac{3072(1+\sqrt{2})}{N_f^4} \right),$$

have the $(2, 1, 0)$ scaling, and two additional mixed fixed points have the $(\frac{2}{3}, \frac{1}{3}, 0)$ scaling

$$(\lambda_{SSS}, \lambda_{SAA}, \lambda_{AAA}) : \left(\frac{-64\sqrt{6}}{N_f^{2/3}}, \frac{64\sqrt{6}}{N_f^{1/3}}, 192 - \frac{256}{N_f^{2/3}} \right), \left(\frac{64\sqrt{6}}{N_f^{2/3}}, \frac{-64\sqrt{6}}{N_f^{1/3}}, 192 - \frac{256}{N_f^{2/3}} \right). \quad (5.11)$$

Note that the points in (5.10) and (5.11) have additional higher order corrections in all of their components. The way they are written here is to emphasize that different subleading orders in several couplings can affect the leading order of others. For example, in the first point in (5.10), we have $\lambda_{AAA} = 192 + \frac{3072(-1+\sqrt{2})}{N_f^4} + \mathcal{O}\left(\frac{1}{N_f^5}\right)$, and the correction to the leading order of λ_{AAA} (i.e. $\frac{3072(-1+\sqrt{2})}{N_f^4}$) affects the leading values of y_{SSS} .

In total we find 7 solutions, as indeed expected from table 5.

5.4.2 Very small λ

As in the $\lambda = 0$ case, we can apply the $N_f \rightarrow \infty$ limit to (5.3) and find analytically the leading order (in $\frac{1}{N_f}$) dependence of the fixed points arising from the splitting of the $\lambda_{SSS} = \lambda_{SAA} = \lambda_{AAA} = 0$ degenerate point.

In section 5.3.3, we saw that (5.3) predicted that there are six such fixed points for $N_f \geq 5$ (see table 6), with two of them given exactly by (5.8), both of which have the scaling $(2, 1, 0)$.

Using the same methods as in section 5.4.1, we can find the leading scalings of the additional fixed points. There is one additional mixed ($\gamma = 1$) fixed point with leading $(2, 1, 0)$ scaling

$$(\lambda_{SSS}, \lambda_{SAA}, \lambda_{AAA}) : \left(\frac{294}{25} \frac{1}{N_f^2} \left(\frac{\lambda}{4\pi} \right)^2, -\frac{18}{5} \frac{1}{N_f} \left(\frac{\lambda}{4\pi} \right)^2, \left(3 + \frac{1}{N_f^2} \frac{576}{25} \right) \left(\frac{\lambda}{4\pi} \right)^2 \right). \quad (5.12)$$

These are only 3 points. In order to find the other 3 we must relax the assumption that the leading powers in (5.9) are constrained by (4.26) (we'll explain what this relaxation

³⁶Note that higher-order corrections of N_f do not necessarily appear with powers of $\frac{1}{N_f}$. In the $(\frac{2}{3}, \frac{1}{3}, 0)$ scaling, they may also involve fractional powers, such as $\frac{1}{N_f^{1/3}}$. This is seen explicitly in (5.11).

means momentarily). Doing this, we find two points with leading $(0, 0, 0)$ scaling

$$(\lambda_{SSS}, \lambda_{SAA}, \lambda_{AAA}) : \left(\frac{2}{3} (5 - \sqrt{5}) \left(\frac{\lambda}{4\pi} \right)^2, -\frac{2}{3} \sqrt{6\sqrt{5} - 10} \left(\frac{\lambda}{4\pi} \right)^2, \frac{1}{3} (2\sqrt{5} - 1) \left(\frac{\lambda}{4\pi} \right)^2 \right), \\ \left(\frac{2}{3} (5 - \sqrt{5}) \left(\frac{\lambda}{4\pi} \right)^2, \frac{2}{3} \sqrt{6\sqrt{5} - 10} \left(\frac{\lambda}{4\pi} \right)^2, \frac{1}{3} (2\sqrt{5} - 1) \left(\frac{\lambda}{4\pi} \right)^2 \right), \quad (5.13)$$

(both mixed with $\gamma = 2, 1$, respectively), and an IR-stable fixed point with the leading $(0, 1, 0)$ scaling

$$(\lambda_{SSS}, \lambda_{SAA}, \lambda_{AAA}) : \left(\frac{8}{3} \left(\frac{\lambda}{4\pi} \right)^2, \frac{2}{N_f} \left(\frac{\lambda}{4\pi} \right)^2, 3 \left(\frac{\lambda}{4\pi} \right)^2 \right). \quad (5.14)$$

Overall we found 6 points as indeed was expected.

While the points in (5.8) and (5.12) have one of the three allowed scalings presented in (4.26), the points in (5.13) and (5.14) have different scalings. This “contradiction” is resolved by a careful analysis of the different limits; (4.26) was derived under the assumption of taking $N_f \rightarrow \infty$ at a constant λ , while (5.3) assumes that λ is the smallest parameter (and, in particular, $\lambda \ll \frac{1}{N_f^2}$).

Indeed, one can check explicitly for the IR fixed point in (5.14) that the approximation which leads to (5.3) breaks. Since $\lambda_{SSS} \sim \lambda^2$, the cubic term in β_{SSS} (see (4.22) and (5.2)), which always exists, has the scaling of $N_f^3 \lambda_{SSS}^3 \sim N_f^3 \lambda^6$, while the linear term in (5.3) scales as $\lambda^2 N_f \lambda_{SSS} \sim N_f \lambda^4$. Thus, for $\lambda \sim \frac{1}{N_f}$, the cubic term is of the same order of magnitude as some of the terms in (5.3), and it is unjustified to ignore it. One can do the same scaling analysis for different terms in (5.3), and show that for the cubic terms to be smaller than all of them, we must demand $\lambda \ll \frac{1}{N_f^2}$.

We therefore expect that as we increase λ for constant, but large, values of N_f ³⁷ the 3 fixed points in (5.13) and (5.14) that have “wrong scalings” will merge in pairs with other fixed points (or with themselves) and disappear. More concretely, for large enough N_f , we expect that (for each of these fixed points) there exist $l_0, \alpha > 0$ with $\lambda_{crit} \simeq \frac{4\pi l_0}{N_f^\alpha}$ such that these fixed points merge with others at $\lambda = \lambda_{crit}$.

5.4.3 Tracking the IR-stable fixed point

In this section, we show explicitly how the IR-stable fixed point (5.14) merges with another fixed point, as we increase λ beyond the perturbative regime in which (5.3) holds. In order to see this we take a double scaling limit in which λ scales as $\lambda = \frac{4\pi l_0}{N_f}$, with l_0 a constant which does not scale with N_f .

The appropriate beta functions that describe this phenomenon are given by adding the cubic term in (5.2) to (5.3). By itself this will not yield a well defined expression in perturbation theory. It is not the beta function at leading order in λ , as there are also λ^2

³⁷Or equivalently, increase N_f for constant small λ .

corrections to the quadratic and cubic terms. Nor is it the leading order beta function in $\frac{1}{N_f}$, as it mixes different orders of $\frac{1}{N_f}$.

However, it is still useful in the double scaling limit, as it captures the leading order contribution in $\frac{1}{N_f}$ of each term separately³⁸. Now (in accordance with (5.14)) we scale

$$\lambda_{SSS} = \frac{y_{SSS}}{N_f^2}, \quad \lambda_{SAA} = \frac{y_{SAA}}{N_f^3}, \quad \lambda_{AAA} = \frac{y_{AAA}}{N_f^2}. \quad (5.15)$$

The beta functions (that contain the terms from both (5.2) and (5.3)) in this scaling become

$$\begin{aligned} \pi^2 N_c N_f^3 \beta_{SSS} &= - \frac{y_{SSS} (y_{SSS}^2 - 384 y_{SSS} + 1024 l_0^2)}{1024} + \mathcal{O}\left(\frac{1}{N_f}\right), \\ \pi^2 N_c N_f^4 \beta_{SAA} &= \frac{y_{SSS} + y_{AAA} - 3l_0^2}{4} y_{SAA} + \frac{3l_0^4 + y_{AAA}^2 - 2l_0^2 y_{SSS} - 4l_0^2 y_{AAA}}{4} + \mathcal{O}\left(\frac{1}{N_f}\right), \\ \pi^2 N_c N_f^3 \beta_{AAA} &= \frac{3 \left(y_{AAA} - \frac{l_0^2}{3}\right) (y_{AAA} - 3l_0^2)}{16} + \mathcal{O}\left(\frac{1}{N_f}\right), \end{aligned} \quad (5.16)$$

which now include all the leading order contributions.

From the first of these equations we see that the possible values of y_{SSS} at a fixed point are

$$y_{SSS} = 0, \quad 32 \left(6 - \sqrt{36 - l_0^2}\right), \quad 32 \left(6 + \sqrt{36 - l_0^2}\right), \quad (5.17)$$

and those of y_{AAA} are

$$y_{AAA} = \frac{1}{3} l_0^2, \quad 3l_0^2, \quad (5.18)$$

³⁸Consider for example, the constant term in β_{SSS} . It scales as $\frac{\lambda^4}{N_f} \sim \frac{1}{N_f^5}$. All higher corrections in $\frac{1}{N_f}$ of this term will scale with at least $\mathcal{O}\left(\frac{1}{N_f^6}\right)$.

It is possible to prove this statement by looking at the general case directly. We can compute this term by taking (4.22), and shifting G_{SAA} and G_{SSS} according to (4.9). We find

$$\begin{aligned} \text{Constant term in } \beta_{SSS} &= 6 \frac{\gamma'_S}{N_f^2} (\bar{G}_{3,3,\bar{g}_3=0}) - \delta G_{SSS} + \frac{1}{N_f} \frac{3(G_{5F} + G_{5N})}{\pi^2 G_2} \\ &\quad + \frac{1}{N_f} \frac{3(G_{4,1,F} + 2G_{4,1,N}) (\bar{G}_{3,3,\bar{g}_3=0})}{\pi^2 G_2^2} + \frac{1}{N_f} \frac{4(\bar{G}_{3,3,\bar{g}_3=0})^3}{\pi^2 G_2^3}, \end{aligned}$$

where we denoted $\bar{G}_{3,3,\bar{g}_3=0} \equiv \left\langle \tilde{J}_1^2(-p_1) \tilde{J}_2^3(-p_2) \tilde{J}_3^1(-p_3) \right\rangle_{\text{leading}}$. By going over the sum, and using the $N_f \rightarrow \infty$ scaling laws presented in section 4.4 (and the fact that $\bar{G}_{3,3,\bar{g}_3=0}$ has no scaling with N_f) we see that for constant λ , this term must be proportional to $\frac{1}{N_f}$ for large N_f . Thus, if we expand the constant term in β_{SSS} as a series in λ and $\frac{1}{N_f}$

$$\text{Constant term in } \beta_{SSS} = \sum_{i \in 2\mathbb{N}} f_i(N_f) \lambda^i,$$

we must have for all i that $f_i(N_f)$ scales as at most as $\frac{1}{N_f}$. Since we take a double scaling limit in which $\lambda \sim \frac{1}{N_f}$, the term $\frac{\lambda^4}{N_f}$ has the highest order in $\frac{1}{N_f}$ (as there are no terms with λ^0 or λ^2 ; otherwise, they would have appeared in (5.3)).

We can now go term by term in (4.22) and show that it gives the leading order in $\frac{1}{N_f}$, in a similar fashion.

and for each choice y_{SSA} is determined (except for the choice $y_{SSS} = 0, y_{AAA} = 3l_0^2$, for which its beta function vanishes at leading order).

The solutions with $y_{SSS} = 32 \left(6 + \sqrt{36 - l_0^2} \right)$, which are

$$\left(\frac{32 \left(6 + \sqrt{36 - l_0^2} \right)}{N_f^2}, \frac{2 \left(l_0^2 - 24\sqrt{36 - l_0^2} + 144 \right)}{3N_f^3}, \frac{l_0^2}{3N_f^2} \right), \left(\frac{32 \left(6 + \sqrt{36 - l_0^2} \right)}{N_f^2}, \frac{2l_0^2}{N_f^3}, \frac{3l_0^2}{N_f^2} \right), \quad (5.19)$$

correspond to two fixed points which originate from the degenerate point at $\left(\frac{384}{N_f^2}, 0, 0 \right)$ ³⁹.

The other solutions describe the splitting of the free degenerate fixed point $(0, 0, 0)$, one of them is the IR fixed point, which corresponds to $\left(\frac{32(6 - \sqrt{36 - l_0^2})}{N_f^2}, \frac{2l_0^2}{N_f^3}, \frac{3l_0^2}{N_f^2} \right)$ ⁴⁰. Note that there is a degeneracy for β_{SSA} when $y_{SSS} = 0, y_{AAA} = 3l_0^2$. This means that in order to determine the fixed points for this case we must go to subleading corrections in N_f , which will result in three different points (this is inferred by counting, as we showed in section 5.3.3 that there are in total six fixed points)⁴¹.

As we increase l_0 from 0 to 6, the two points with $y_{SSS} = 32 \left(6 - \sqrt{36 - l_0^2} \right)$ and the two points with $y_{SSS} = 32 \left(6 + \sqrt{36 - l_0^2} \right)$ get closer to each other. At $l_0 = 6$ those points merge to a degenerate point, and for $l_0 > 6$ they no longer exist.

Thus, we managed to show analytically that the IR-stable fixed point disappears, at least at large values of N_f , at $\lambda_{crit} \simeq \frac{24\pi}{N_f}$. Since the perturbative parameter in the equations is $\left(\frac{\lambda}{4\pi} \right)^2 = \frac{l_0^2}{N_f^2}$, we can trust this analysis as long as $\frac{l_0^2}{N_f^2} \ll 1$. A visualization of the merging of points is presented in figure 14 for $N_f = 1000$ and different values of λ . We see that the two degenerate points for $\lambda = 0$ split, and 2 pairs of points merge at the critical value of λ .

5.4.4 The $(2, 1, 0)$ case

The $(2, 1, 0)$ scaling possesses a specific physical significance, and so here we examine this case in greater detail. For this scaling, the beta functions at leading order in $1/N_f$ and at

³⁹Indeed $32 \left(6 + \sqrt{36 - l_0^2} \right) \rightarrow 384$ in the limit $l_0 \rightarrow 0$. This also justifies our claim in the end of section 5.3.3.

⁴⁰For very small l_0 , this indeed reproduces (5.14), and one can check explicitly the derivative matrix of (5.16) and see that this is a fixed point.

⁴¹It is instructive to revisit the fixed points found in the regime $\lambda \ll 1$ and identify their corresponding solutions in the language used here. The second point in (5.8), which is a UV fixed point, corresponds to $y_{SSS} = 0$ and $y_{AAA} = \frac{1}{3}l_0^2$. This is confirmed by examining the beta functions in (5.16), where the structure of the derivative matrix indicates a UV fixed point.

The first point in (5.8), as well as the point in (5.12), both correspond to the degenerate solution $y_{SSS} = 0, y_{AAA} = 3l_0^2$. There is another point corresponds to the degenerate solution, as well as to the case of $y_{SSS} = 32 \left(6 - \sqrt{36 - l_0^2} \right), y_{AAA} = \frac{1}{3}$. Those two correspond (by elimination of other possibilities) to the two fixed points in (5.13). However, this correspondence is not immediately evident from the expression in (5.13), as that result is valid only in the regime $\lambda \ll \frac{1}{N_f}$, while in this section we consider a different scaling.

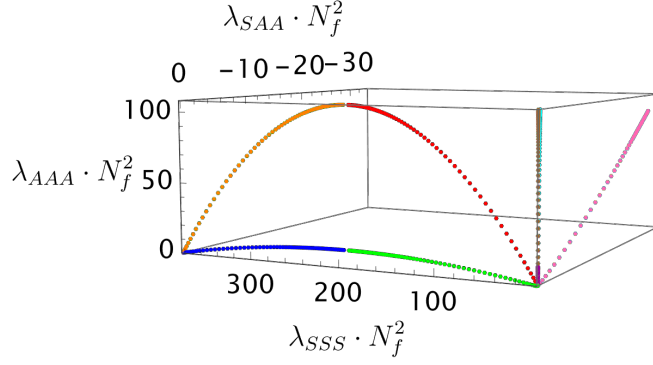


Figure 14. The fixed points of (5.16) (including next order corrections that break the degeneracy) at different values of $0 < l_0 < 6$. The degenerate fixed points at $(0, 0, 0)$ and $(\frac{384}{N_f^2}, 0, 0)$ (for $\lambda = 0$) split and some of the resulting fixed points merge and disappear at $l_0 = 6$. The IR-stable fixed point is denoted in red, the other fixed points discussed in the text appear as well (note that the purple, brown and cyan fixed points appear very close to one another).

$\lambda = 0$ are given by (substituting into (4.29) the values in table 3)

$$\begin{aligned} \pi^2 N_c \frac{\beta_{y_{SSS}}}{N_f} &= -\frac{(y_{SAA} - 384) y_{SAA}^2}{1024} + \mathcal{O}\left(\frac{1}{N_f}\right), \\ \pi^2 N_c \frac{\beta_{y_{SAA}}}{N_f} &= \frac{y_{AAA} (128 y_{AAA} - y_{SAA} (y_{AAA} - 128))}{512} + \mathcal{O}\left(\frac{1}{N_f}\right), \\ \pi^2 N_c \frac{\beta_{y_{AAA}}}{N_f} &= -\frac{(y_{AAA} - 192) y_{AAA}^2}{1024} + \mathcal{O}\left(\frac{1}{N_f}\right), \end{aligned} \quad (5.20)$$

where the y_n are given by (see table 3 and the definition of Y_n in (4.28))

$$y_{SSS} = N_c^2 Y_{SSS} + 128, \quad y_{SAA} = N_c^2 Y_{SAA} + 128, \quad y_{AAA} = N_c^2 Y_{AAA} + 64. \quad (5.21)$$

We see that the degeneracies discussed in section 4.4.1 apply in this case for (5.20), since both $\gamma'_S = 0$, and the condition (4.30) is satisfied. First, solving $\beta_{y_{AAA}} = 0$, we find $y_{AAA} = 0$ or $y_{AAA} = 192$. In the $y_{AAA} = 0$ case, $\beta_{y_{SAA}}$ automatically vanishes, and we cannot determine y_{SAA} from the equation $\beta_{y_{SAA}} = 0$. Second, y_{SSS} does not appear in the leading order beta functions, but instead the equation $\beta_{y_{SSS}} = 0$ becomes an additional condition for y_{SAA} . Solving for y_{SAA} , we find the following possibilities⁴²

$$(y_{SAA}, y_{AAA}) : (0, 0), (384, 192), (384, 0). \quad (5.22)$$

To remove the degeneracies mentioned above, we must go to the next order of $\frac{1}{N_f}$, and apply the approach presented by (5.9). Doing so, we find in total 5 points - the 3 points in (5.6) and the 2 points in (5.10).

⁴²Note that the solution $(384, 0)$ in (5.22) disappears at the next order in $\frac{1}{N_f}$ (i.e, there are no perturbed solutions of the form (5.9) around this solution), and so there are no solutions with these values.

We see explicitly how a degeneracy adds possible solutions. In the generic case described in (4.4.1), there should be only one fixed point with $y_{AAA} = 192$, corresponding to the single root in β_{AAA} in (5.20). However, we find explicitly three such solutions - the last point in (5.6), and the two points (5.10).

As we turn on finite λ , our generic expectation is that the degeneracies of (4.29), which appear for the $\lambda = 0$ case in (5.20), will disappear. It is easy to see that this is the case for at least one of the degeneracies: in the region $\lambda \ll \frac{1}{N_f^2}$ we have $\gamma'_S/N_f \sim \lambda^2$, and this adds a linear term in λ_{SSS} in β_{SSS} . Indeed, taking the $N_f \rightarrow \infty$ limit of (4.28) in equation (5.3) we find

$$\begin{aligned}\pi^2 N_c \frac{\beta_{y_{SSS}}}{N_f} &= \frac{1}{8} \left(-8y_{SSS} + 3 \left(y_{SAA} - 2 \left(\frac{\lambda}{4\pi} \right)^2 \right)^2 \right) + \mathcal{O} \left(\frac{1}{N_f}, \lambda^2 \right), \\ \pi^2 N_c \frac{\beta_{y_{SAA}}}{N_f} &= \frac{1}{4} \left(y_{AAA} - 3 \left(\frac{\lambda}{4\pi} \right)^2 \right) \left(y_{SAA} + y_{AAA} - \left(\frac{\lambda}{4\pi} \right)^2 \right) + \mathcal{O} \left(\frac{1}{N_f}, \lambda^2 \right), \\ \pi^2 N_c \frac{\beta_{y_{AAA}}}{N_f} &= \frac{3}{16} \left(y_{AAA} - 3 \left(\frac{\lambda}{4\pi} \right)^2 \right) \left(y_{AAA} - \frac{1}{3} \left(\frac{\lambda}{4\pi} \right)^2 \right) + \mathcal{O} \left(\frac{1}{N_f}, \lambda^2 \right),\end{aligned}\quad (5.23)$$

and there is a linear term of y_{SSS} in β_{SSS} .

The second degeneracy is not removed in (5.23). We see that for $y_{AAA} = 3 \left(\frac{\lambda}{4\pi} \right)^2$, we have $\beta_{y_{AAA}} = \beta_{y_{SAA}} = 0$ at leading order of $\frac{1}{N_f}$. There are thus two possibilities: the first is that this degeneracy is removed when going to the next order of perturbation theory in λ . The second is that the condition (4.30) persists to all values of λ (in the large N_f limit).

Whether the degeneracy is removed or not, we can use (5.3), (5.20), and (5.23) to search for the possible points with the scaling (5.9) for $(a, b, c) = (2, 1, 0)$ and $\lambda \ll \frac{1}{N_f^2}$. Solving for y_{AAA} , the three possibilities are:

1. $y_{AAA} = 192 + \mathcal{O}(\lambda^2)$: For this solution, there is no degeneracy of β_{SAA} , and so by (5.20) we get $y_{SAA} = 384 + \mathcal{O}(\lambda^2)$. Since the degeneracy in y_{SSS} is removed, there will be for finite $\lambda \ll 1$ only one point with the leading scaling of $(2, 1, 0)$. One might think that since $\gamma'_S \sim \mathcal{O}(\lambda^2)$, the solution of y_{SSS} will be $y_{SSS} \sim \mathcal{O}(\lambda^{-2})$, but this is not true because the other terms in the beta function also vanish as $\lambda \rightarrow 0$ for this fixed point and depend on even powers of λ . In any case, one of the 3 points with $y_{AAA} = 192$ and $y_{SAA} = 384$ (that is, the two points in (5.10) and the last point in (5.6)) will preserve the scaling of $(2, 1, 0)$ as we turn on λ , even beyond perturbation theory, while the other two points will presumably get a different scaling.
2. $y_{AAA} = \frac{1}{3} \left(\frac{\lambda}{4\pi} \right)^2$: For this solution, there is no degeneracy in (5.23) and so there will be only one solution with the scaling of $(2, 1, 0)$, and we already found this point at small λ : the second point in (5.8).
3. $y_{AAA} = 3 \left(\frac{\lambda}{4\pi} \right)^2$: For this solution, there is a degeneracy in (5.23), and so, at least at leading order in λ^2 , there might be several points with this scaling. The possible points are the first point in (5.8) and the point in (5.12). From this analysis only, it

is also possible that the fixed point $\left(\frac{384}{N_f^2}, 0, 0\right)$, splits under perturbation theory into two points with $y_{AAA} = 3\left(\frac{\lambda}{4\pi}\right)^2$, and gives two more candidates for fixed points with the scaling of $(2, 1, 0)$. However, from the analysis in section 5.4.3 we see that those two points have different scalings. If the degeneracy is removed at higher orders in λ , then one of the points necessarily loses the scaling of $(2, 1, 0)$ as we go to higher orders of perturbation theory in λ . If the degeneracy remains then possibly both can have the scaling.

5.5 General discussion – elimination, splitting, and merging of fixed points

Our objective in this section is twofold - first, we wish to gain additional understanding of the structure of solutions to the vanishing of the beta functions (5.2) and (5.3). Second, we develop tools to analyze what can happen to the fixed points beyond the perturbative region of small λ .

In section 5.5.1, we take a ‘static’ approach by focusing on the fixed points as roots of a system of polynomials. This will involve mostly elementary complex analysis. In section 5.5.2, we look at the flow induced by the beta functions, and classify the points according to their Poincaré–Hopf index. This gives topological constraints for the possible splittings and mergings of fixed points.

5.5.1 Complex analysis perspective

We showed in section 4 that the general form of the beta functions of the marginal couplings λ_n is exactly (at order $\frac{1}{N_c}$) a system of cubic polynomials in the couplings. As such, searching for fixed points of the flow is equivalent to finding the roots of a system of three polynomials of degree three in three variables (with coefficients that depend on λ).

By Bézout’s Theorem, the total number of zeros (including degeneracies) over the complex plane of three polynomials of degree three in three variables is equal to or lower than 27^{43} . Since all the coefficients of the polynomials are real, solutions with an imaginary part must come in pairs (i.e. if $(\lambda_{SSS}, \lambda_{SAA}, \lambda_{AAA})$ is a complex root of the beta functions, so is $(\lambda_{SSS}^*, \lambda_{SAA}^*, \lambda_{AAA}^*)$). Thus, the number of real solutions (including degeneracies) must be odd.

To emphasize this point, we work out explicitly the example of (5.2) with $N_f = 3$. The algebraic degeneracy of the point $(0, 0, 0)$ is $2^3 = 8$, while for the point $\left(\frac{384}{N_f^2}, 0, 0\right)$ the

⁴³This is sometimes known as the Bézout bound. The exact statement of Bézout’s Theorem for n homogeneous polynomials in $n + 1$ variables is that the number of solutions on the projective plane is the multiplication of their degrees. Our polynomials are not homogeneous, but using homogenization (i.e, defining $P^h(x_0, x_1, \dots) = x_0^d P\left(\frac{x_1}{x_0}, \dots\right)$ with d the degree of p) we can apply the theorem, any solution with $x_0 \neq 0$ corresponds to a complex solution in our case, while solutions with $x_0 = 0$ are solutions “at infinity” and therefore the statement in the text is only an upper bound (that is generically saturated). If the polynomials have a common component, the number of solutions might be uncountable.

degeneracy is 2⁴⁴. Adding the other 5 real non degenerate fixed points, one finds in total $2 + 8 + 5 = 15$ real solutions. Indeed, solving (5.2) with $N_f = 3$ over the complex plane, one finds 12 solutions with non-zero imaginary part. This analysis extends to all $N_f \geq 3$ (with different numbers of complex solutions).

We now turn to see how the solutions change under continuous changes in the coefficients of the polynomials, which in our case corresponds to turning on a finite λ . As a consequence of the pairing of points with imaginary part, real roots can't be eliminated on their own (that is, lifted from the real line to the complex plane), but must do so in pairs. That is to say, for a point to gain an imaginary part and be lifted from the real line, there must be another point with the same real part, which gains the opposite imaginary part. For this process to occur, the two points must have the same real part, before the small perturbation lifts them. This means that the only way a point can be eliminated in the process of continuously changing the polynomial coefficients, is by first merging with another point, and only after this merger the resulting degenerate point can be eliminated (see figure 4 for a pictorial example in one variable).

The conclusion of the analysis above, is that from the perspective of complex analysis, fixed points cannot be added or removed arbitrarily, but only in pairs, and then there must be a critical value of λ for which there is a degenerate point. At such a degenerate point the CFT has a marginal deformation.

A similar analysis can be done to investigate the $N_f \rightarrow \infty$ limit, and in particular the $(2, 1, 0)$ scaling. As discussed in section 5.4.4, generically (i.e, assuming that (4.30) does not hold, and $\gamma'_S \neq 0$) (4.29) has exactly 3 solutions (including multiplicity), but (4.22) can, and indeed does, have many more solutions (see tables 5 and 6). It is therefore interesting to ask what happens to these solutions as $N_f \rightarrow \infty$?

To answer this question, we define Y_n as in (4.28) and look at $\delta \equiv \frac{1}{N_f}$ as a continuous variable. For $\delta = 0$, and λ now held constant at some non-zero value, we get equation (4.29) exactly (without higher order corrections). It is therefore evident from the discussion above that (assuming generic behavior) only 3 solutions can have the scaling (4.27): if two solutions merge into one in that limit, it is counted as a multiplicity and the resulting point will be degenerate. Every other solution must either merge and be eliminated at finite N_f , or go to infinity in the Y_n coordinates.

5.5.2 Topological perspective

There is a deep connection between the local properties of the flow around the fixed points, and the overall topology of the flow. We can use such connections to restrain if and how fixed points can split, merge, or be eliminated. We start by looking at the process of degenerate point splitting, and then use the Poincaré–Hopf theorem to gain insight into global restrictions on the fixed point structure.

⁴⁴One can see that by Taylor expanding around these points. Around the free fixed point all the beta functions are polynomials of degree 2, while around $\left(\frac{384}{N_f^2}, 0, 0\right)$, $\beta_{SSS/AAA}$ are linear and β_{AAA} is of degree 2.

For each fixed point we evaluate the derivative matrix of the beta functions $\partial_i \beta_j$ for this point. The eigenvectors and eigenvalues of the $\partial_i \beta_j$ matrix characterize the structure of the flow around this fixed point. Each positive eigenvalue corresponds to an irrelevant deformation (when decreasing the energy scale) in the direction of its corresponding eigenvector, and each negative eigenvalue corresponds to a relevant deformation. If one or more of the eigenvalues is zero, we call this point a *degenerate* point (the point is degenerate in that sense, if and only if it is algebraically degenerate).

Perturbations of a given flow can either split or eliminate degenerate fixed points (as discussed above), while non-degenerate fixed points are protected under infinitesimal changes of the flow⁴⁵. Note that due to continuity, if the original degenerate point had non-degenerate directions (i.e, non-zero eigenvalues), the signs of the eigenvalues in these directions stays the same for the resulting fixed points after the splitting.

There are also global constraints on the types and numbers of fixed points. As discussed in point 5 of section 4.3, the flow at large values of λ_n is the same for every value of λ . One can then assign a “Poincaré–Hopf index” to the flow at infinity, that is constant for any value of λ . The index of a point ind_p is defined as the degree of the map $u : \partial D \rightarrow S^{n-1}$, where D is a closed ball around the fixed point, and u is the normalized flow⁴⁶.

The Poincaré–Hopf theorem asserts that the sum of the Poincaré–Hopf indices of all the fixed points + infinity is constant. Since in our case the index at infinity is constant for every λ , so is the sum of all the fixed points (not including infinity). We summarize this as

$$\sum_{p \text{ fixed point}} \text{ind}_p = \text{Constant in } \lambda. \quad (5.24)$$

The Poincaré–Hopf index of a nondegenerate fixed point is the sign of the determinant of the $\partial_i \beta_j$ matrix, i.e $(-1)^\gamma$ where γ is the number of negative eigenvalues [54, 55]. Finding the Poincaré–Hopf index of a degenerate fixed point is in general more complicated, however, in our case the index of the degenerate points is zero⁴⁷.

The fact that this sum is related to the flow at infinity shows why it is different for the cases $N_f = 3$ and $N_f > 3$ (see table 5): this is because the flow at infinity of these 2 cases is topologically very different, as was shown in figure 13.

Another implication of (5.24) is that if several points merge to a single degenerate point, then the sum of their indices is the index of the resulting point. In particular, if they annihilate, the sum of their indices must be 0. Indeed, we can check explicitly using tables 4 and 6 that in our case the sum of the indices of the non-degenerate points that split from the degenerate one is 0.

⁴⁵To see how perturbations can eliminate a fixed point with only one degenerate direction, it is instructive to look at the example $\beta_x = x, \beta_y = y^2$, with a degenerate fixed point at $(0,0)$ and a perturbation that gives $\beta_x = x, \beta_y = y^2 + \epsilon$, and eliminates the fixed point

⁴⁶Intuitively, it counts how many times the function u wraps the S^{n-1} manifold. To define this quantity at infinity one must compactify the plane.

⁴⁷We can see from (5.2) that in the vicinity of the free fixed point $\beta_{SSS} \geq 0$ so the map $u : \partial D \rightarrow S^2$, of the normalized flow is not surjective, and so the degree of the map is zero (i.e. it does not wrap S^2). Similar arguments also hold for the other degenerate fixed point for $N_f > 4$. For $N_f = 3$ one can apply the Eisenbud–Levine–Khimshiashvili formula.

The implications extracted from (5.24) persist as we go beyond the perturbative regime in λ . Note that the opposite of merging can also occur – it may be that for some finite value of λ , a new degenerate fixed point will appear, and it will then split into additional non-degenerate fixed points.

To give a concrete example of the consequences of the type of analysis above, we can compute the sum of indices for $N_f = 2$ as shown in table 4, and find it is -1 . Since for $N_f = 2$, UV and IR-stable fixed points both contribute positively to this sum, this means that *for any value of λ* there must be at least one mixed point.

6 The Critical Fermion theory with $\lambda_F = 0$

In this section, we'll analyze the CF theory described in section 2.1.1 in the particular limit where $\lambda_F = 0$ (this is the same as the $SU(N_c)$ -singlet sector of the Gross-Neveu model). First, in section 6.1, we'll outline how to compute the beta function for this theory. Then, in section 6.2, we'll analyze the flows due to the beta functions at large N_c , and in particular the absence of IR-stable fixed points. Finally, in section 6.3, we will consider the large N_f limit. Since this section only deals with fermion theories we'll drop the sub/superscript F in all the equations that follow.

Unlike the RB theory, we'll find that there are no degenerate fixed points for $\lambda = 0$ that can split into IR-stable points, and therefore we will not need to carry out any computations for small λ .

6.1 Computation of the β functions

As in section 4, we compute the effective action for ζ_j^i in terms of the correlation functions of the meson operators M_i^j . These correlation functions are computed in the RF theory with $\lambda = 0$ (a free fermion theory) and they are therefore relatively simple. In fact, in this limit the 2, 3 and 5-point correlation functions are trivial to compute:

- The leading term of the **two-point** function, G_2 , is equal to its value for the $N_f = 1$ case in section 3, and given by $G_2 = 2\pi^2 \frac{N_c}{\kappa_F}$ (see footnote 22).
- Since the RF theory is free when $\lambda \rightarrow 0$, we find that the anomalous dimensions are $\gamma_S = 0$ and $\gamma_A = 0$.
- The 3 and 5-point correlation functions must vanish. This follows from parity invariance, as the RF theory (2.3) for $\lambda = 0$ contains only parity conserving terms. Under parity, the mesons transform to themselves with a minus sign, and so all correlation functions with an odd number of mesons are equal to minus themselves, and so they need to be zero. In particular, this means that $\bar{G}_{3,n} = \bar{g}_n$ (see (4.9)), and therefore $G_{SSS} = g_{SSS}$, $G_{SAA} = g_{SAA}$ and $G_{AAA} = g_{AAA}$.

The only non-trivial correlation function is the 4-point correlation function, which (as explained in section 4) we only need to know in a specific kinematical limit. The computation is a straightforward, yet cumbersome, loop integral. We leave the full derivation to

Appendix C. The result for the leading orders in k/p is

$$(G_4)_{i_1, i_2, i_3, i_4}^{j_1, j_2, j_3, j_4}(p, -p, k, -k) = - \left(\frac{4\pi}{\kappa} \right)^4 N_c \left(\begin{aligned} & \left(\delta_{i_2}^{j_1} \delta_{i_3}^{j_2} \delta_{i_4}^{j_3} \delta_{i_1}^{j_4} + \delta_{i_4}^{j_1} \delta_{i_3}^{j_2} \delta_{i_2}^{j_3} \delta_{i_1}^{j_4} \right) \left(\frac{1}{8|p|} + \frac{k \cdot p}{8p^3} - \frac{k \cdot p}{8|k|p^2} - \frac{(k \cdot p)^2}{8|k|p^4} \right) + \\ & \left(\delta_{i_2}^{j_1} \delta_{i_4}^{j_2} \delta_{i_3}^{j_3} \delta_{i_1}^{j_4} + \delta_{i_3}^{j_1} \delta_{i_4}^{j_2} \delta_{i_2}^{j_3} \delta_{i_1}^{j_4} \right) \left(\frac{1}{8|p|} - \frac{k \cdot p}{8p^3} + \frac{k \cdot p}{8|k|p^2} - \frac{(k \cdot p)^2}{8|k|p^4} \right) + \\ & \left(\delta_{i_3}^{j_1} \delta_{i_2}^{j_2} \delta_{i_4}^{j_3} \delta_{i_1}^{j_4} + \delta_{i_4}^{j_1} \delta_{i_2}^{j_2} \delta_{i_3}^{j_3} \delta_{i_1}^{j_4} \right) \left(\frac{1}{4|p|} - \frac{|k|}{4p^2} \right) \end{aligned} \right), \quad (6.1)$$

where the third line is different because the large-momentum meson operators are not adjacent to each other in the cyclic ordering of the mesons around the fermion loop⁴⁸.

The results are summarized in table 3. Inserting these values into (4.22), we find the beta functions

$$\begin{aligned} 16\pi^8 N_c \cdot \beta_{SSS} &= 256\pi^6 \left(3\lambda_{SAA} \frac{N_f^2 - 1}{N_f^2} - \lambda_{SSS} \frac{N_f^2 - 3}{N_f} \right) - (N_f^3 \lambda_{SSS}^3 + (N_f^2 - 1) \lambda_{SAA}^3), \\ 16\pi^8 N_c \cdot \beta_{SAA} &= 256\pi^6 \left(\lambda_{SSS} + 2\lambda_{AAA} \frac{N_f^2 - 4}{N_f^2} + \lambda_{SAA} \frac{3}{N_f} \right) \\ &\quad - \left(N_f^2 \lambda_{SSS} \lambda_{SAA}^2 + N_f \lambda_{SAA}^3 + 2 \frac{N_f^2 - 4}{N_f} \lambda_{SAA} \lambda_{AAA}^2 \right), \\ 16\pi^8 N_c \cdot \beta_{AAA} &= 128\pi^6 \left(\lambda_{AAA} \frac{N_f^2 - 12}{N_f} + 6\lambda_{SAA} \right) - \left(3N_f \lambda_{SAA}^2 \lambda_{AAA} + \frac{N_f^2 - 12}{N_f} \lambda_{AAA}^3 \right). \end{aligned} \quad (6.2)$$

Note that the couplings λ_n are parity-odd in this case, so parity implies that only odd powers of the couplings can appear in their beta functions. This implies that

- $(0, 0, 0)$ is always a fixed point, and unlike the RB case with $\lambda_B = 0$ in (5.2), there are linear terms in λ_n which prevent this point from being degenerate. Thus, turning on a very small but finite λ (which would break the parity symmetry) does not change the behavior of this fixed point.
- Except for the fixed point at $(0, 0, 0)$, all other fixed points come in pairs, and the two points in the pair are of the same type (they have the same number of relevant/irrelevant directions). In particular, this means that if the point at $(0, 0, 0)$ is non-degenerate as we argued above, then the sum of the Poincaré-Hopf indices will be odd.

6.2 Analysis of the flow

The beta functions found above can be compared to the $N_f = 1$ case. In that case, β_{SSS} decouples from the other equations, it is only dependent on λ_{SSS} and it is equal to the result given in (3.8), which has an IR-stable fixed point.

For the case $N_f = 2$ we get that β_{SSS} and β_{SAA} are independent of λ_{AAA} , as is expected in this case and as was also observed for the scalar theories and for the general

⁴⁸As mentioned in footnote 24, we use only the symmetrized version of the 4-point function (6.1). Under symmetrization, (6.1) has the form of the general parametrization in (4.11).

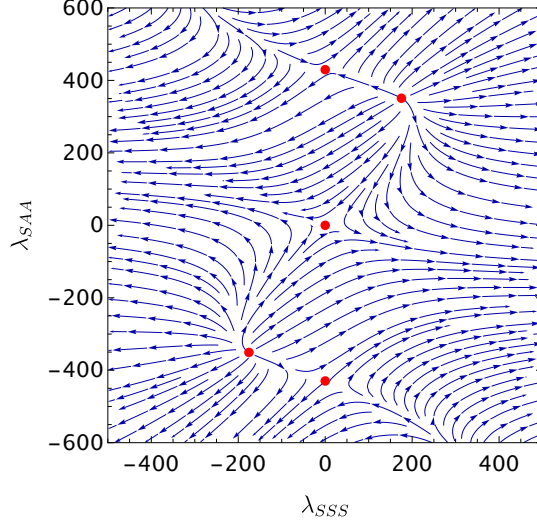


Figure 15. Stream plot of the flow to the IR of (minus) the fermion beta functions (6.2) for $N_f = 2$. The fixed points are shown in Red.

case. The flow to the IR for this case is seen in figure 15. The fixed points can all be found analytically as

$$(\lambda_{SSS}, \lambda_{SAA}) : \pm \left(4\sqrt{2}\pi^3, 8\sqrt{2}\pi^3 \right), \pm \left(0, 8\sqrt{3}\pi^3 \right) \quad (6.3)$$

(and the extra point $(0,0)$). The first point is UV-stable, and both the second and the one at $(0,0)$ are mixed fixed points. There is no IR-stable fixed point for this number of flavors.

The absence of an IR-stable fixed point continues as we take $N_f \geq 3$. For $N_f \geq 3$ there are 5 or 9 fixed points. Two of the points are given analytically by

$$(\lambda_{SSS}, \lambda_{SAA}, \lambda_{AAA}) : \pm \left(\frac{16\sqrt{2}\pi^3}{N_f^2}, \frac{16\sqrt{2}\pi^3}{N_f}, 8\sqrt{2}\pi^3 \right). \quad (6.4)$$

For $N_f > 3$ the points (6.4) are UV-stable points, while for $N_f = 3$ they have one degenerate direction and two relevant directions⁴⁹. Therefore, for $N_f = 3$, under a small perturbation to finite λ , these points can either disappear, or split to one mixed and one UV-stable

⁴⁹It is possible to show analytically that the Poincaré-Hopf index of these points at $N_f = 3$ is zero, as expected for a simple degeneration (where higher order derivatives do not vanish). To do so, we shift the couplings to be zero at this point, and change variables to v_i such that

$$\begin{pmatrix} v_1 \\ v_2 \\ v_3 \end{pmatrix} = \begin{pmatrix} \frac{9}{\sqrt{2977}} & -\frac{36}{\sqrt{2977}} & \frac{40}{\sqrt{2977}} \\ \frac{4}{\sqrt{17}} & \frac{1}{\sqrt{17}} & 0 \\ -\frac{40}{\sqrt{50609}} & \frac{160}{\sqrt{50609}} & 9\sqrt{\frac{17}{2977}} \end{pmatrix} \begin{pmatrix} \lambda_{SSS} \\ \lambda_{SAA} \\ \lambda_{AAA} \end{pmatrix}.$$

In these variables, the beta function of v_1 at quadratic order is $\beta_{v_1} = -144\sqrt{\frac{2}{2977}}\pi^3 (9\lambda_{SSS}^2 + 8\lambda_{SAA}^2)$ where λ_{SSS} and λ_{SAA} are linear combinations of the v_i 's. Thus, $\beta_{v_1} \leq 0$ in the vicinity of this point, and the map u is not surjective, and so the index is zero.

N_f	$\gamma = 0$ IR-stable	$\gamma = 1$	$\gamma = 2$	$\gamma = 3$ UV stable	Degenerate points	Total num. of fixed points	$\sum \text{ind}_p$
3	0	0	3	0	2	5	3
4-13	0	0	3	2	0	5	1
14\leq	0	2	5	2	0	9	1

Table 7. Summary of the $N_f \geq 3$ fixed points in the fermionic theory with $\lambda = 0$. We denote by γ the number of relevant directions at each point. The degenerate points do not contribute to the sum in the last column (see footnote 49). The fact that this sum differs between $N_f = 3$ and $N_f > 3$, and is equal to the same sum in the RB theory (see table 5), is discussed in section 5.5.2.

point, but not to an IR-stable fixed point. The summary of the fixed points and their type for $N_f \geq 3$ is found in table 7.

Finally, we note that as discussed in point 5 of section 4.3, the cubic terms are the same as in the RB theory (up to a common pre-factor). Therefore the large λ_n analysis done in sections 5.2.2 and 5.3.2 holds in this case as well. This also implies that the sum of the Poincaré-Hopf indices, defined in section 5.5.2, should be the same as in the RB theories, as can be verified by comparing table 7 with table 5.

6.3 Solutions in the limit $N_f \rightarrow \infty$

We can now take the $N_f \rightarrow \infty$ limit, in which it is possible to find analytically (to leading order) all nine fixed points which appear for $N_f \geq 14$. Three of the points were already found: the $(0, 0, 0)$ point, and the two points given by (6.4) with the $(2, 1, 0)$ scaling law.

Using the methods presented in section 5.4.1, we find six additional points. Two mixed fixed points with the leading scaling of $(2, 1, 0)$ are given by

$$(\lambda_{SSS}, \lambda_{SAA}, \lambda_{AAA}) : \pm \left(\frac{48\sqrt{6}\pi^3}{N_f^2}, -\frac{16\sqrt{6}\pi^3}{N_f}, 0 + \frac{96\sqrt{6}\pi^3}{N_f^2} \right), \quad (6.5)$$

and four mixed fixed points with the leading scaling of $(\frac{2}{3}, \frac{1}{3}, 0)$ are given by

$$(\lambda_{SSS}, \lambda_{SAA}, \lambda_{AAA}) : \pm \left(\frac{-16\pi^3}{N_f^{2/3}}, \frac{16\pi^3}{N_f^{1/3}}, -8\sqrt{2}\pi^3 \right), \pm \left(\frac{-16\pi^3}{N_f^{2/3}}, \frac{16\pi^3}{N_f^{1/3}}, 8\sqrt{2}\pi^3 \right). \quad (6.6)$$

Note that, although the formal scaling of the points in (6.5) is $(2, 1, 2)$, this is not a contradiction to the allowed scaling laws presented in (4.26), since we can classify it under the $(2, 1, 0)$ scaling class. This is just a special case in which the leading order result for λ_{AAA} happens to be zero.

In a similar fashion, it is not clear from the $\lambda = 0$ analysis what is the large N_f scaling of the free fixed point at the origin, and one has to check how it behaves for non-zero λ in order to determine this.

6.3.1 The (2, 1, 0) case

We see that there are 5 fixed points which we can classify under the scalings laws of (2, 1, 0): The free point (0, 0, 0), the two points in (6.4) and the two points in (6.5). As explained in section 4.4.1, this is possible only if there is a degeneracy in the leading order (in $\frac{1}{N_f}$) terms in the beta functions.

Indeed, taking the limit $N_f \rightarrow \infty$ with the scaling of (4.28), the beta functions are⁵⁰

$$\begin{aligned} 16\pi^8 N_c \frac{\beta_{y_{SSS}}}{N_f} &= (256\pi^6 (y_{SSS} - 3y_{SAA}) + y_{SAA}^3) + \mathcal{O}\left(\frac{1}{N_f}\right), \\ 16\pi^8 N_c \frac{\beta_{y_{SAA}}}{N_f} &= 2y_{AAA} (y_{SAA}y_{AAA} - 256\pi^6) + \mathcal{O}\left(\frac{1}{N_f}\right), \\ 16\pi^8 N_c \frac{\beta_{y_{AAA}}}{N_f} &= y_{AAA} (y_{AAA}^2 - 128\pi^6) + \mathcal{O}\left(\frac{1}{N_f}\right). \end{aligned} \quad (6.7)$$

We see from (6.7) that there are 3 possible solutions for y_{AAA} , two of them are described by (6.4) and are non-degenerate. The third solution $y_{AAA} = 0$ is degenerate (the condition (4.30) is satisfied for the CF theory with $\lambda = 0$), and one has to expand to next order in $\frac{1}{N_f}$ to find which solutions for y_{SSS} and y_{SAA} are consistent with this value of y_{AAA} . This process results in three points (the free point, and the two points given by (6.5)).

As discussed in section 5.4.4, once we turn on a finite λ there are two options: either the degeneracy is lifted and then only one⁵¹ of these solutions keeps its N_f scaling to all orders in λ , or it is not lifted and then it is also possible that two or all of them keep the scaling.

7 Semi-Critical theories

In this section we analyze the Semi-Critical theories, presented in sections 2.1.2 and 2.2.2, in the limits $\lambda_F = 0$ and $\lambda_B = 0$. We start by presenting the general formalism of how to calculate the beta functions for them, and then analyze the results in these limits.

7.1 Calculation of the beta functions

The beta functions of the Semi-Critical theories defined in (2.9) and (2.15) are much simpler than those of the RB and CF theories, since there is only one marginal coupling constant in each of them.

However, one has to be wary, as the calculation of the beta functions does not directly follow from (4.22). This is due to the fact that the Lagrange multiplier which sets the field combinations ζ_A or ζ_S to zero, should be applied *before* calculating the 1-loop diagrams in section 4.2, and not after.

Consider, for example, the simple G_5 diagram on the left of figure 3, which contributes to the constant terms of the beta functions. The contribution of this diagram to $\beta_{G_{SSS}}$ in

⁵⁰In (6.7) we use $y_n = N_c^2 Y_n$, as in (5.9).

⁵¹Note that non-zero λ breaks the $\lambda_n \rightarrow -\lambda_n$ symmetry, and therefore it is possible that only one of the non-trivial solutions loses its scaling.

(4.22) comes from setting the three external legs to ζ_S , and integrating over all the possible ζ_j^i fields propagating in the loop diagram. This is *not* the same calculation that needs to be done in the CF_S and CB_A theories, since in these theories the combinations of fields in ζ_A do not propagate at all, and so the internal loop contains only the ζ_S structure (see also figure 7).

This has important consequences for the semiclassical boson theories with $\lambda_B = 0$. In (5.2), there is no constant term in the beta function, as the contributions of all the terms exactly match to cancel each other⁵². In particular, the contribution of the G_5 diagram in figure 3 cancels the term in δG_3 which originated from calculating a diagram with the same topology (see Appendix B.2.3 in [25] for the full details, Appendix B.5 here, or compare the $s_{5,N/F}$ terms in δG_3 in table 3 to the constants in (4.22)).

To apply the Lagrange multiplier properly and project out the vanishing modes in the effective action (4.2) before calculating the 1-loop diagrams, we define the projectors to the singlet and adjoint representation

$$P_{j'i}^{i'j} = \begin{cases} \frac{1}{N_f} \delta_{j'}^{i'} \delta_i^j & S \\ \delta_i^{i'} \delta_{j'}^j - \frac{1}{N_f} \delta_{j'}^{i'} \delta_i^j & A \end{cases} \quad (7.1)$$

and use them on the ζ fields. This is equivalent to applying the projections on the G_n 's in (4.2). The end result is that the action of the Semi-Critical theories is similar in form to (4.2), with either only ζ_S fields or only ζ_A fields, and with the prefactors⁵³

$$(G_n^{SC})_{i_1, i_2, \dots}^{j_1, j_2, \dots} = (G_n)_{i'_1, i'_2, \dots}^{j'_1, j'_2, \dots} P_{j'_1 i_1}^{i'_1 j_1} P_{j'_2 i_2}^{i'_2 j_2} \dots \quad (7.2)$$

The superscript SC stands for Semi-Critical effective action.

The rest of the computations go on exactly as described in section 4.2 but now with the G_n replaced by G_n^{SC} .

For the CB_A and CF_S Semi-Critical theories, in which the adjoint field combinations vanish $\zeta_A = 0$ (see table 1), we find that the one loop corrected anomalous dimension of the ζ_S field is

$$\gamma'_S = \gamma_S + \frac{3G_{4,2,F} + G_{4,3,F} + 6G_{4,2,N} + 2G_{4,3,N}}{12\pi^2 G_2^2 N_f}, \quad (7.3)$$

and the beta function is

$$\begin{aligned} \beta_{G_{SSS}} &= \frac{1}{\pi^2 G_2} \frac{3(G_{5,F} + G_{5,N})}{N_f^3} - \delta G_{SSS} \\ &- G_{SSS} \left(3\gamma'_S + \frac{3(G_{4,1,F} + 2G_{4,1,N})}{2\pi^2 G_2^2 N_f} \right) - \frac{1}{2\pi^2 G_2^3} N_f^3 G_{SSS}^3. \end{aligned} \quad (7.4)$$

Note that (7.3) and (7.4) reproduce the $N_f = 1$ results in section 3, as one would expect, since for $N_f = 1$, the Semi-Critical singlet theories are the same as the one flavor theory (there is no adjoint structure to project out).

⁵²This is of course no accident, but results from the fact that the RB theory is free when $\lambda_B = \lambda_n^B = 0$. However, in the Semi-Critical theories at $\lambda_B = 0$ one sector is a critical bosonic theory, so they are not free.

⁵³Equivalently one can project only the propagator.

Also, the prefactor of the cubic and linear terms in (7.4) are the same as in (4.22) (ignoring the change in γ'_S), as the only diagrams that contribute to $\beta_{G_{SSS}}$ and that are proportional only to the G_{SSS} coupling in the non projected theories, contain only ζ_S fields as internal propagators. The anomalous dimension and the constant term in (7.4) change however, as the closed loops in the right diagram in figure 2 and the left diagrams in figure 3 contain internal propagation of ζ_A in the non projected theories.

For the CB_S and CF_A Semi-Critical theories, in which the singlet field combination vanishes $\zeta_S = 0$, we find that the one-loop corrected anomalous dimension of the ζ_A field is

$$\gamma'_A = \gamma_A + \frac{3G_{4,2,F} + G_{4,3,F} - 2(N_f^2 - 1)(3G_{4,2,N} + G_{4,3,N})}{12\pi^2 G_2^2 N_f}, \quad (7.5)$$

and the beta function is

$$\begin{aligned} \beta_{G_{AAA}} = & \frac{3(N_f^2 - 1)G_{5,N} - 3G_{5,F}}{2\pi^2 G_2 N_f} - \delta G_{AAA} \\ & - G_{AAA} \left(3\gamma'_A + \frac{3(N_f^2 - 4)G_{4,1,N} - 6G_{4,1,F}}{2\pi^2 G_2^2 N_f} \right) - \frac{1}{2\pi^2 G_2^3} \frac{N_f^2 - 12}{N_f} G_{AAA}^3. \end{aligned} \quad (7.6)$$

In addition to the similar comments made above regarding the cubic, linear and constant coefficients, note that for $N_f \rightarrow \infty$, the leading order results of (7.5), (7.6) and of (4.21), (4.22) (setting $G_{SAA} = 0$ in $\beta_{G_{AAA}}$) are the same, respectively. This stems from the fact that in ζ_A there are $N_f^2 - 1$ degrees of freedom and in ζ_S only 1, so projecting it out doesn't change the leading large N_f behavior.

More remarkably, for $N_f = 3$ the prefactor of the cubic term is positive for every λ (see a similar discussion in item 5 of section 4). This means that there is at least 1 (and up to 2) IR-stable fixed points *for every value of λ* , and the basin of attraction of these points is all of λ_{AAA} .

The conclusion of this section is that one can use the results obtained for the correlation functions of the mesons G_n in the CB and RF theories to compute also the beta function in the Semi-Critical theories. In the following, we will use the results summarized in table 3 (which were obtained in Appendices B and C) to explicitly calculate the beta functions in the scalar and fermionic theories with $\lambda_{B/F} = 0$.

7.2 Semi-Critical Singlet theories

In this section, we apply the results obtained for the singlet theories in (7.3) and (7.4) to the scalar and fermionic theories with $\lambda_B = 0$ and $\lambda_F = 0$, respectively.

7.2.1 Scalar theories CB_A

For CB_A theories with $\lambda_B = 0$, the anomalous dimension is (the super-script B stands for Boson)

$$\gamma_S^{B'} = -\frac{16(N_f^2 - 1)}{3\pi^2 N_c^B N_f}, \quad (7.7)$$

and the beta function is

$$2^{10}\pi^2 N_c^B \beta_S^B = 2^{21} \frac{(N_f^2 - 1)(1 - 6(s_{5,F} + s_{5,N}))}{N_f^3} + 2^{14} \frac{N_f^2 - 1}{N_f} \lambda_{SSS} + 384 N_f \lambda_{SSS}^2 - N_f^3 \lambda_{SSS}^3. \quad (7.8)$$

We see explicitly that for the case $N_f = 1$, $\gamma_S^{B'}$ and β_S^B reproduce the result of (3.10). Although the beta function depends on $s_{5,N/F}$, which are unknown in the literature, the dependence is only through the sum $s_{5,N} + s_{5,F}$, which may be easier to compute than each one separately, as the sum appears also in the $N_f = 1$ theory.

We already observe an interesting behavior from the anomalous dimension (7.7). Specifically, since $\gamma_S^{B'} \neq 0$ for $N_f > 1$, the two-point correlation function of the mesons \tilde{M}_S no longer resembles that of a free theory. As a result, even if $\lambda_{SSS} = 0$ corresponds to a fixed point, the resulting theory is not equivalent to a free theory.

The beta function (7.8) is a cubic polynomial, and thus has generically either 1 or 3 zeros (see figure 4 and the discussion in section 3). Because of the unknown quantity, we cannot find whether in general these theories have an IR-stable fixed point, however we can find the range of its values for which such an IR-stable fixed point appears. By evaluating the discriminant of the polynomials we find an IR-stable fixed point if

$$\frac{9N_f^2 - \sqrt{3}(N_f^2 + 2)^{\frac{3}{2}}}{27(N_f^2 - 1)} < s_{5,F} + s_{5,N} < \frac{9N_f^2 + \sqrt{3}(N_f^2 + 2)^{\frac{3}{2}}}{27(N_f^2 - 1)}. \quad (7.9)$$

Since $s_{5,N} + s_{5,F}$ is just a number which is currently unknown, and the right and left sides in condition (7.9) go to positive/negative infinity as $N_f \rightarrow \infty$, there exists a value of N_f^* from which there will be an IR-stable fixed point for any $N_f > N_f^*$.

The conclusion of this section is that for large enough N_f , the CB_A theory has a non-trivial IR-stable fixed point for $\lambda_B = 0$.

7.2.2 Fermionic theories CF_S

For the CF_S theories with $\lambda_F = 0$, the anomalous dimension is (the super-script F stands for Fermions)

$$\gamma_S^{F'} = \frac{16}{3\pi^2 N_c N_f^F}, \quad (7.10)$$

and the beta function is

$$16\pi^8 N_c^F \cdot \beta_S^F = \frac{512\pi^6}{N_f} \lambda_{SSS} - N_f^3 \lambda_{SSS}^3. \quad (7.11)$$

Once again, we see that for $N_f = 1$, the beta function reproduces the beta function (3.8) of the CF theory.

The beta function (7.11) always exhibits an IR-stable fixed point at $\lambda_{SSS} = 0$, for any N_f .

7.2.3 Conclusions and duality

We will now analyze these results in light of the dualities presented in section 2.3 that relate the fermion theory to the scalar theory. We found that for large enough values of N_f there is a single IR-stable fixed point for both the perturbative regions of the scalar and fermion theories (i.e. in small neighborhoods of $\lambda_B = 0, 1$), as is the case for $N_f = 1$. It is then natural to conjecture that such an IR-stable fixed point also exists for every intermediate value of λ .

For small N_f the situation is more complicated because of the unknown sum $s_{5,F} + s_{5,N}$. We know that in this case there is a fixed point for $|\lambda_B| \simeq 1$ (i.e. $\lambda_F \simeq 0$) but it is yet unknown whether there is one for $\lambda_B \simeq 0$.

7.3 Semi-Critical Adjoint theories

In this section, we repeat the analysis in the previous section for the adjoint theories, by using (7.5) and (7.6). We emphasize that those theories are defined only for $N_f \geq 3$ (more precisely, the theory exists also for $N_f = 2$, but it does not have a marginal coupling in this case).

7.3.1 Scalar theories CB_S

For the CB_S theories with $\lambda_B = 0$, the anomalous dimension is

$$\gamma_A^{B'} = -\frac{16}{3\pi^2 N_c^B N_f}, \quad (7.12)$$

and the beta function is

$$2^{10}\pi^2 N_c^B \beta_A^B = 2^{21} \frac{1 - 3(s_{5,F} + s_{5,N})}{N_f} + \frac{2^{16}}{N_f} \lambda_{AAA} + 192 \frac{N_f^2 - 12}{N_f} \lambda_{AAA}^2 - \frac{N_f^2 - 12}{N_f} \lambda_{AAA}^3. \quad (7.13)$$

We explicitly see that, as expected, for $N_f \rightarrow \infty$ the beta function (7.13) reproduces the coefficients of the beta function β_{AAA} in (5.2), and, as in the singlet theory, also here the theory is not free even for $\lambda_{AAA} = 0$.

The beta function (7.13) results in one IR-stable fixed point if either $N_f = 3$ (since the beta function in that case is monotonically increasing), or if

$$\frac{9N_f^2 - \sqrt{3 \frac{(3N_f^2 - 20)^3}{N_f^2 - 12}}}{108} < s_{5,F} + s_{5,N} < \frac{9N_f^2 + \sqrt{3 \frac{(3N_f^2 - 20)^3}{N_f^2 - 12}}}{108} \quad \text{and} \quad N_f \geq 4. \quad (7.14)$$

Unlike the singlet case, the left hand side of (7.14) is bounded from below as $N_f \rightarrow \infty$ by $\frac{1}{3}$, and so if $s_{5,F} + s_{5,N} > \frac{1}{3}$, there always exists a value of N_f^* such that there will be an IR-stable fixed point for any $N_f > N_f^*$, but if $s_{5,F} + s_{5,N} < \frac{1}{3}$ there is no IR-stable fixed point for large enough N_f .

7.3.2 Fermionic theories CF_A

For the CF_A theories with $\lambda_F = 0$, the anomalous dimension is

$$\gamma_A^{F'} = \frac{4(N_f^2 - 4)}{3\pi^2 N_c^F N_f}, \quad (7.15)$$

and the beta function is

$$16\pi^8 N_c^F \cdot \beta_A^F = 128\pi^6 \frac{N_f^2 - 10}{N_f} \lambda_{AAA} - \frac{N_f^2 - 12}{N_f} \lambda_{AAA}^3. \quad (7.16)$$

Once again, we see that in the $N_f \rightarrow \infty$ limit the beta function (7.16) reproduces the coefficients of β_{AAA} in (6.2) for that limit. This beta function has 2 IR-stable fixed points (and one UV-stable) for $N_f = 3$, and a single IR-stable point at $\lambda_{AAA} = 0$ for any $N_f > 3$.

7.3.3 Conclusions and duality

Again we analyze these results in light of the dualities of section 2.3. As was noted below (7.6), for $N_f = 3$ there is an IR-stable point for every value of λ_B . However, we see that for $\lambda_B = 0$ there is only one such point, while for $|\lambda_B| = 1$ there are two. Thus, in this case an IR-stable point *emerges* as one increases λ_B . This theory is also the only system we find with two IR-stable fixed points.

For $N_f > 3$, at $|\lambda_B| = 1$ there is an IR-stable fixed point. Whether this point emerges for some critical value of λ_B or exists for any value of λ_B is unknown, due to the unknown factor $s_{5,F} + s_{5,N}$. In particular, if $\frac{1}{3} < s_{5,F} + s_{5,N} < \frac{2}{3}$ then there would be an IR-stable fixed point for all the (perturbative regions of the) Semi-Critical theories (singlet and adjoint) and for every value of N_f .

8 Conclusions and future directions

The main result of this paper is the computation of the beta functions for the marginal couplings in the RB, CF, and Semi-Critical theories, for a general flavor number N_f , at first non-trivial order in $\frac{1}{N_c}$. For small $|\lambda|$ (in one of the descriptions of these theories) we compute the beta functions explicitly, and we also analyze their general structure for all values of λ . Using the dualities described in section 2.3, our explicit computations describe the beta functions of the RB/CF theory in the limits $|\lambda_B| \rightarrow 0, 1$. Adopting this viewpoint, we describe the beta functions in the rest of this section in terms of λ_B .

For the RB/CF theory, we find that the beta function behavior for general values of N_f is qualitatively different from the $N_f = 1$ case described in [25]. For $|\lambda_B| = 1$ there are no IR-stable fixed points for any $N_f > 1$, in contrast to the $N_f = 1$ case. Moreover, we find that for $\lambda_B \rightarrow 0$ there is an IR-stable fixed point for any $N_f \neq 3, 4$, which means that the structure of the fixed points changes as we go between $0 < \lambda_B < 1$. In particular, this means that there is a critical value $\lambda_{B,crit}$ for which the IR-stable fixed point merges with another fixed point and then disappears.

We were able to find this value, and to show the merging explicitly, for large (but finite) values of N_f . For small N_f this merger happens outside the perturbative regime, so its analysis requires an expression for the beta functions beyond the perturbative regime.

As in the $N_f = 1$ case, we were able to construct a general expression for the beta functions, as a third degree polynomial in the marginal couplings, which depends on some unknown n -point correlation functions of meson operators. Nevertheless this formal expression gives meaningful results that are true for any λ_B , such as the large λ_n behavior, and restrictions on types and numbers of possible fixed points.

We also managed to find general restrictions in the large N_f limit, in which we showed that the fixed points must scale in some way with N_f , and we showed that for the natural scaling of $(2, 1, 0)$ there are generically three fixed points. However, we showed that this is not the case for $|\lambda_B| = 0, 1$, and we conjectured that this is resolved as we go to higher orders of perturbation theory in $\lambda_{B,F}$ ⁵⁴.

For both Semi-Critical theories, we found there is always an IR-stable fixed point for $|\lambda_B| = 1$. For $\lambda_B = 0$ the situation is more complex, as the beta function depends on the unknown values of the 5-point function. An exception is the $N_f = 3$ Adjoint (CF_A/CB_S) theories, for which we were able to prove that there exists an IR-stable fixed point *for every value of λ_B* . It is therefore evident that finding the 5-point function would greatly contribute to the understanding of the Semi-Critical theories as well as the RB/CF theories.

One obvious direction for future work is the computation of the n -point correlation functions of the meson operators at large N_c , which enter the beta functions of the theory. A complete understanding of these correlation functions for arbitrary values of λ would enable the determination of the beta functions even in the strongly coupled regime. Some conjectures about the structures of these correlation functions for arbitrary values of λ appeared in [46].

A particular concrete computation that can be pursued involves the 5-point function of mesons. It would be interesting to compute it even just at $\lambda_B = 0$, since this would tell us if the Semi-Critical theories possess IR fixed points in that case. If they do, then one could conjecture that the fixed points survive for all λ ; while if they don't, then it would mean that new fixed points must appear as λ_B is increased, and those theories could serve as simple candidates for scenarios in which fixed-point merging occurs.

In addition, computing the correlation functions of the CF theory at finite but small $\lambda_F \ll 1$, or evaluating the beta function of the RB theory at small $\lambda_B \ll 1$ to the next order in perturbation theory, would allow us to test whether the degeneracy we identified in the $N_f \rightarrow \infty$ limit for the $(2, 1, 0)$ scaling at weak coupling stops holding (i.e. the condition (4.30) is not satisfied) at higher orders in perturbation theory, as we propose, or whether this limit introduces a new type of symmetry in the theory, that implies (4.30).

In this paper we have not used the approximate higher-spin symmetry of the CS-matter theories, and it would be interesting to generalize the analysis of [6] to the case of higher N_f , where in addition to the energy-momentum tensor there is another spin-2 $SU(N_f)$ -

⁵⁴Alternatively, if one finds that the beta functions *do* degenerate, then this would imply a non-trivial relation between the 5 and 3-point functions and the anomalous dimension, see (4.30).

adjoint operator that becomes conserved in the large- N_c limit (and similarly for all other spins). Proving that the large N_c 3-point functions of the “quasi-fermionic” theories in this case are still uniquely determined by one parameter (corresponding to λ), and that the “quasi-bosonic” ones are determined up to four parameters (corresponding to λ and the three marginal deformations), would provide more evidence for the $N_f > 1$ dualities between the scalar and fermion theories. It would be particularly interesting to compute the anomalous dimension of the extra spin-2 flavor-adjoint operator in all of these theories at leading order in $1/N_c$.

Additional computations that would be interesting to do for general values of N_f involve the phase diagram of the theory as a function of its three relevant operators, that can be accessed by computing the large- N_c effective potential (as done for $N_f = 1$ in [25, 38]). The naive expectation is that by tuning two of the three relevant operators one should be able to flow from the RB/CF theories to the Semi-Critical Adjoint or Semi-Critical Scalar theories, while by tuning one operator one should be able to flow to the CB/RF theory. However, this may not be true for all values of the marginal couplings, and in addition some values of these couplings may correspond to unstable theories (as found for $N_f = 1$ in [25]).

It would be interesting to understand what happens to all these fixed points when N_f increases to become of order N_c or larger, though it is no longer known how to sum all the large- N_c diagrams in this case. In addition, it would be interesting to understand the flows from QCD-Chern-Simons theories to all these theories; currently we do not have the tools to sum all the planar diagrams involved, even in the large N_c limit for small N_f , but it may still be possible to understand these flows, at least at small λ .

Our analysis in this paper can be generalized to many other theories, and in particular to theories with both scalars and fermions. For some values of the couplings one has supersymmetric theories with various amounts of supersymmetry, and the beta functions for this case were computed for all values of N_f in [24], but there should also be many non-supersymmetric fixed points, and it would be interesting to know if some of them are IR-stable.

Acknowledgments

The authors would like to thank Netanel Barel, Sachin Jain, Trivko Kukulj, Jiangyuan Qian and Shimon Yankielowicz for useful discussions. This work was supported in part by ISF grant no. 2159/22, by Simons Foundation grant 994296 (Simons Collaboration on Confinement and QCD Strings), by the Minerva foundation with funding from the Federal German Ministry for Education and Research, and by the German Research Foundation through a German-Israeli Project Cooperation (DIP) grant “Holography and the Swampland”. OA is the Samuel Sebba Professorial Chair of Pure and Applied Physics.

A Calculations for finite λ_B

In this appendix we'll compute the beta function of the RB theory in the weak 't Hooft coupling limit. First, we'll lay out our conventions for the CS action and the $SU(N_c)$ generators, from which we'll derive the Feynman rules of the theory. Then, we'll compute the beta function to first non-vanishing order (in the 't Hooft large N_c expansion) when $\lambda_B = 0$. The result is valid to all orders in the ϕ^6 couplings λ_n^B .

We then move on to perturbative computations when both λ_B and λ_n^B are small but non-zero. We compute the beta function to first non-vanishing order in both of these couplings, for any value of N_c and N_f . Since this appendix deals only with the RB theory, we drop the sub/superscript B in all of the following equations (e.g., write λ instead of λ_B).

A.1 The action and Feynman rules

A.1.1 Conventions for generators

In the calculation below, we use a convention in which the generators of the $SU(N_c)$ algebra are anti-hermitian, which is $(T_{ab}^{\bar{a}})^\dagger = -T_{ab}^{\bar{a}}$, orthogonal with respect to the Killing form $\text{tr}(T^{\bar{a}} T^{\bar{b}}) \propto \delta^{\bar{a}\bar{b}}$, and with the structure constants defined by $[T^{\bar{b}}, T^{\bar{c}}] = -f^{\bar{a}\bar{b}\bar{c}} T^{\bar{a}}$.

The generators of $SU(N_c)$ obey [49, 50]

$$T_{ij}^{\bar{a}} T_{kl}^{\bar{a}} = C_3 I_{ij;kl}; \quad I_{ij;kl} \equiv \delta_{il} \delta_{kj} - \frac{1}{N_c} \delta_{ij} \delta_{kl}, \quad (\text{A.1})$$

where $C_3 < 0$, and so

$$\text{tr}(T^{\bar{a}} T^{\bar{b}}) = C_3 \delta^{\bar{a}\bar{b}}; \quad f^{\bar{a}\bar{b}\bar{c}} = -\frac{1}{C_3} \text{tr}(T^{\bar{a}} [T^{\bar{b}}, T^{\bar{c}}]). \quad (\text{A.2})$$

In the following, we use the normalization $C_3 = -1$.

A.1.2 The Chern-Simons action

The normalization for the Chern-Simons action which we use is

$$S_{CS} = \frac{\kappa}{4\pi} \int d^3x \left(-\frac{i}{2} \epsilon^{\mu\nu\rho} A_\mu^{\bar{a}} \partial_\nu A_\rho^{\bar{a}} - \frac{i}{6} \epsilon^{\mu\nu\rho} f^{\bar{a}\bar{b}\bar{c}} A_\mu^{\bar{a}} A_\nu^{\bar{b}} A_\rho^{\bar{c}} \right). \quad (\text{A.3})$$

In this normalization, the level κ for the $SU(N_c)$ gauge group is an integer. We now rescale the gauge field $A \rightarrow \sqrt{\frac{4\pi}{|\kappa|}} A$ such that

$$S = \text{sign}(\kappa) \int d^3x \left(\frac{-i}{2} \epsilon^{\mu\nu\rho} A_\mu^{\bar{a}} \partial_\nu A_\rho^{\bar{a}} - \frac{i}{6} \sqrt{\frac{4\pi}{|\kappa|}} f^{\bar{a}\bar{b}\bar{c}} A_\mu^{\bar{a}} A_\nu^{\bar{b}} A_\rho^{\bar{c}} \right). \quad (\text{A.4})$$

The full action also contains gauge-fixing and ghost terms. The latter will not play a role in our calculations (they only appear at higher orders, see [49]). We work in the Landau gauge, in which the gluon propagator is given by [49, 50]

$$\langle A_\mu^{\bar{a}}(p) A_\nu^{\bar{b}}(-p) \rangle = -\delta^{\bar{a}\bar{b}} \epsilon_{\mu\nu\lambda} \frac{p^\lambda}{p^2}. \quad (\text{A.5})$$

The non-linear term in the Chern-Simons action generates an interaction vertex with no momentum dependence

$$\langle A_\mu^{\bar{a}} A_\nu^{\bar{b}} A_\rho^{\bar{c}} \rangle_{vertex} = i \sqrt{\frac{4\pi}{|\kappa|}} \epsilon_{\mu\nu\rho} f^{\bar{a}\bar{b}\bar{c}}. \quad (\text{A.6})$$

A.1.3 The scalar kinetic term

The kinetic term of the scalars in the bosonic theory (2.2) can be written as

$$\begin{aligned} S_B(A, \phi) &= \int d^3x \left(D_\mu^{ba} \phi_{i,a} \right)^\dagger \left(D_{bc}^\mu \phi^{i,c} \right) \\ &= \int d^3x \left(\partial_\mu \bar{\phi}_{a,i} \partial_\mu \phi_{a,i} + T_{ba}^{\bar{a}} A_\mu^{\bar{a}} (\partial_\mu \bar{\phi}_{b,i} \phi_{a,i} - \bar{\phi}_{b,i} \partial_\mu \phi_{a,i}) - \left\{ T^{\bar{b}}, T^{\bar{a}} \right\}_{cb} A_\mu^{\bar{b}} A_\mu^{\bar{a}} \bar{\phi}_{c,i} \phi_{b,i} \right), \end{aligned} \quad (\text{A.7})$$

where the covariant derivative is given by $D_\mu = \partial_\mu + T^{\bar{a}} A_\mu^{\bar{a}}$. The propagator of the scalar is given by

$$\langle \phi_{a,i}(p) \bar{\phi}_{b,j}(-p) \rangle = \frac{\delta_{a,b} \delta_{i,j}}{p^2}, \quad (\text{A.8})$$

and the interaction terms which follows from (A.7), after rescaling $A \rightarrow \sqrt{\frac{4\pi}{|\kappa|}} A$, are

$$\begin{aligned} \langle A_\mu^{\bar{a}} \bar{\phi}_{a,i}(p_1) \phi_{b,j}(p_2) \rangle_{vertex} &= i \sqrt{\frac{4\pi}{|\kappa|}} (p_1 - p_2)_\mu T_{ab}^{\bar{a}} \delta_{i,j}, \\ \langle A_\mu^{\bar{a}} A_\nu^{\bar{b}} \bar{\phi}_{a,i} \phi_{b,j} \rangle_{vertex} &= \frac{4\pi}{|\kappa|} \left\{ T^{\bar{a}}, T^{\bar{b}} \right\}_{ab} \delta_{\mu\nu} \delta_{i,j}. \end{aligned} \quad (\text{A.9})$$

A.1.4 The scalar self interaction term

The last term in the RB action is the scalar self-interactions, given in (2.10), which we repeat here for clarity

$$\mathcal{L}_{int} = \frac{\bar{g}_1}{3!} (\bar{\phi}_{c,i} \phi^{c,i})^3 + \frac{\bar{g}_2}{2} \bar{\phi}_{a,i} \phi^{a,i} \bar{\phi}_{b,j} \phi^{b,k} \bar{\phi}_{c,k} \phi^{c,j} + \frac{\bar{g}_3}{3} \bar{\phi}_{a,i} \phi^{a,j} \bar{\phi}_{b,j} \phi^{b,k} \bar{\phi}_{c,k} \phi^{c,i}. \quad (\text{A.10})$$

This leads to the following vertex:

$$\begin{aligned} \langle \bar{\phi}_{a_1,i_1} \phi^{a_2,i_2} \bar{\phi}_{a_3,i_3} \phi^{a_4,i_4} \bar{\phi}_{a_5,i_5} \phi^{a_6,i_6} \rangle_{vertex} &= -\bar{g}_1 (\delta_{a_1 a_2} \delta_{a_3 a_4} \delta_{a_5 a_6} \delta_{i_1 i_2} \delta_{i_3 i_4} \delta_{i_5 i_6} + (5 \text{ terms})) \\ &\quad -\bar{g}_2 (\delta_{a_1 a_2} \delta_{a_3 a_4} \delta_{a_5 a_6} \delta_{i_1 i_2} \delta_{i_3 i_6} \delta_{i_5 i_4} + (17 \text{ terms})) \\ &\quad -\bar{g}_3 (\delta_{a_1 a_2} \delta_{a_3 a_4} \delta_{a_5 a_6} \delta_{i_1 i_4} \delta_{i_3 i_6} \delta_{i_5 i_2} + (11 \text{ terms})). \end{aligned} \quad (\text{A.11})$$

A.1.5 Renormalization Conditions

The renormalization conditions chosen in this paper are such that, at the energy scale we are working with, the connected six-point correlation functions of ϕ are given by

$$\begin{aligned} \bar{\Gamma}_1^{(6)} &\equiv \langle \bar{\phi}_{a,i} \phi^{a,i} \bar{\phi}_{b,j} \phi^{b,j} \bar{\phi}_{c,k} \phi^{c,k} \rangle_{amp} = -\bar{g}_1 \\ \bar{\Gamma}_2^{(6)} &\equiv \langle \bar{\phi}_{a,i} \phi^{a,i} \bar{\phi}_{b,j} \phi^{b,k} \bar{\phi}_{c,k} \phi^{c,j} \rangle_{amp} = -\bar{g}_2, \quad \text{no sum over all indices,} \\ \bar{\Gamma}_3^{(6)} &\equiv \langle \bar{\phi}_{a,i} \phi^{a,j} \bar{\phi}_{b,j} \phi^{b,k} \bar{\phi}_{c,k} \phi^{c,i} \rangle_{amp} = -\bar{g}_3 \end{aligned} \quad \begin{matrix} i \neq j \neq k \\ a \neq b \neq c \end{matrix}, \quad (\text{A.12})$$

where the subscript amp indicates a connected amputated diagram, and all momenta are taken to lie at the same scale.

In the 't Hooft limit one can contract the color indices to get the *leading* N_c expressions

$$\begin{aligned}\langle \bar{\phi}_{a,i} \phi^{a,i} \bar{\phi}_{b,j} \phi^{b,j} \bar{\phi}_{c,k} \phi^{c,k} \rangle_{\text{amp}} &= -N_c^3 \bar{g}_1 \\ \langle \bar{\phi}_{a,i} \phi^{a,i} \bar{\phi}_{b,j} \phi^{b,k} \bar{\phi}_{c,k} \phi^{c,j} \rangle_{\text{amp}} &= -N_c^3 \bar{g}_2, \quad \text{no sum over flavor indices, } i \neq j \neq k. \\ \langle \bar{\phi}_{a,i} \phi^{a,j} \bar{\phi}_{b,j} \phi^{b,k} \bar{\phi}_{c,k} \phi^{c,i} \rangle_{\text{amp}} &= -N_c^3 \bar{g}_3\end{aligned}\quad (\text{A.13})$$

Alternatively, one can consider the six-point correlation function in terms of the representation basis. The renormalization conditions for the three mesons (at leading order in $\frac{1}{N_c}$) are

$$\begin{aligned}\Gamma_{SSS}^{(6)} &\equiv \langle \tilde{M}_S \tilde{M}_S \tilde{M}_S \rangle_{\text{amp}} = -N_c^3 N_f^3 g_{SSS}, \\ \Gamma_{SAA}^{(6)} &\equiv \left\langle \tilde{M}_S \left(\tilde{M}_A \right)_j^i \left(\tilde{M}_A \right)_i^j \right\rangle_{\text{amp}} = -N_c^3 N_f (N_f^2 - 1) g_{SAA}, \\ \Gamma_{AAA}^{(6)} &\equiv \left\langle \left(\tilde{M}_A \right)_j^i \left(\tilde{M}_A \right)_k^j \left(\tilde{M}_A \right)_i^k \right\rangle_{\text{amp}} = -N_c^3 \frac{(N_f^2 - 1)(N_f^2 - 4)}{N_f} g_{AAA}.\end{aligned}\quad (\text{A.14})$$

At leading order, choosing (A.14) is equivalent to choosing (A.13), as can be shown by projecting (A.13) to the representation basis, and using (2.8).

A.2 The $\lambda = 0$ case

In this section we calculate the β function of the scalar self-interaction terms at leading order in $\frac{1}{N_c}$, in the 't Hooft limit where the couplings scale as $g_n \sim \frac{1}{N_c^2}$. The computation is a simple generalization of the single flavor $N_f = 1$ case studied long ago in [47] (for real scalars). First, we present the answer for the $N_f = 1$ case, and then we generalize this to multiple flavors.

Note that in this section we use a momentum cutoff regularization, unlike in the next section, in which dimensional regularization is used.

A.2.1 Calculation for $N_f = 1$

For the $\lambda = 0$, $N_f = 1$ case, the Euclidean Lagrangian with UV momentum cutoff Λ is

$$\mathcal{L} = \partial_\mu \bar{\phi} \partial_\mu \phi + \frac{g_{SSS}}{3!} (\bar{\phi} \phi)^3 \big|_\Lambda, \quad (\text{A.15})$$

where the color summations are implicit (as was noted before, for $N_f = 1$ only the g_{SSS} structure exists). The connection between the regularized and bare scalar field is given by $\phi_B = \sqrt{Z} \phi$, and the Lagrangian is

$$\mathcal{L} = \partial_\mu \bar{\phi} \partial_\mu \phi + \frac{g_{SSS}}{3!} (\bar{\phi} \phi)^3 + (Z - 1) \partial_\mu \bar{\phi} \partial_\mu \phi + \frac{1}{3!} (Z^3 g_{SSS,B} - g_{SSS}) (\bar{\phi}_B \phi_B)^3, \quad (\text{A.16})$$

where the second term provides the tree-level six point correlation function (A.12), and the last two terms serve as counter-terms.

There are only two diagrams that contribute to the beta function β_{SSS} at leading order, shown in figure 8. The first, which is a 4-loop diagram, contributes to the zero-momentum amputated correlator $\bar{\Gamma}_1^{(6)}$ a UV divergence

$$\begin{aligned} A0 &= (-g_{SSS})^3 N_c^3 \int \frac{d^3 q_1}{(2\pi)^3} \frac{d^3 q_2}{(2\pi)^3} \frac{d^3 q_3}{(2\pi)^3} \frac{d^3 k}{(2\pi)^3} \frac{1}{q_2^2 (k - q_2)^2 q_3^2 (k - q_3)^2 q_1^2 (k - q_1)^2} \\ &= -g_{SSS}^3 N_c^3 \frac{1}{2^{10} \pi^2} \ln(\Lambda). \end{aligned} \quad (\text{A.17})$$

The second, which is a two-loop diagram, contributes

$$A8a = 6g_{SSS}^2 N_c \int \frac{d^3 q}{(2\pi)^3} \frac{d^3 k}{(2\pi)^3} \frac{1}{q^2 k^2 (q + k)^2} = 6 \cdot g_{SSS}^2 N_c \frac{1}{16\pi^2} \ln(\Lambda). \quad (\text{A.18})$$

At leading order, there are no diagrams which contribute to $Z - 1$, and so we can set $Z = 1$. We find from the renormalization condition that:

$$-(Z^3 g_{SSS,B} - g_{SSS}) + A0 + A8a = 0 \quad (\text{A.19})$$

and so, by taking a derivative with respect to Λ ,

$$2^{10} \pi^2 \beta_{g_{SSS}} = 2^6 \cdot 6 N_c g_{SSS}^2 - g_{SSS}^3 N_c^3. \quad (\text{A.20})$$

Finally, in the 't Hooft limit $\lambda_{SSS} \equiv g_{SSS} N_c^2$ is a finite quantity, and by writing the β function for λ_{SSS} we get

$$2^{10} \pi^2 \beta_{SSS} = \frac{2^6 \cdot 6 \lambda_{SSS}^2 - \lambda_{SSS}^3}{N_c}. \quad (\text{A.21})$$

The form of the $\frac{1}{N_c}$ leading term of the β function is cubic in the coupling, which must be the case, as proved in [25] and reviewed in section 3 of this paper. The proof that only the two diagrams contribute to the β -function proceeds as follows. To calculate the β function, we consider amputated diagrams with $E = 6$ external legs, as well as possible contributions from the field strength renormalization Z . We are interested in contributions to the 6-point correlation functions (see (A.12)) that scale like $\log(\Lambda)$, without any additional powers of the cutoff Λ , that is, diagrams that do not contain factors of Λ . Thus, we ignore diagrams with self-connected vertices, and so for a diagram with E external legs, I internal legs, and V 6-point interaction vertices, we have the relation

$$E + 2I = 6V. \quad (\text{A.22})$$

For a diagram with $E = 6$ external legs, we have the relation $I = 3V - 3$. A factor of N_c comes when summing over the color index of two internal lines, so given I internal lines, the maximum power of N_c a diagram can produce is $\lfloor \frac{I}{2} \rfloor$. The vertices contribute N_c^{-2V} (since $g = \frac{\lambda}{N_c^2}$), so the total power of N_c of a Feynman diagram is (the plus two is since $\beta_{SSS} = N_c^2 \beta_{g_{SSS}}$)

$$\# \text{ maximal power of } N_c = \left\lfloor \frac{I}{2} \right\rfloor - 2V + 2 = \left\lfloor \frac{-V + 1}{2} \right\rfloor, \quad (\text{A.23})$$

i	$\#_{tree,n}$	$\#_{2loop,n}$	$\#_{4loop,n}$
SSS	N_f^3	$6N_f^4 g_{SSS}^2 + 6N_f^2 (N_f^2 - 1) g_{SAA}^2$	$N_f^3 (g_{SSS}^3 N_f^3 + g_{SAA}^3 (N_f^2 - 1))$
$\frac{SAA}{N_f^2 - 1}$	N_f	$4N_f^2 g_{SSS} g_{SAA} + 8N_f g_{SAA}^2 + 4(N_f^2 - 4) g_{SAA} g_{AAA} + 4 \frac{N_f^2 - 4}{N_f} g_{AAA}^2$	$N_f^3 g_{SSS} g_{SAA}^2 + N_f^2 g_{SAA}^3 + 2(N_f^2 - 4) g_{SAA} g_{AAA}^2$
$\frac{AAA}{(N_f^2 - 1)(N_f^2 - 4)}$	$\frac{1}{N_f}$	$3g_{SAA}^2 + 3 \frac{N_f^2 - 12}{N_f^2} g_{AAA}^2 + \frac{12}{N_f} g_{SAA} g_{AAA}$	$3g_{SAA}^2 g_{AAA} + \frac{N_f^2 - 12}{N_f^2} g_{AAA}^3$

Table 8. The prefactors which correspond to the flavor structure part in the calculation of the β functions in (A.24). Note the factor of $N_f^2 - 1$ and $(N_f^2 - 1)(N_f^2 - 4)$ common to all the SAA and AAA contributions respectively. This is to be expected because for $N_f = 1$ (respectively 2) both (respectively the AAA) structures do not exist.

and so there will be contributions to subleading order only for $V = 2$ or $V = 3$. Furthermore, in order to obtain the maximal power of N_c , all the available propagators of ϕ must be paired to give factors of N_c . This leaves only the two diagrams drawn in figure 8⁵⁵.

Next, we claim that there is no contribution of the field strength renormalization Z at the leading order in $\frac{1}{N_c}$. For such diagrams, the number of external lines is $E = 2$ and so the number of internal lines is given by the equation $I = 3V - 1$. By the same power counting, the maximal power of N_c is $\lfloor \frac{I}{2} \rfloor - 2V = \lfloor \frac{-V-1}{2} \rfloor$. However, the only possibility to get a contribution at order $\frac{1}{N_c}$ is by taking $V = 1$, and this cannot be the case, since we do not allow interaction vertices connected to themselves. This completes the proof.

A.2.2 Calculation for $N_f > 1$

The calculation for the $N_f > 1$ case follows directly from the $N_f = 1$ case. The only difference is that the vertex (A.11) also contains a flavor structure. The integrals over the internal loop momenta are the same, and so one has only to calculate the prefactor which comes from the symmetry factor and the flavor structure.

We find it illuminating to work with the renormalization condition in the representation basis (A.14). The analog of (A.19) is (for $n = SSS, SAA, AAA$)

$$\#_{tree,n} (g_{n,B} - g_n) = \#_{2loop,n} \frac{N_c}{16\pi^2} \ln(\Lambda) - \#_{4loop,n} \frac{N_c^3}{2^{10}\pi^2} \ln(\Lambda), \quad (\text{A.24})$$

where the coefficients which correspond to the different flavor structures are given in table 8.

⁵⁵An example with “unpaired” propagators is diagram A8b, shown in figure 9. The contribution of this diagram is subleading to the A8a diagram.

Taking the derivative with respect to the UV cutoff Λ , we find that the β functions are

$$\begin{aligned}
2^{10}\pi^2 N_c \beta_{SSS} &= 2^6 \left(6N_f \lambda_{SSS}^2 + 6 \frac{(N_f^2 - 1)}{N_f} \lambda_{SAA}^2 \right) - (N_f^3 \lambda_{SSS}^3 + (N_f^2 - 1) \lambda_{SAA}^3), \\
2^{10}\pi^2 N_c \beta_{SAA} &= 2^6 \left(4N_f \lambda_{SSS} \lambda_{SAA} + 8\lambda_{SAA}^2 + 4 \frac{(N_f^2 - 4)}{N_f} \lambda_{SAA} \lambda_{AAA} + 4 \frac{(N_f^2 - 4)}{N_f^2} \lambda_{AAA}^2 \right) \\
&\quad - \left(N_f^2 \lambda_{SSS} \lambda_{SAA}^2 + N_f \lambda_{SAA}^3 + 2 \frac{(N_f^2 - 4)}{N_f} \lambda_{SAA} \lambda_{AAA}^2 \right), \\
2^{10}\pi^2 N_c \beta_{AAA} &= 2^6 \left(3N_f \lambda_{SAA}^2 + \frac{3(N_f^2 - 12)}{N_f} \lambda_{AAA}^2 + 12\lambda_{SAA} \lambda_{AAA} \right) \\
&\quad - \left(3N_f \lambda_{SAA}^2 \lambda_{AAA} + \frac{(N_f^2 - 12)}{N_f} \lambda_{AAA}^3 \right),
\end{aligned} \tag{A.25}$$

which is equation (5.2) in the main text.

The advantage of working with the couplings in the representation basis, compared to the index basis, is that the contributions of the Feynman diagrams to each of the beta functions is more transparent. In complete analogy to the beta functions (4.22) in the main text (explained in section 4.3 in item 7), one can extract the possible monomials which can appear in the beta function by treating each pair of particle ϕ and anti particle $\bar{\phi}$ entering a vertex of type (A.11) as a composite meson \tilde{M} . For example, the contribution of the four-loop diagram to Γ_{SSS}^6 involves three scalar mesons, each entering the diagram at a different vertex. The internal loops correspond to exchanging mesons between the vertices, which in our example, can be either all scalar mesons, or all adjoint mesons, but not both. As a result, the only two cubic structures which contribute to β_{SSS} are λ_{SSS}^3 and λ_{SAA}^3 (as one cannot construct a scenario in which there is $\lambda_{SSS}^2 \lambda_{SAA}$ or $\lambda_{SSS} \lambda_{SAA}^2$). This way, each two lines in diagram A0 in figure 7 are viewed in the same way as a ζ line in the G_3^3 diagrams in figure 3. The same reasoning can be applied for the other two couplings β_{SAA} and β_{AAA} and for the two-loop diagram. This shows which monomials of the couplings can appear in the β function. Also, each λ_{SAA} in β_{SSS} is accompanied by a factor of $(N_f^2 - 1)$, and each λ_{AAA} in β_{SAA} is accompanied by a factor of $(N_f^2 - 4)$, which makes the reduction to the $N_f = 1$ and $N_f = 2$ cases natural (as discussed in item 6 in section 4.3).

Diagram	Momentum Integral	Symmetry Factor	Overcounting Factor	Factors of $4\pi/ \kappa $
A1a	$-\frac{1}{32\pi^2}$	$\frac{1}{2}$	4	$(4\pi/ \kappa)^2$
A1b/c	$-\frac{1}{32\pi^2}$	$\frac{1}{2}$	12	$(4\pi/ \kappa)^2$
A2	$\frac{1}{32\pi^2}$	1	1	$(4\pi/ \kappa)^4$
A3	$\frac{1}{32\pi^2}$	1	2	$(4\pi/ \kappa)^4$
A4	$-\frac{1}{16\pi^2}$	1	4	$(4\pi/ \kappa)^2$
A5	$\frac{1}{32\pi^2}$	1	2	$(4\pi/ \kappa)^4$
A6	$\frac{3}{64\pi^2}$	$\frac{1}{2}$	6	$(4\pi/ \kappa)^4$
A7	$\frac{3}{64\pi^2}$	1	2	$(4\pi/ \kappa)^4$
A8a	$\frac{1}{32\pi^2}$	$\frac{1}{2}$	4	1
A8b	$\frac{1}{32\pi^2}$	$\frac{1}{2}$	36	1

Table 9. The factors contributing to the diagrams of figure 9, as explained in the text. The momentum integral column is the coefficient of $\frac{1}{\epsilon}$. The last column indicates the factors of $4\pi/|\kappa|$ which come from the gauge field interactions. For color and flavor structures see table 10.

A.3 The $\lambda \ll 1$ case

Turning on a small λ we can also perturbatively compute the beta function, in the regime where also g_n are small and of order $\frac{\lambda^2}{N_c^2}$ (without necessarily taking the 't Hooft large N_c limit).

To second order in both g_n and λ^2 there are 11 diagrams that contribute to the 6-point vertex (figure 9) and 4 that contribute to the propagator (figure 10) [49]. The momentum structure of these diagrams is the same as in the $N_f = 1$ case, so we can use the known results [49, 50] to extract the divergent part in **dimensional regularization** with $d = 3 - \epsilon$, as is shown in the first column of table 9. The symmetry factor for these diagrams is also shown in that table.

Each of the diagrams of figure 9 also has a color and flavor structure (some sum of delta functions in the external indices). In order to extract the correct contribution to the different delta function structures of (A.11) one must sum over every permutation of the external color-flavor indices **that gives a different diagram**. This is not the full $3! \cdot 3!$ possible permutations (e.g. permuting two of the upper scalars in diagram A1b will not result in a different diagram). We call the number of permutations of external indices that leaves the diagram the same an “Overcounting Factor” and it is given in the second to right column of table 9.

The computations of the color and flavor structures of these diagrams are straightforward given the Feynman rules above. We can then extract the corrections to the beta functions using the renormalization conditions in (A.12). The results are shown in table 10, except for the contributions to the A4 and A8a diagrams that are too long to fit in the table, and

Contribution to:	Diagram	Contribution
$\delta\bar{\Gamma}_1^{(6)}$	A1a	$3\bar{g}_1 N_c^2 + 6\bar{g}_2 N_c + \frac{18\bar{g}_1}{N_c^2} - \frac{24\bar{g}_2}{N_c} - 3\bar{g}_1$
	A1b/c	$\frac{6\bar{g}_1}{N_c^2} + 3\bar{g}_2 N_c - \frac{12\bar{g}_2}{N_c} + 3\bar{g}_1$
	A2	$\frac{96}{N_c^4} + 12$
	A3	-12
	A4	see (A.26)
	A5	$-\frac{24N_f}{N_c^3}$
	A6	-2
	A7	$\frac{48}{N_c^4} + \frac{48}{N_c^2} + 6$
	A8a	see (A.26)
	A8b	$\bar{g}_1^2 + 3\bar{g}_2^2 + 2\bar{g}_3^2$
$\delta\bar{\Gamma}_2^{(6)}$	A1a	$3\bar{g}_2 N_c^2 + 2(\bar{g}_1 + 2\bar{g}_3) N_c + \frac{18\bar{g}_2}{N_c^2} - \frac{8(\bar{g}_1 + 2\bar{g}_3)}{N_c} - 3\bar{g}_2$
	A1b/c	$\frac{6\bar{g}_2}{N_c^2} + (\bar{g}_1 + 2\bar{g}_3) N_c - \frac{4(\bar{g}_1 + 2\bar{g}_3)}{N_c} + 3\bar{g}_2$
	A2	$10N_c - \frac{96}{N_c^3} - \frac{16}{N_c}$
	A3	$-10N_c - \frac{8}{N_c}$
	A4	see (A.26)
	A5	$\frac{24N_f}{N_c^2} + 6N_f$
	A6	$-2N_c$
	A7	$6N_c - \frac{64}{N_c^3} - \frac{32}{N_c}$
	A8a	see (A.26)
	A8b	$2\bar{g}_2(\bar{g}_1 + 2\bar{g}_3)$
$\delta\bar{\Gamma}_3^{(6)}$	A1a	$3\bar{g}_3 N_c^2 + 6\bar{g}_2 N_c + \frac{18\bar{g}_3}{N_c^2} - \frac{24\bar{g}_2}{N_c} - 3\bar{g}_3$
	A1b/c	$3\bar{g}_2 N_c - \frac{12\bar{g}_2}{N_c} + \frac{6\bar{g}_3}{N_c^2} + 3\bar{g}_3$
	A2	$3N_c^2 + \frac{144}{N_c^2} - 48$
	A3	$36 - 3N_c^2$
	A4	$\frac{3(N_c^2 - 4)(\bar{g}_3 N_f + 2\bar{g}_2)}{N_c}$
	A5	$-\frac{36N_f}{N_c} + 3N_c N_f$
	A6	4
	A7	$\frac{96}{N_c^2} - 12$
	A8a	see (A.26)
	A8b	$3\bar{g}_2^2 + \bar{g}_3(2\bar{g}_1 + \bar{g}_3)$

Table 10. Color and flavor structures that contribute to the 2-loop corrections to (A.12), from the diagrams in figure 9, after accounting for symmetry and overcounting factors (but not the momentum integrals).

are given by

$$\begin{aligned}
A4_1 &= \frac{6(\bar{g}_1(N_c^3 N_f - N_c N_f + N_c^2 + 2) + \bar{g}_2(N_c^2 N_f + 2N_c^3 - 2N_c + 2N_f) + \bar{g}_3(N_c^2 + 2))}{N_c^2}, \\
A4_2 &= 2 \left(N_c(2\bar{g}_2 N_f + \bar{g}_1 + 3\bar{g}_3) + \frac{2\bar{g}_3 N_f + 4\bar{g}_2}{N_c^2} - \frac{5\bar{g}_2 N_f + 4\bar{g}_1 + 6\bar{g}_3}{N_c} + \bar{g}_3 N_f + 2\bar{g}_2 \right), \\
A8a_1 &= 3(\bar{g}_1^2(2N_c N_f + 7) + 8\bar{g}_1(\bar{g}_2(N_c + N_f) + \bar{g}_3) + \bar{g}_2^2(2N_c N_f + 19) + 4\bar{g}_2\bar{g}_3(N_c + N_f) + 4\bar{g}_3^2), \\
A8a_2 &= 2(7\bar{g}_2^2(N_c + N_f) + \bar{g}_1\bar{g}_2(2N_c N_f + 17) + 2\bar{g}_3\bar{g}_2(N_c N_f + 16) + 3\bar{g}_3^2(N_c + N_f) + 4\bar{g}_1\bar{g}_3(N_c + N_f)), \\
A8a_3 &= 3(\bar{g}_2^2(N_c N_f + 15) + 8\bar{g}_3\bar{g}_2(N_c + N_f) + \bar{g}_3(\bar{g}_3(N_c N_f + 9) + 6\bar{g}_1)). \tag{A.26}
\end{aligned}$$

Diagram	Momentum Integral	Symmetry Factor	Total Color- Flavor Factor
B1	$\frac{1}{24\pi^2}$	1	$N_c^2 - 1$
B2	$\frac{1}{96\pi^2}$	$\frac{1}{2}$	$\frac{N_c^4 - 3N_c^2 + 2}{N_c^2}$
B3	$\frac{1}{12\pi^2}$	1	$\frac{1}{N_c^2} - 1$
B4	$\frac{1}{24\pi^2}$	1	$\frac{N_c^2 - 1}{N_c} N_f$

Table 11. The factors contributing to the diagrams of figure 10, as explained in the text. The momentum integral column is the coefficient of $\frac{1}{\epsilon}$, the color structure is after multiplication by the symmetry factor. All the diagrams are of order $\left(\frac{4\pi}{|\kappa|}\right)^2$.

We also need the contribution that comes from the corrections to the propagators. This is simpler, as the overall structure is just $\delta_{ij}\delta_{ab}$ and there are no overcounting factors. The results are shown in table 11.

Summing all the contributions we can get the beta functions for $\bar{g}_{1/2/3}$. By the Callan-Symanzik equation we have

$$\begin{aligned} \beta_{\bar{g}_i} = & 2 \sum_{A \text{ diagrams}} \left(\frac{\text{Factors}}{\text{of } 4\pi/|\kappa|} \right) \times \left(\frac{\text{Momentum}}{\text{Integration}} \right) \times \left(\frac{\text{Symmetry}}{\text{Factor}} \right) \times \frac{3! \cdot 3!}{\text{Overcounting Factor}} \times \delta \bar{\Gamma}_i^{(6)} \\ & - 6 \times \left(\frac{4\pi}{|\kappa|} \right)^2 \times \bar{g}_i \times \sum_{B \text{ diagrams}} \left(\frac{\text{Momentum}}{\text{Integration}} \right) \times \left(\frac{\text{Symmetry}}{\text{Factor}} \right) \times (\text{factors in table 11}). \end{aligned} \quad (\text{A.27})$$

In the paper, we are interested in the 't Hooft limit $N_c \rightarrow \infty$, with the finite 't Hooft parameters $\bar{g}_n = \frac{\bar{\lambda}_n}{(N_c)^2}$ and $\lambda = \frac{N_c}{\kappa}$. In this limit, the beta functions are (at leading order in $\frac{1}{N_c}$)

$$16\pi^2 N_c \beta_{\bar{1}} = 6 \left(\bar{\lambda}_1^2 N_f + \bar{\lambda}_2 (\bar{\lambda}_2 N_f + 2\bar{\lambda}_3) + 4\bar{\lambda}_2 \bar{\lambda}_1 \right) - 4 \left(\frac{\lambda}{4\pi} \right)^2 (4\bar{\lambda}_1 N_f + 9\bar{\lambda}_2), \quad (\text{A.28})$$

$$16\pi^2 N_c \beta_{\bar{2}} = 4\bar{\lambda}_2 (\bar{\lambda}_1 + \bar{\lambda}_3) N_f + 14\bar{\lambda}_2^2 + 2\bar{\lambda}_3 (4\bar{\lambda}_1 + 3\bar{\lambda}_3) - 4 \left(\frac{\lambda}{4\pi} \right)^2 (3\bar{\lambda}_2 N_f + 2\bar{\lambda}_1 + 5\bar{\lambda}_3) + 6 \left(\frac{\lambda}{4\pi} \right)^4, \quad (\text{A.29})$$

$$16\pi^2 N_c \beta_{\bar{3}} = 3 \left(\bar{\lambda}_2^2 N_f + \bar{\lambda}_3^2 N_f + 8\bar{\lambda}_3 \bar{\lambda}_2 \right) - 2 \left(\frac{\lambda}{4\pi} \right)^2 (5\bar{\lambda}_3 N_f + 12\bar{\lambda}_2) + 3N_f \left(\frac{\lambda}{4\pi} \right)^4. \quad (\text{A.30})$$

As in the case $\lambda = 0$, it is more convenient to write this in the representation basis. Using

the conversion (2.8) we find

$$\begin{aligned}
16\pi^2 N_c \beta_{SSS} &= \left(\frac{\lambda}{4\pi}\right)^4 \frac{24}{N_f} - \left(\frac{\lambda}{4\pi}\right)^2 \frac{8 \left(\lambda_{SSS} N_f (2N_f^2 + 3) + 3\lambda_{SAA} (N_f^2 - 1) \right)}{N_f^2} \\
&\quad + 6\lambda_{SSS}^2 N_f + \frac{6\lambda_{SAA}^2 (N_f^2 - 1)}{N_f}, \\
16\pi^2 N_c \beta_{SAA} &= 12 \left(\frac{\lambda}{4\pi}\right)^4 - \left(\frac{\lambda}{4\pi}\right)^2 \frac{4 \left(N_f (2\lambda_{SSS} N_f + 3\lambda_{SAA} (N_f^2 + 2)) + 4\lambda_{AAA} (N_f^2 - 4) \right)}{N_f^2} \\
&\quad + \frac{4 \left(\lambda_{SAA} N_f^2 (\lambda_{SSS} N_f + 2\lambda_{SAA}) + \lambda_{SAA} \lambda_{AAA} (N_f^2 - 4) N_f + \lambda_{AAA}^2 (N_f^2 - 4) \right)}{N_f^2}, \\
16\pi^2 N_c \beta_{AAA} &= 3N_f \left(\frac{\lambda}{4\pi}\right)^4 + \left(\frac{\lambda}{4\pi}\right)^2 \left(-10\lambda_{AAA} N_f + \frac{48\lambda_{AAA}}{N_f} - 24\lambda_{SAA} \right) \\
&\quad + 3 \left(\lambda_{SAA}^2 N_f + \frac{\lambda_{AAA}^2 (N_f^2 - 12)}{N_f} + 4\lambda_{AAA} \lambda_{SAA} \right),
\end{aligned} \tag{A.31}$$

which is equation (5.3) we use in the main text. We note that as expected from the general proof in the paper, and as shown in the $N_f = 1$ case [49], the highest power of N_c^2 cancels between diagrams A1a, A2, B1 and B2, and we are left with a leading contribution to the beta function of order $\frac{1}{N_c}$.

A.3.1 IR-stable points at finite N_c

The results presented in table 10 were obtained using perturbation theory in $\sqrt{\frac{4\pi}{|\kappa|}}$, with $g_n \sim \frac{\lambda^2}{N_c^2}$, and are valid for arbitrary N_c and N_f . Although this is not the main focus of the paper, the calculations performed can also be applied to analyze systems with finite N_c .

One particular question of interest is whether there exists an IR-stable fixed point for the marginal running couplings g_n . The results, for different values of N_c and N_f , are shown in figure 16.

As we see from the figure, the existence of of an IR fixed point depends both on the number of colors and on the number of flavors. For the $N_f = 1, 2$ (or $N_c = 2$) cases, there exist only 1 or 2 marginal couplings, we see that an IR-stable fixed point exists for any N_c (N_f).

For the cases with all three marginal couplings, the existence of the IR-stable fixed point depends on the specific values chosen. An interesting result is that for $N_f = 3, 4$ (with the exception of $N_c = N_f = 3$) there is no IR fixed point for any N_c (we see this explicitly for $N_c \leq 30$ and is in accordance with the result for $N_c \rightarrow \infty$ we saw in the main text, see table 6).

Another interesting observation from the figure is that for $3 \leq N_c \leq 6$, there is no IR-stable fixed point for any value of $N_f \geq 3$ (with the exception of $N_c = N_f = 3$).

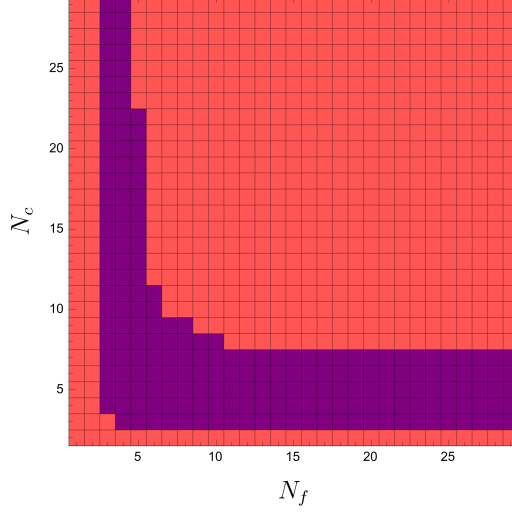


Figure 16. Existence of a weakly coupled IR-stable point for different values of $N_c \geq 2$ and $N_f \geq 1$. **Violet-** no IR-stable fixed point **Red-** one IR-stable fixed point. The large N_c behavior that was derived in the main text appears here for $N_c > 22$.

B Correlation functions for the critical boson theory at $\lambda = 0$

In this appendix, we calculate correlation functions of the σ_i^j operators, for the critical boson theory (2.15a) with $\lambda = 0$. As described in [25] and in the main text, in order to calculate the β_{λ_n} functions at leading order in $\frac{1}{N_c}$, we need the leading expansion in terms of $\frac{1}{N_c}$ for the four-point and five-point correlation functions, as well as the leading and first subleading terms of the two-point and three-point functions.

To calculate the desired correlation functions, we do the following⁵⁶:

- In section B.1, we integrate out the scalar fields $\phi, \bar{\phi}$ and obtain an effective action for the σ field. While the formal expression for the effective action is an infinite series, we truncate it to obtain a polynomial in σ . The coefficients of this expansion, denoted by S_n , correspond to the amputated correlation functions.
- In section B.2, we present the amputated tree level n -point correlation functions of σ , G_n , and derive an expression for the amputated correlation functions of four σ fields, in a particular limit of external momenta.
- In section B.3, we summarize the tree-level correlation functions of σ in the limit that we use in the paper, and in this appendix afterwards.
- In section B.4 we calculate the first sub-leading correction to the two-point correlation function of σ , which depends on $\ln(\Lambda)$. From this, we extract the anomalous dimensions $\gamma_{S/A}$ of the singlet σ_S and adjoint σ_A operators.
- In section B.5, we present the first sub-leading correction to the three-point correlation function of σ , which in the main text we denote as δG_3 .

⁵⁶We closely follow Appendix B of [25], extending their results to multiple flavors.

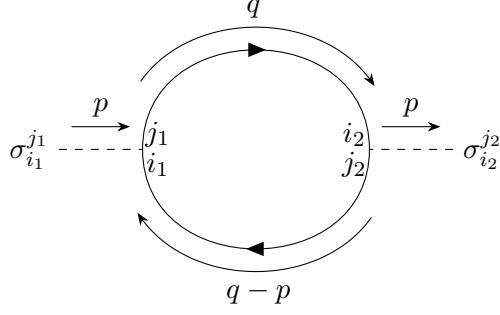


Figure 17. Feynman diagram for calculating S_2 . Broken lines denote σ fields and solid lines the scalars ϕ .

B.1 Effective action for σ

In the $\lambda = 0$ limit, the gauge fields do not interact with the ϕ and σ fields in the theory, and can be trivially integrated out. The scalar fields ϕ can also be integrated out, providing the effective action for σ

$$\int D\phi D\bar{\phi} e^{-\int (\sum_i \partial_\mu \bar{\phi} \partial_\mu \phi + \sigma_i^j \bar{\phi}_j \phi^i)} = e^{-S_{eff}(\sigma_i^j)},$$

$$S_{eff}(\sigma_i^j) = \sum_{n=2}^{\infty} \frac{1}{n!} \int d\Pi_n (S_n)_{j_1 \dots j_n}^{i_1 \dots i_n} (p_1, \dots, p_n) \sigma_{i_1}^{j_1}(p_1) \dots \sigma_{i_n}^{j_n}(p_n), \quad (\text{B.1})$$

where $d\Pi_n$ is given by (3.2).

The $(S_n)_{j_1 \dots j_n}^{i_1 \dots i_n} (p_1, \dots, p_n)$ coefficients of the effective action can be found (at least formally) by taking the derivatives with respect to σ_i^j on both sides of (B.1). For each n , $(S_n)_{j_1 \dots j_n}^{i_1 \dots i_n} (p_1, \dots, p_n)$ can be calculated by summing over all the connected diagrams of the ϕ 's. For the purpose of our calculations, we need only the terms with $n \leq 5$.

For $n = 2$, there is only one connected diagram, and one finds (see figure 17)

$$(S_2)_{j_1 j_2}^{i_1 i_2} (p) = \delta_{j_2}^{i_1} \delta_{j_1}^{i_2} \tilde{S}_2(p); \quad \tilde{S}_2(p) = -N_c \int \frac{d^3 q}{(2\pi)^3} \frac{1}{q^2 (q-p)^2} = -N_c \frac{1}{8|p|}. \quad (\text{B.2})$$

For $n = 3$, there are two connected diagrams, as shown in figure 18: one in which the i_1 index is contracted with j_2 to provide $\delta_{j_2}^{i_1}$ and one in which we have $\delta_{j_3}^{i_1}$. It is evident (as can be shown by explicit calculation) that the momentum dependence in both cases is the same, and we find

$$(S_3)_{j_1, j_2, j_3}^{i_1, i_2, i_3} (p_1, p_2, p_3) = \tilde{S}_3 \left(\delta_{j_2}^{i_1} \delta_{j_3}^{i_2} \delta_{j_1}^{i_3} + \delta_{j_3}^{i_1} \delta_{j_2}^{i_3} \delta_{j_1}^{i_2} \right),$$

$$\tilde{S}_3(p_1, p_2, p_3) = N_c \int \frac{d^3 q}{(2\pi)^3} \frac{1}{q^2 (q+p_1)^2 (q-p_3)^2} = \frac{N_c}{8} \frac{1}{|p_1| |p_2| |p_3|}. \quad (\text{B.3})$$

For $n = 4$ there are $(4-1)! = 6$ connected diagrams, corresponding to permutations of $(1, 2, 3, 4)$ up to cyclic shifts. An example of one of the diagrams is given in figure 19.

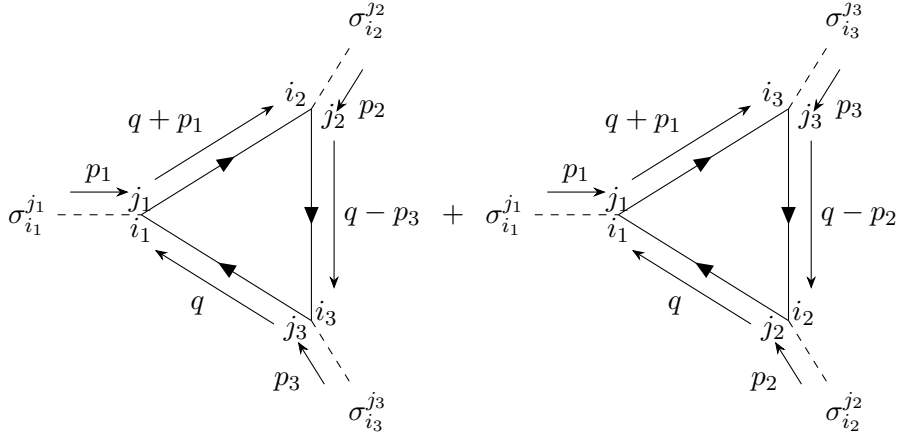


Figure 18. Feynman diagrams for calculating S_3 , with the same notations as in figure 17.

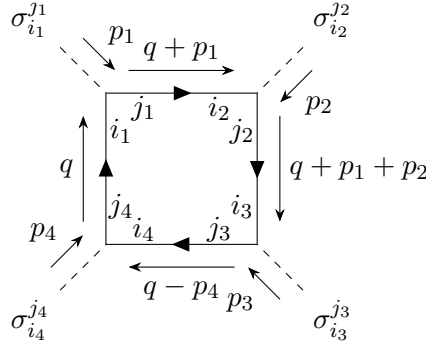


Figure 19. A Feynman diagram which contributes to the calculation of S_4 . The other 5 diagrams are given by permutations of the external legs.

We have:

$$(S_4)^{i_1, i_2, i_3, i_4}_{j_1, j_2, j_3, j_4}(p_1, p_2, p_3, p_4) = \left(\delta_{j_2}^{i_1} \delta_{j_3}^{i_2} \delta_{j_4}^{i_3} \delta_{j_1}^{i_4} \tilde{S}_4(p_1, p_2, p_3, p_4) + (\text{permutations of } \{2, 3, 4\}) \right),$$

$$\tilde{S}_4(p_1, p_2, p_3, p_4) = -N_c \int \frac{d^3 q}{(2\pi)^3} \frac{1}{q^2 (q + p_1)^2 (q + p_1 + p_2)^2 (q - p_4)^2}. \quad (\text{B.4})$$

The explicit expression of \tilde{S}_4 for arbitrary momenta is unknown.

A similar expression can be written for $n = 5$, with $(5 - 1)! = 24$ connected diagrams

$$(S_5)^{i_1, i_2, i_3, i_4, i_5}_{j_1, j_2, j_3, j_4, j_5}(p_1, p_2, p_3, p_4, p_5) = \left(\delta_{j_2}^{i_1} \delta_{j_3}^{i_2} \delta_{j_4}^{i_3} \delta_{j_5}^{i_4} \delta_{j_1}^{i_5} \tilde{S}_5(p_1, p_2, p_3, p_4, p_5) + (\text{permutations of } \{2, 3, 4, 5\}) \right), \quad (\text{B.5})$$

with $\tilde{S}_5(p_1, p_2, p_3, p_4, p_5)$ containing the momentum part. We do not use the explicit form of \tilde{S}_5 in this work, and refer the reader to [25].

B.2 Amputated tree-level correlation functions for σ

In this section, we use (B.1), the effective action for σ , to obtain the tree-level amputated correlation functions of σ , in the desired momenta limits.

First, we note that the coefficient of the quadratic term serves as the inverse of the σ propagator. The σ propagator (at tree-level) is thus⁵⁷

$$-(G_2)_{i_1, i_2}^{j_1, j_2}(p) \equiv \left\langle \sigma_{i_1}^{j_1}(p) \sigma_{i_2}^{j_2}(-p) \right\rangle = (S_2^{-1})_{i_1, i_2}^{j_1, j_2}(p) = -\frac{8|p|}{N_c} \delta_{i_2}^{j_1} \delta_{i_1}^{j_2}. \quad (\text{B.6})$$

For the amputated three-point correlation function of σ , the only diagram at tree-level is that which contains only the 3-point vertex S_3 , that is⁵⁸

$$\left\langle \sigma_{j_1}^{i_1}(p_1) \sigma_{j_2}^{i_2}(p_2) \sigma_{j_3}^{i_3}(p_3) \right\rangle_{\text{amp}} = -(S_3)_{j_1, j_2, j_3}^{i_1, i_2, i_3}(p_1, p_2, p_3). \quad (\text{B.7})$$

For the amputated four-point σ correlation function, there are four Feynman diagrams contributing to this correlation function, shown in figure 20. They are given by

$$\begin{aligned} & \left\langle \sigma_{j_1}^{i_1}(p_1) \sigma_{j_2}^{i_2}(p_2) \sigma_{j_3}^{i_3}(p_3) \sigma_{j_4}^{i_4}(p_4) \right\rangle_{\text{amp}} = -(S_4)_{j_1, j_2, j_3, j_4}^{i_1, i_2, i_3, i_4}(p_1, p_2, p_3, p_4) \\ & + (S_3)_{j_1, j_2, j_a}^{i_1, i_2, i_a}(p_1, p_2, -p_1 - p_2) (S_3)_{j_3, j_4, j_b}^{i_3, i_4, i_b}(p_3, p_4, p_1 + p_2) (S_2^{-1})_{i_a, i_b}^{j_a, j_b}(p_1 + p_2) \\ & + \left[(S_3)_{j_1, j_3, j_a}^{i_1, i_3, i_a}(p_1, p_3, -p_1 - p_3) (S_3)_{j_2, j_4, j_a}^{i_2, i_4, i_a}(p_2, p_4, p_1 + p_3) (S_2^{-1})_{i_a, i_b}^{j_a, j_b}(p_1 + p_3) + (3 \leftrightarrow 4) \right], \end{aligned} \quad (\text{B.8})$$

where we used (B.6), and we sum over i_a, j_a, i_b, j_b .

For the purpose of calculating the β functions, we are interested in the limit where $p_1 = -p_2 = p, p_3 = -p_4 = k$ and $|p| \gg |k|$ (see section 3 in this paper, and section 3 in [25]). This limit cannot be plugged in directly, since both $\tilde{S}_4(p, -p, k, -k)$ and $S_3(p, -p, 0)$ have an IR divergence, and so although the full tree-level 4-point function in this limit is well-defined, two of the Feynman diagrams contributing to (B.8) diverge separately.

To see that (B.8) for the single-flavor case $N_f = 1$ is free from IR singularities, the authors in [25] used an IR regulator δ . They calculated the four-point function with $p_1 = p, p_2 = p + \delta, p_3 = k, p_4 = -k - \delta$, in the $|p| \gg |k| \gg |\delta|$ limit, and showed that the resulting expression is well-defined, finite, and single-valued at $\delta \rightarrow 0$.

Adding flavors adds a subtlety to this procedure, since for specific indices, (B.8) with $p_1 = -p_2 = p, p_3 = -p_4 = k$ is not IR-finite. This can be fixed by symmetrizing over p_3 and p_4 . We define

$$\begin{aligned} (S_4^{\text{eff}})_{j_1, j_2, j_3, j_4}^{i_1, i_2, i_3, i_4}(p, -p, k, -k) \equiv & -\lim_{\delta \rightarrow 0} \frac{1}{2} \left[\left\langle \sigma_{j_1}^{i_1}(p) \sigma_{j_2}^{i_2}(-p + \delta) \sigma_{j_3}^{i_3}(k) \sigma_{j_4}^{i_4}(-k - \delta) \right\rangle_{\text{amp}} \right. \\ & \left. + \left\langle \sigma_{j_1}^{i_1}(p) \sigma_{j_2}^{i_2}(-p + \delta) \sigma_{j_3}^{i_3}(-k - \delta) \sigma_{j_4}^{i_4}(k) \right\rangle_{\text{amp}} \right]. \end{aligned} \quad (\text{B.9})$$

⁵⁷Note that here, and in the following, we ignore trivial factors of δ functions over the momenta.

⁵⁸Note that we flip the role of the i 's and j 's indices comparing to section B.1. This is because when taking the amputated diagram, we have to multiply each external leg by the inverse of S_2 , as in (B.12).

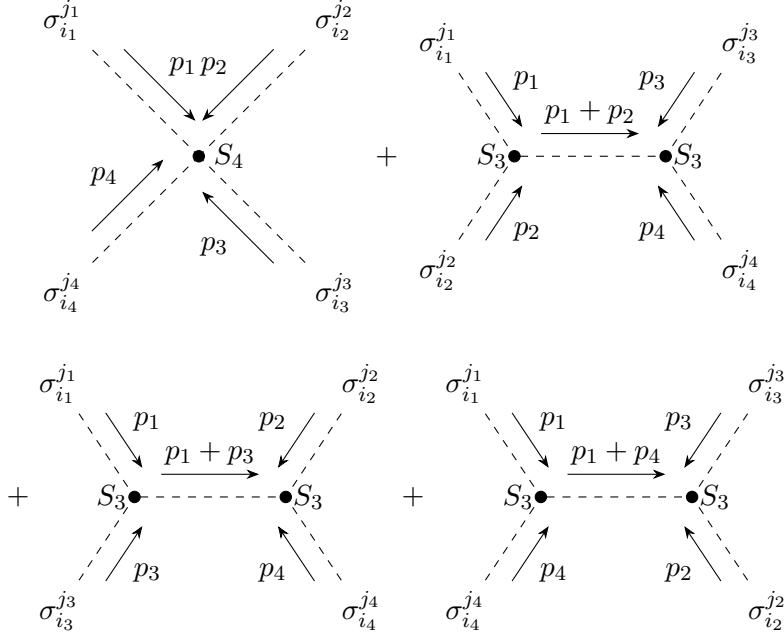


Figure 20. Feynman diagrams for calculating S_4 .

Then, (B.9) is free from IR divergences, even though each term on the right-hand side diverges. This should not concern us, since in the calculation involving the 4-point function in this limit, we need to include both the case that $p_3 = k$ and the case $p_3 = -k$.

The calculation of S_4^{eff} follows the same lines as in [25]. The only difference is that one needs to compute the two different index structures (the near and far structures presented in (4.11)) separately. We find that in the limit $|p| \gg |k|$, the effective amputated four-point function is

$$\begin{aligned}
 & \left(S_4^{eff} \right)_{j_1, j_2, j_3, j_4}^{i_1, i_2, i_3, i_4} (p, -p, k, -k) \simeq \\
 & -\frac{N_c}{2} \left[\left(\left(\delta_{j_2}^{i_1} \delta_{j_3}^{i_2} \delta_{j_4}^{i_3} \delta_{j_1}^{i_4} + (3 \leftrightarrow 4) \right) + (1 \leftrightarrow 2) \right) \left(-\frac{1}{8} \frac{1}{p^2 k^2 |p-k|} - \frac{1}{8} \frac{1}{p^2 k^2 |p+k|} + \frac{1}{4p^4} \frac{1}{|k|} \frac{(k \cdot p)^2}{p^2 k^2} \right) + \right. \\
 & \left. \left(\delta_{j_3}^{i_1} \delta_{j_2}^{i_3} \delta_{j_4}^{i_2} \delta_{j_1}^{i_4} + \delta_{j_4}^{i_1} \delta_{j_2}^{i_4} \delta_{j_3}^{i_2} \delta_{j_1}^{i_3} \right) \left(-\frac{1}{4} \frac{1}{p^2 k^2 |p-k|} - \frac{1}{4} \frac{1}{p^2 k^2 |p+k|} + \frac{1}{2|k|p^4} \right) \right].
 \end{aligned} \tag{B.10}$$

The calculation of the amputated five-point function follows the same idea [25]. Besides the original 5 point interaction term S_5 , we have two additional types of diagrams, one involving S_3 and S_4 , and one involving three S_3 vertices (see figures 17, 18, and 19 in [25]).

We will not attempt to calculate the final expression for the amputated five-point correlation function explicitly, nor will we show that for momenta in the limit of interest, it is free from IR singularities. Instead, we will use our knowledge of the full five-point correlation function G_5 in (4.12), to construct the proper expression for S_5 .

For $|p| \gg |p_1|, |p_2|, |p_3|$, the form of G_5 , which is the full correlation function, is given by (4.12). To get the amputated correlation function, we remove the external legs by

multiplying by $S_2(k_i)$ for each external leg carrying a momentum k_i . The end result is

$$\left(S_5^{eff}\right)_{j_1, j_2, j_3, j_4, j_5}^{i_1, i_2, i_3, i_4, i_5}(p, -p, p_1, p_2, p_3) = \frac{N_c}{|p|^4 |p_1| |p_2| |p_3|} \begin{pmatrix} s_{5,N} \left(\left(\delta_{j_2}^{i_1} \delta_{j_3}^{i_2} \delta_{j_4}^{i_3} \delta_{j_5}^{i_4} \delta_{j_1}^{i_5} + (3, 4, 5) \right) + (1 \leftrightarrow 2) \right) \\ s_{5,F} \left(\left(\delta_{j_3}^{i_1} \delta_{j_2}^{i_3} \delta_{j_4}^{i_2} \delta_{j_5}^{i_4} \delta_{j_1}^{i_5} + (3, 4, 5) \right) + (1 \leftrightarrow 2) \right) \end{pmatrix}, \quad (\text{B.11})$$

where $s_{5,N}$ and $s_{5,F}$ are unknown coefficients, which do not scale with N_c , and we sum over permutations of $\{3, 4, 5\}$.

As a final comment, it should be clear that $S_n \propto N_c$ (at leading order at large N_c) for any n . As a result, the effective action (B.1) is proportional to N_c , and we can think of N_c as taking the role of \hbar^{-1} . Thus, the contribution of loop diagrams goes as $\frac{1}{N_c}$ to the power of the number of loops.

B.3 Tree-level correlation functions

In the main text, we use the full (not amputated) n -point correlation functions of the σ operators, which we denote by G_n (up to minus sign)⁵⁹. To obtain them from the amputated correlation function, we multiply each external leg with momentum p by the propagator $(S_2^{-1})_{i_a, i_b}^{j_a, j_b}(p)$. This fixes the N_c dependence of the tree-level contribution to G_n to be $G_n \sim N_c^{-n+1}$.⁶⁰ The expression for the tree-level 2-point correlation function is given in (B.6), while for the 3-point function it is a contact term

$$\begin{aligned} (G_3)_{i_1, i_2, i_3}^{j_1, j_2, j_3}(p_1, p_2, p_3) &\equiv - \left\langle \sigma_{i_1}^{j_1}(p_1) \sigma_{i_2}^{j_2}(p_2) \sigma_{i_3}^{j_3}(p_3) \right\rangle \\ &= (S_2^{-1})_{i_1, i_a}^{j_1, j_a}(p_1) (S_2^{-1})_{i_2, i_b}^{j_2, j_b}(p_2) (S_2^{-1})_{i_3, i_c}^{j_3, j_c}(p_3) (S_3)_{\{j\}_3}^{\{i\}_3}(p_1, p_2, p_3) \\ &= -\frac{64}{N_c^2} \left(\delta_{i_2}^{j_1} \delta_{i_3}^{j_2} \delta_{i_1}^{j_3} + \delta_{i_3}^{j_1} \delta_{i_2}^{j_2} \delta_{i_1}^{j_3} \right), \end{aligned} \quad (\text{B.12})$$

and for the four-point function in the desired momenta limit it is⁶¹

$$\begin{aligned} \left(G_4^{eff}\right)_{i_1, i_2, i_3, i_4}^{j_1, j_2, j_3, j_4}(p, -p, k, -k) &\equiv \left\langle \sigma_{i_1}^{j_1}(p) \sigma_{i_2}^{j_2}(-p) \sigma_{i_3}^{j_3}(k) \sigma_{i_4}^{j_4}(-k) \right\rangle \\ &\simeq \frac{8^4}{N_c^3} \left[\left(\left(\delta_{i_2}^{j_1} \delta_{i_3}^{j_2} \delta_{i_4}^{j_3} \delta_{i_1}^{j_4} + (3 \leftrightarrow 4) \right) + (1 \leftrightarrow 2) \right) \left(-\frac{1}{16} \frac{1}{|p-k|} - \frac{1}{16} \frac{1}{|p+k|} + \frac{1}{8p^4} \frac{(k \cdot p)^2}{|k|} \right) + \right. \\ &\quad \left. \left(\delta_{i_3}^{j_1} \delta_{i_2}^{j_3} \delta_{i_4}^{j_2} \delta_{i_1}^{j_4} + \delta_{i_4}^{j_1} \delta_{i_2}^{j_4} \delta_{i_3}^{j_2} \delta_{i_1}^{j_3} \right) \left(-\frac{1}{8} \frac{1}{|p-k|} - \frac{1}{8} \frac{1}{|p+k|} + \frac{|k|}{4p^2} \right) \right] \\ &\approx \frac{8^4}{N_c^3} \left[\left(\left(\delta_{i_2}^{j_1} \delta_{i_3}^{j_2} \delta_{i_4}^{j_3} \delta_{i_1}^{j_4} + (3 \leftrightarrow 4) \right) + (1 \leftrightarrow 2) \right) \left(-\frac{1}{8} \frac{1}{p} + \frac{1}{8} \frac{(k \cdot p)^2}{p^4 |k|} \right) + \right. \\ &\quad \left. \left(\delta_{i_3}^{j_1} \delta_{i_2}^{j_3} \delta_{i_4}^{j_2} \delta_{i_1}^{j_4} + \delta_{i_4}^{j_1} \delta_{i_2}^{j_4} \delta_{i_3}^{j_2} \delta_{i_1}^{j_3} \right) \left(-\frac{1}{4} \frac{1}{p} + \frac{|k|}{4p^2} \right) \right], \end{aligned} \quad (\text{B.13})$$

where we assume $|p| \gg |k|$.

⁵⁹Note that we define G_2 and G_3 with minus the corresponding correlation functions, and G_4 and G_5 with a plus sign, to have compatibility with the notation in (4.2).

⁶⁰Multiplying by $(S_2^{-1})_{i_a, i_b}^{j_a, j_b}(p)$ also flips the role of the j and i indices in our notation.

⁶¹See the discussion in section B.2 for the meaning of the superscript *eff*.

For the five-point function, we take the same result in (4.12), which for completeness we copy here

$$\begin{aligned}
(G_5)_{i_1, i_2, i_3, i_4, i_5}^{j_1, j_2, j_3, j_4, j_5}(p, -p, 0, 0, 0) &\equiv - \left\langle \sigma_{i_1}^{j_1}(p) \sigma_{i_2}^{j_2}(-p) \sigma_{i_3}^{j_3}(0) \sigma_{i_4}^{j_4}(0) \sigma_{i_5}^{j_5}(0) \right\rangle \\
&= \frac{1}{p^2} \left(G_{5,N} \left(\delta_{i_2}^{j_1} \delta_{i_3}^{j_2} \delta_{i_4}^{j_3} \delta_{i_5}^{j_4} \delta_{i_1}^{j_5} + (3, 4, 5) + (1 \leftrightarrow 2) \right) + \right. \\
&\quad \left. G_{5,F} \left(\delta_{i_3}^{j_1} \delta_{i_2}^{j_2} \delta_{i_4}^{j_3} \delta_{i_5}^{j_4} \delta_{i_1}^{j_5} + (3, 4, 5) + (1 \leftrightarrow 2) \right) \right). \tag{B.14}
\end{aligned}$$

The connections between $G_{5,N}$, $G_{5,F}$ and $s_{5,N}$, $s_{5,F}$ in (B.11) are

$$s_{5,F/N} = \frac{N_c^4}{8^5} G_{5,F/N}. \tag{B.15}$$

B.4 First $\ln(\Lambda)$ dependent sub-leading contribution to G_2

At first subleading order in $\frac{1}{N_c}$, there are two diagrams that contribute to the two-point function of the σ operators, shown in figure 21. In the leading order calculation of the β function, we use only the leading order dependence of the anomalous dimension (see sections 3 and 4 in this paper and section 2 and Appendix B in [25]), which is extracted from the $\ln(\Lambda)$ -dependent terms in the two-point function. Using the expressions for S_n , we evaluate the diagrams and find

$$\begin{aligned}
(\delta S_2)_{j_1, j_2}^{i_1, i_2}(p) &= \left\langle \sigma_{j_1}^{i_1}(p) \sigma_{j_2}^{i_2}(-p) \right\rangle_{amp, loop} \\
&\supset \frac{1}{2} \int \frac{d^3 q}{(2\pi)^3} \lim_{\delta \rightarrow 0} \left(S_4^{eff} \right)_{j_3, j_4, j_1, j_2}^{i_3, i_4, i_1, i_2}(q, -q + \delta, p, -p - \delta) (S_2^{-1})_{i_3, i_4}^{j_3, j_4}(q) \tag{B.16} \\
&\supset \left(\delta s_{20} \delta_{j_2}^{i_1} \delta_{j_1}^{i_2} + \delta s_{22} \delta_{j_1}^{i_1} \delta_{j_2}^{i_2} \right) \frac{1}{p} \ln \left(\frac{\Lambda}{|p|} \right),
\end{aligned}$$

where

$$\delta s_{20} = \frac{N_f}{3\pi^2}, \quad \delta s_{22} = \frac{1}{\pi^2}, \tag{B.17}$$

and⁶²

$$\begin{aligned}
(G_{2,tot})_{i_1, i_2}^{j_1, j_2}(p) &= - \left((S_2 + \delta S_2)^{-1} \right)_{i_1, i_2}^{j_1, j_2}(p) \\
&= - (S_2^{-1})_{i_1, i_2}^{j_1, j_2}(p) + (S_2^{-1})_{i_1, i_3}^{j_1, j_3}(p) (\delta S_2)_{j_3, j_4}^{i_3, i_4}(p) (S_2^{-1})_{i_4, i_2}^{j_4, j_2}(p) \tag{B.18} \\
&\supset + G_2 p \delta_{i_2}^{j_1} \delta_{i_1}^{j_2} + G_2^2 p \ln \left(\frac{\Lambda}{p} \right) \left(\delta s_{20} \delta_{i_2}^{j_1} \delta_{i_1}^{j_2} + \delta s_{22} \delta_{i_1}^{j_1} \delta_{i_2}^{j_2} \right).
\end{aligned}$$

Note that, unlike the tree-level correlation function, the first subleading correction at order $\frac{1}{N_c}$ introduces additional structures involving delta functions over the flavor indices, which do not correspond to a single-cycle permutation, specifically $\delta_{i_1}^{j_1} \delta_{i_2}^{j_2}$.

⁶²The inclusion symbol, instead of an equality symbol, is due to a subleading correction in $\frac{1}{N_c}$ to the p term with no logarithm, which we ignore.

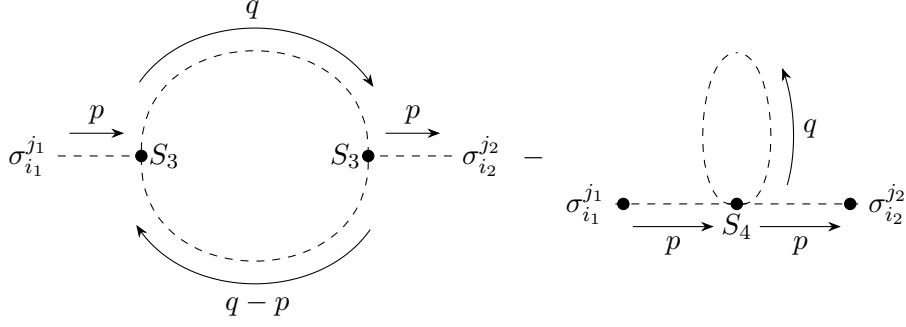


Figure 21. Feynman diagrams for the first sub-leading correction to G_2 .

To extract the anomalous dimensions of the singlet and adjoint structures, we multiply $(G_{2,tot})_{i_1,i_2}^{j_1,j_2}$ by $\zeta_{j_1}^{i_1} \zeta_{j_2}^{i_2}$ and use (4.6). We find⁶³

$$\begin{aligned} (G_{2,tot})_{i_1,i_2}^{j_1,j_2} \zeta_{j_1}^{i_1} \zeta_{j_2}^{i_2} &= p G_2 \left(1 - G_2 \delta s_{20} \ln \left(\frac{p}{\Lambda} \right) \right) (\zeta_A)_j^i (\zeta_A)_i^j \\ &\quad + p \frac{1}{N_f} G_2 \left(1 - (G_2 \delta s_{20} + N_f G_2 \delta s_{22}) \ln \left(\frac{p}{\Lambda} \right) \right) \zeta_S \zeta_S, \end{aligned} \quad (\text{B.19})$$

and plugging in the numbers, we get

$$\gamma_A = -\frac{1}{2} G_2 \delta s_{20} = -\frac{1}{N_c} \frac{4 N_f}{3 \pi^2}, \quad \gamma_S = -\frac{1}{2} (G_2 \delta s_{20} + N_f G_2 \delta s_{22}) = -\frac{1}{N_c} \frac{16 N_f}{3 \pi^2}. \quad (\text{B.20})$$

For $N_f = 1$, there is only a singlet structure, and γ_S in (B.20) matches the result in the literature [2, 25].

B.5 First sub-leading contribution to G_3

The first subleading contribution to G_3 , which we denote in the main text as δG_3 , comes from three diagrams, shown in figure 22. The calculations proceed in exactly the same manner as in section B.2.2 of [25], and the only difference is adding flavors indices. We find that⁶⁴

$$\begin{aligned} \delta \bar{G}_{3,3} &= \frac{1}{N_c^3} \frac{512 N_f (12 s_{5,N} - 1)}{\pi^2}, \\ \delta \bar{G}_{3,2} &= \frac{1}{N_c^3} \frac{1024 (4 s_{5,F} - 1)}{\pi^2}, \\ \delta \bar{G}_{3,1} &= 0. \end{aligned} \quad (\text{B.21})$$

Note that, at leading order in $\frac{1}{N_c}$, there is no contribution to $\delta \bar{G}_{3,1}$, as it involves three non-diagonal delta functions in the flavor indices. Such a structure requires diagrams with

⁶³Note that $G_{2,tot}$ and ζ have an implicit momentum dependence.

⁶⁴Alternatively, and as in the $N_f = 1$ case, these conditions can be found by requiring that (4.22) vanish for $\lambda = \lambda_n = 0$. This is true since the RB theory (2.11) is free at this point, and thus the beta function should vanish.

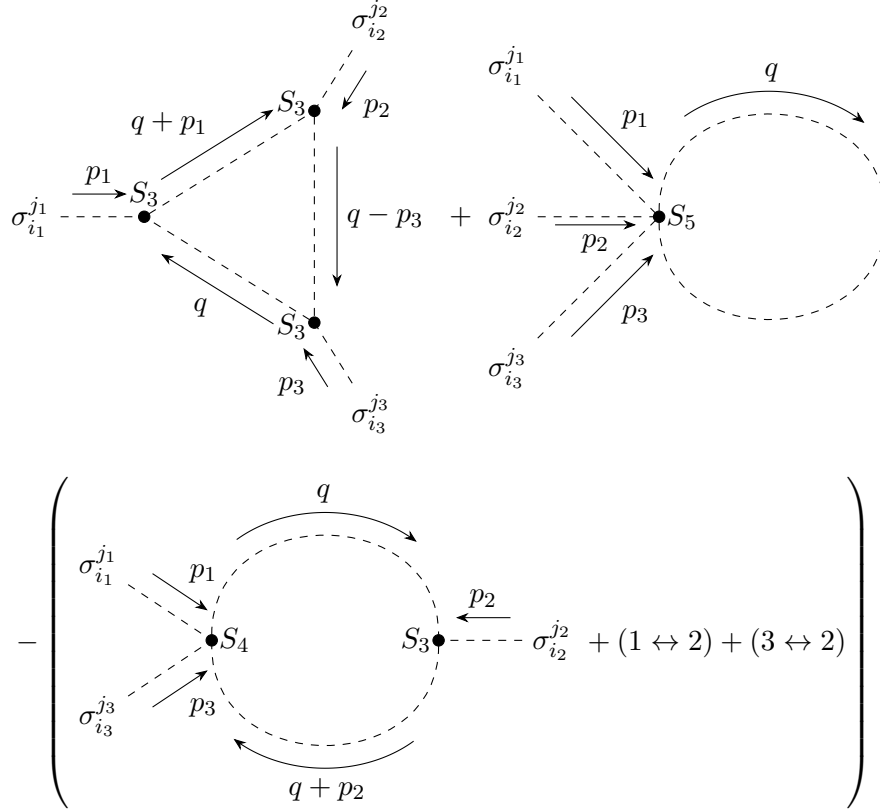


Figure 22. Feynman diagrams for calculating the first sub-leading contribution to G_3 .

a different topology in order to be realized. We expect contributions to it only at order $\delta\bar{G}_{3,1} \sim \frac{1}{N_c^5}$ (that is three loops).

Transformation to the representation basis is done using (2.8). The results of this appendix are summarized in table 3.

C Correlation functions for the free fermion theories

In this appendix we present the calculations of correlation functions of the fermion bilinear mesons $M_i^j \equiv \frac{4\pi}{\kappa_F} \bar{\psi}_{c,i} \psi^{c,j}$ in the limit $\lambda_F = 0$. We follow Appendix C of [25], generalizing their results to multiple flavors.

The calculation of the two-point function is given by⁶⁵

$$\langle M_{i_1}^{j_1}(p) M_{i_2}^{j_2}(-p) \rangle = \delta_{i_2}^{j_1} \delta_{i_1}^{j_2} \left(\frac{4\pi}{\kappa_F} \right)^2 N_c \int \frac{d^3 q}{(2\pi)^3} \text{Tr} \left(\frac{\not{q}(\not{q} + \not{p})}{q^2 (q+p)^2} \right). \quad (\text{C.1})$$

Solving the integral using $\text{Tr}(\gamma^\mu \gamma^\nu) = 2\eta^{\mu\nu}$, and ignoring terms which are linear in the

⁶⁵Note that the minus sign from the fermion loop is canceled with the i^2 from the two fermion propagators in Euclidean signature.

cutoff (since we fine tune the relevant operator), we find

$$(G_2)_{i_1 i_2}^{j_1 j_2}(p) = \frac{2\pi^2}{\kappa_F^2} N_c |q| \delta_{i_2}^{j_1} \delta_{i_1}^{j_2}. \quad (\text{C.2})$$

The four-point function is given by

$$(G_4)_{i_1, i_2, i_3, i_4}^{j_1, j_2, j_3, j_4}(p_1, p_2, p_3, p_4) = \left(\frac{4\pi}{\kappa_F} \right)^4 N_c \left(\delta_{i_2}^{j_1} \delta_{i_3}^{j_2} \delta_{i_4}^{j_3} \delta_{i_1}^{j_4} Y(p_1, p_2, p_3, p_4) + (\text{permutations of } \{2,3,4\}) \right), \quad (\text{C.3})$$

where

$$Y(p_1, p_2, p_3, p_4) = - \int \frac{d^3 q}{(2\pi)^3} \text{Tr} \left(\frac{q(q+p_1)(q+p_1+p_2)(q-p_4)}{q^2(q+p_1)^2(q+p_1+p_2)^2(q-p_4)^2} \right). \quad (\text{C.4})$$

The trace over the γ matrices can be simplified by

$$\text{Tr}(\gamma^\mu \gamma^\nu \gamma^\rho \gamma^\sigma) = 2(\eta^{\mu\nu} \eta^{\rho\sigma} - \eta^{\mu\rho} \eta^{\nu\sigma} + \eta^{\mu\sigma} \eta^{\nu\rho}). \quad (\text{C.5})$$

We are interested in the kinematic limit where $p_1 = -p_2 \equiv p$, $p_3 = -p_4 \equiv k$, and $|p| \gg |k|$. In this regime, it is sufficient to solve for $Y(p, -p, k, -k)$ and $Y(p, k, -p, -k)$. The remaining momentum configurations can be obtained either by replacing k with $-k$, or by exploiting the symmetry

$$Y(p_1, p_2, p_3, p_4) = Y(p_1, p_4, p_3, p_2). \quad (\text{C.6})$$

We find

$$\begin{aligned} -Y(p, k, -p, -k) = & \int \frac{d^3 q}{(2\pi)^3} \left[-\frac{1}{2q^2(q+k)^2} - \frac{1}{2q^2(q+p)^2} - \frac{1}{2(q+p)^2(q+k)^2} \right. \\ & + \frac{k^2}{2q^2(q+k)^2(q+p)^2} + \frac{p^2}{2q^2(q+k)^2(q+p)^2} + \frac{3}{2q^2(q+p+k)^2} + \frac{1}{q^2(q+p)^2} \\ & - \frac{k^2}{2q^2(q+k)^2(q+p+k)^2} - \frac{p^2}{2q^2(q+p)^2(q+p+k)^2} + \frac{3k^2}{2(q+k)^2(q+p)^2(q+p+k)^2} \\ & + \frac{p^2}{2(q+k)^2(q+p)^2(q+p+k)^2} - \frac{k^2 p^2}{2q^2(q+k)^2(q+p)^2(q+p+k)^2} + \frac{p \cdot k}{q^2(q+k)^2(q+p+k)^2} \\ & + \frac{p \cdot k}{q^2(q+p)^2(q+p+k)^2} + \frac{2p \cdot k}{(q+k)^2(q+p)^2(q+p+k)^2} - \frac{k^2 k \cdot p}{q^2(q+k)^2(q+p)^2(q+p+k)^2} \\ & - \frac{p^2 p \cdot k}{q^2(q+k)^2(q+p)^2(q+p+k)^2} + \frac{q \cdot k}{q^2(q+p)^2(q+p+k)^2} \\ & \left. + \frac{q \cdot p}{q^2(q+k)^2(q+p+k)^2} + \frac{2q \cdot k}{(q+k)^2(q+p)^2(q+p+k)^2} \right], \end{aligned} \quad (\text{C.7})$$

and

$$\begin{aligned}
-Y(p, -p, k, -k) = & \int \frac{d^3 q}{(2\pi)^3} \left[\frac{1}{2q^2 (q+p)^2} - \frac{k^2}{2q^2 (q+k)^2 (q+p)^2} + \frac{q \cdot p}{q^2 (q+k)^2 (q+p)^2} \right. \\
& \left. + \frac{2(q \cdot p)(q \cdot k)}{q^4 (q+k)^2 (q+p)^2} + \frac{1}{2(q+k)^2 (q+p)^2} - \frac{p \cdot k}{q^2 (q+k)^2 (q+p)^2} \right]. \tag{C.8}
\end{aligned}$$

Using the integral identities (where we denote $p_0 = p_1 - p_2$)

$$\int \frac{d^3 q}{(2\pi)^3} \frac{1}{q^2 (q+p)^2} = \frac{1}{8|p|}, \tag{C.9}$$

$$\int \frac{d^3 q}{(2\pi)^3} \frac{1}{q^2 (q+p_1)^2 (q+p_2)^2} = \frac{1}{8} \frac{1}{|p_1| |p_2| |p_0|}, \tag{C.10}$$

$$\int \frac{d^3 q}{(2\pi)^3} \frac{q_\mu}{q^2 (q+p_1)^2 (q+p_2)^2} = -\frac{1}{8|p_0|(|p_1|+|p_2|+|p_0|)} \left(\frac{1}{|p_1|} p_{1\mu} + \frac{1}{|p_2|} p_{2\mu} \right), \tag{C.11}$$

$$\begin{aligned}
\int \frac{d^3 q}{(2\pi)^3} \frac{q_\mu q_\nu}{q^4 (q+p_1)^2 (q+p_2)^2} = & \frac{1}{16} \frac{1}{(p_1+p_2+p_0)} \left[\frac{\eta_{\mu\nu}}{|p_1| |p_2|} \right. \\
& + \frac{(2|p_1|+|p_2|+|p_0|) p_{1,\mu} p_{1,\nu}}{|p_1|^3 |p_0| (|p_1|+|p_2|+|p_0|)} + \frac{p_{1,\mu} p_{2,\nu}}{|p_1| |p_2| |p_0| (|p_1|+|p_2|+|p_0|)} \\
& \left. + \frac{p_{1,\nu} p_{2,\mu}}{|p_1| |p_2| |p_0| (|p_1|+|p_2|+|p_0|)} + \frac{(|p_1|+2|p_2|+|p_0|) p_{2,\nu} p_{2,\mu}}{|p_2|^3 |p_0| (|p_1|+|p_2|+|p_0|)} \right], \tag{C.12}
\end{aligned}$$

and for $|p| \gg |k|$ the identity [25]

$$\int \frac{d^3 p}{(2\pi)^3} \frac{1}{q^2 (q+k)^2 (q+p)^2 (q+p+k)^2} \simeq \frac{1}{4|p|^4 |k|}, \tag{C.13}$$

we find after Taylor expanding in $|k|/|p|$ that at the leading orders

$$\begin{aligned}
-Y(p, -p, k, -k) = & \frac{1}{8|p|} + \frac{k \cdot p}{8p^3} - \frac{k \cdot p}{8|k|p^2} - \frac{(k \cdot p)^2}{8|k|p^4}, \\
-Y(p, k, -p, -k) = & \frac{1}{4|p|} - \frac{|k|}{4p^2}. \tag{C.14}
\end{aligned}$$

The four-point function is thus

$$\begin{aligned}
(G_4)_{i_1, i_2, i_3, i_4}^{j_1, j_2, j_3, j_4}(p, -p, k, -k) = & -\left(\frac{4\pi}{\kappa}\right)^4 N_c \left(\left(\delta_{i_2}^{j_1} \delta_{i_3}^{j_2} \delta_{i_4}^{j_3} \delta_{i_1}^{j_4} + \delta_{i_4}^{j_1} \delta_{i_3}^{j_4} \delta_{i_2}^{j_3} \delta_{i_1}^{j_2} \right) \left(\frac{1}{8|p|} + \frac{k \cdot p}{8p^3} - \frac{k \cdot p}{8|k|p^2} - \frac{(k \cdot p)^2}{8|k|p^4} \right) + \right. \\
& \left(\delta_{i_2}^{j_1} \delta_{i_4}^{j_2} \delta_{i_3}^{j_4} \delta_{i_1}^{j_3} + \delta_{i_3}^{j_1} \delta_{i_4}^{j_3} \delta_{i_2}^{j_4} \delta_{i_1}^{j_2} \right) \left(\frac{1}{8|p|} - \frac{k \cdot p}{8p^3} + \frac{k \cdot p}{8|k|p^2} - \frac{(k \cdot p)^2}{8|k|p^4} \right) + \\
& \left. \left(\delta_{i_3}^{j_1} \delta_{i_2}^{j_3} \delta_{i_4}^{j_2} \delta_{i_1}^{j_4} + \delta_{i_4}^{j_1} \delta_{i_2}^{j_4} \delta_{i_3}^{j_2} \delta_{i_1}^{j_3} \right) \left(\frac{1}{4|p|} - \frac{|k|}{4p^2} \right) \right). \tag{C.15}
\end{aligned}$$

Note that when using the G_4 term in the main text, since we integrate over the large momenta when using G_4 , we can ignore the $p \cdot k$ term, since it will give an antisymmetric integrand with respect to $p \leftrightarrow -p$, and so the full integral will vanish.

We summarize the results obtained in this appendix in table 3.

References

- [1] S. Giombi, S. Minwalla, S. Prakash, S.P. Trivedi, S.R. Wadia and X. Yin, *Chern-Simons Theory with Vector Fermion Matter*, *Eur. Phys. J. C* **72** (2012) 2112 [[1110.4386](#)].
- [2] O. Aharony, G. Gur-Ari and R. Yacoby, *Correlation Functions of Large N Chern-Simons-Matter Theories and Bosonization in Three Dimensions*, *JHEP* **12** (2012) 028 [[1207.4593](#)].
- [3] O. Aharony, *Baryons, monopoles and dualities in Chern-Simons-matter theories*, *JHEP* **02** (2016) 093 [[1512.00161](#)].
- [4] N. Seiberg, T. Senthil, C. Wang and E. Witten, *A Duality Web in 2+1 Dimensions and Condensed Matter Physics*, *Annals Phys.* **374** (2016) 395 [[1606.01989](#)].
- [5] J. Maldacena and A. Zhiboedov, *Constraining Conformal Field Theories with A Higher Spin Symmetry*, *J. Phys. A* **46** (2013) 214011 [[1112.1016](#)].
- [6] J. Maldacena and A. Zhiboedov, *Constraining conformal field theories with a slightly broken higher spin symmetry*, *Class. Quant. Grav.* **30** (2013) 104003 [[1204.3882](#)].
- [7] I.R. Klebanov and A.M. Polyakov, *AdS dual of the critical $O(N)$ vector model*, *Phys. Lett. B* **550** (2002) 213 [[hep-th/0210114](#)].
- [8] E. Sezgin and P. Sundell, *Massless higher spins and holography*, *Nucl. Phys. B* **644** (2002) 303 [[hep-th/0205131](#)].
- [9] S. Giombi and X. Yin, *Higher Spin Gauge Theory and Holography: The Three-Point Functions*, *JHEP* **09** (2010) 115 [[0912.3462](#)].
- [10] C.-M. Chang, S. Minwalla, T. Sharma and X. Yin, *ABJ Triality: from Higher Spin Fields to Strings*, *J. Phys. A* **46** (2013) 214009 [[1207.4485](#)].
- [11] S. Giombi, *Higher Spin — CFT Duality*, in *Theoretical Advanced Study Institute in Elementary Particle Physics: New Frontiers in Fields and Strings*, pp. 137–214, 2017, DOI [[1607.02967](#)].
- [12] A. Giveon and D. Kutasov, *Seiberg Duality in Chern-Simons Theory*, *Nucl. Phys. B* **812** (2009) 1 [[0808.0360](#)].
- [13] F. Benini, C. Closset and S. Cremonesi, *Comments on 3d Seiberg-like dualities*, *JHEP* **10** (2011) 075 [[1108.5373](#)].
- [14] J. Park and K.-J. Park, *Seiberg-like Dualities for 3d $N=2$ Theories with $SU(N)$ gauge group*, *JHEP* **10** (2013) 198 [[1305.6280](#)].
- [15] O. Aharony, S.S. Razamat, N. Seiberg and B. Willett, *3d dualities from 4d dualities*, *JHEP* **07** (2013) 149 [[1305.3924](#)].
- [16] S. Jain, S. Minwalla and S. Yokoyama, *Chern Simons duality with a fundamental boson and fermion*, *JHEP* **11** (2013) 037 [[1305.7235](#)].
- [17] K. Inbasekar, S. Jain, S. Mazumdar, S. Minwalla, V. Umesh and S. Yokoyama, *Unitarity, crossing symmetry and duality in the scattering of $\mathcal{N} = 1$ susy matter Chern-Simons theories*, *JHEP* **10** (2015) 176 [[1505.06571](#)].
- [18] G. Gur-Ari and R. Yacoby, *Three Dimensional Bosonization From Supersymmetry*, *JHEP* **11** (2015) 013 [[1507.04378](#)].

- [19] A. Kapustin, B. Willett and I. Yaakov, *Tests of Seiberg-like dualities in three dimensions*, *JHEP* **08** (2020) 114 [[1012.4021](#)].
- [20] B. Willett and I. Yaakov, *$\mathcal{N} = 2$ dualities and Z -extremization in three dimensions*, *JHEP* **10** (2020) 136 [[1104.0487](#)].
- [21] A. Kapustin, *Seiberg-like duality in three dimensions for orthogonal gauge groups*, [1104.0466](#).
- [22] K. Intriligator and N. Seiberg, *Aspects of 3d $N=2$ Chern-Simons-Matter Theories*, *JHEP* **07** (2013) 079 [[1305.1633](#)].
- [23] K. Jensen and P. Patil, *Chern-Simons dualities with multiple flavors at large N* , *JHEP* **12** (2019) 043 [[1910.07484](#)].
- [24] O. Aharony and A. Sharon, *Large N renormalization group flows in 3d $\mathcal{N} = 1$ Chern-Simons-Matter theories*, *JHEP* **07** (2019) 160 [[1905.07146](#)].
- [25] O. Aharony, S. Jain and S. Minwalla, *Flows, Fixed Points and Duality in Chern-Simons-matter theories*, *JHEP* **12** (2018) 058 [[1808.03317](#)].
- [26] D. Radićević, *Disorder Operators in Chern-Simons-Fermion Theories*, *JHEP* **03** (2016) 131 [[1511.01902](#)].
- [27] S. Kapoor and S. Prakash, *Bifundamental multiscalar fixed points in $d=3-\epsilon$* , *Phys. Rev. D* **108** (2023) 026002 [[2112.01055](#)].
- [28] G. Gur-Ari and R. Yacoby, *Correlators of Large N Fermionic Chern-Simons Vector Models*, *JHEP* **02** (2013) 150 [[1211.1866](#)].
- [29] A. Bedhotiya and S. Prakash, *A test of bosonization at the level of four-point functions in Chern-Simons vector models*, *JHEP* **12** (2015) 032 [[1506.05412](#)].
- [30] S. Jain, M. Mandlik, S. Minwalla, T. Takimi, S.R. Wadia and S. Yokoyama, *Unitarity, Crossing Symmetry and Duality of the S -matrix in large N Chern-Simons theories with fundamental matter*, *JHEP* **04** (2015) 129 [[1404.6373](#)].
- [31] Y. Dandekar, M. Mandlik and S. Minwalla, *Poles in the S -Matrix of Relativistic Chern-Simons Matter theories from Quantum Mechanics*, *JHEP* **04** (2015) 102 [[1407.1322](#)].
- [32] S. Yokoyama, *Scattering Amplitude and Bosonization Duality in General Chern-Simons Vector Models*, *JHEP* **09** (2016) 105 [[1604.01897](#)].
- [33] S. Jain, S.P. Trivedi, S.R. Wadia and S. Yokoyama, *Supersymmetric Chern-Simons Theories with Vector Matter*, *JHEP* **10** (2012) 194 [[1207.4750](#)].
- [34] O. Aharony, S. Giombi, G. Gur-Ari, J. Maldacena and R. Yacoby, *The Thermal Free Energy in Large N Chern-Simons-Matter Theories*, *JHEP* **03** (2013) 121 [[1211.4843](#)].
- [35] S. Jain, S. Minwalla, T. Sharma, T. Takimi, S.R. Wadia and S. Yokoyama, *Phases of large N vector Chern-Simons theories on $S^2 \times S^1$* , *JHEP* **09** (2013) 009 [[1301.6169](#)].
- [36] T. Takimi, *Duality and higher temperature phases of large N Chern-Simons matter theories on $S^2 \times S^1$* , *JHEP* **07** (2013) 177 [[1304.3725](#)].
- [37] S. Minwalla and S. Yokoyama, *Chern Simons Bosonization along RG Flows*, *JHEP* **02** (2016) 103 [[1507.04546](#)].
- [38] A. Dey, I. Halder, S. Jain, L. Janagal, S. Minwalla and N. Prabhakar, *Duality and an exact Landau-Ginzburg potential for quasi-bosonic Chern-Simons-Matter theories*, *JHEP* **11** (2018) 020 [[1808.04415](#)].

- [39] S. Choudhury, A. Dey, I. Halder, S. Jain, L. Janagal, S. Minwalla et al., *Bose-Fermi Chern-Simons Dualities in the Higgsed Phase*, *JHEP* **11** (2018) 177 [[1804.08635](#)].
- [40] A.N. Vasiliev, Y.M. Pismak and Y.R. Khonkonen, *1/N expansion: calculation of the exponent η in the order $1/N^3$ by the conformal bootstrap method*, *Theor. Math. Phys.* **50** (1982) 127.
- [41] R. Yacoby, *Scalar Correlators in Bosonic Chern-Simons Vector Models*, [1805.11627](#).
- [42] G.J. Turiaci and A. Zhiboedov, *Veneziano Amplitude of Vasiliev Theory*, *JHEP* **10** (2018) 034 [[1802.04390](#)].
- [43] O. Aharony, L.F. Alday, A. Bissi and R. Yacoby, *The Analytic Bootstrap for Large N Chern-Simons Vector Models*, *JHEP* **08** (2018) 166 [[1805.04377](#)].
- [44] S. Giombi, V. Gurucharan, V. Kirilin, S. Prakash and E. Skvortsov, *On the Higher-Spin Spectrum in Large N Chern-Simons Vector Models*, *JHEP* **01** (2017) 058 [[1610.08472](#)].
- [45] S. Jain, V. Malvimat, A. Mehta, S. Prakash and N. Sudhir, *All order exact result for the anomalous dimension of the scalar primary in Chern-Simons vector models*, *Phys. Rev. D* **101** (2020) 126017 [[1906.06342](#)].
- [46] P. Jain, S. Jain, B. Sahoo, K.S. Dhruva and A. Zade, *Mapping Large N Slightly Broken Higher Spin (SBHS) theory correlators to free theory correlators*, *JHEP* **12** (2023) 173 [[2207.05101](#)].
- [47] R.D. Pisarski, *Fixed point structure of ϕ^6 in three-dimensions at large N*, *Phys. Rev. Lett.* **48** (1982) 574.
- [48] L.V. Avdeev, D.I. Kazakov and I.N. Kondrashuk, *Renormalizations in supersymmetric and nonsupersymmetric nonAbelian Chern-Simons field theories with matter*, *Nucl. Phys. B* **391** (1993) 333.
- [49] O. Aharony, G. Gur-Ari and R. Yacoby, *d=3 Bosonic Vector Models Coupled to Chern-Simons Gauge Theories*, *JHEP* **03** (2012) 037 [[1110.4382](#)].
- [50] D. Anninos, R. Mahajan, D. Radićević and E. Shaghoulian, *Chern-Simons-Ghost Theories and de Sitter Space*, *JHEP* **01** (2015) 074 [[1405.1424](#)].
- [51] S. Coleman, *Aspects of Symmetry: Selected Erice Lectures*, Online access with purchase: Cambridge Books Online, Cambridge University Press (1988).
- [52] R.R. Kalloor, *Four-point functions in large N Chern-Simons fermionic theories*, *JHEP* **10** (2020) 028 [[1910.14617](#)].
- [53] S. Banerjee and D. Radićević, *Chern-Simons theory coupled to bifundamental scalars*, *JHEP* **06** (2014) 168 [[1308.2077](#)].
- [54] J. Milnor, *Topology from the Differentiable Viewpoint*, University Press of Virginia (1965).
- [55] V. Guillemin and A. Pollack, *Differential Topology*, AMS Chelsea Publishing, AMS Chelsea Pub. (2010).